Spring 2015

Discrete epidemic models with arbitrarily distributed disease stages

Nancy Hernandez Ceron
Purdue University

Graduate School Form 30
Updated 1/15/2015

PURDUE UNIVERSITY
GRADUATE SCHOOL
Thesis/Dissertation Acceptance

This is to certify that the thesis/dissertation prepared

By Hernandez Ceron, Nancy

Entitled

DISCRETE EPIDEMIC MODELS WITH ARBITRARILY DISTRIBUTED DISEASE STAGES

For the degree of Doctor of Philosophy

Is approved by the final examining committee:

Zhilan Feng
Chair

Gregery Buzzard

Aaron Yip

Andrew Hill

To the best of my knowledge and as understood by the student in the Thesis/Dissertation Agreement, Publication Delay, and Certification Disclaimer (Graduate School Form 32), this thesis/dissertation adheres to the provisions of Purdue University's "Policy of Integrity in Research" and the use of copyright material.

Approved by Major Professor(s): Zhilan Feng

Approved by: David Goldberg 04/23/2015

Head of the Departmental Graduate Program Date

DISCRETE EPIDEMIC MODELS WITH ARBITRARILY DISTRIBUTED DISEASE STAGES

A Dissertation

Submitted to the Faculty

of

Purdue University

by

Nancy Hernandez-Ceron

In Partial Fulfillment of the

Requirements for the Degree

of

Doctor of Philosophy

May 2015

Purdue University

West Lafayette, Indiana

To my family, friends and Jonathan

ACKNOWLEDGMENTS

I begin by thanking my PhD adviser Professor Zhilan Feng. Having her as my mentor has been a privilege, her knowledge and guidance have been a fundamental part of my formation as a researcher. Without her advice and support my experience as a graduate student would have never been as rich and enjoyable as it has been.

I thank the committee members, Professors Greg Buzzard, Aaron Nung Kwan Yip and Andrew Hill, for taking the time to revise my work and for their helpful suggestions. I appreciate Dr. Hill is taking the time to travel to Purdue, and I am sure his visit will benefit not only me but also our entire research group and other graduate students in the department.

Along my journey in graduate school I have met people who inspired me. Their ideas gave me a broader vision, while their support provided the confidence to continue though my path. These are too many to list but special acknowledgments go to my collaborators Carlos Castillo-Chavez, Pauline van den Driessche, Jonathan Chavez-Casillas and Linda Allen. With the support of my adviser and Prof. Castillo Chavez I was given the opportunity to attend the MTBI summer program at ASU, during which, I was able to meet wonderful people including Jesse E. Taylor, Anuj Mubayi, Jose Flores and Gerardo Chowell, all of whom encouraged me to grow as a researcher with interesting ideas and insightful discussions. Another summer program that helped shape my formation was the 2012 PIMS-MPrime-CDM Summer School in Edmonton Canada, where I met my collaborators Douglas C. Dover and Erin Kirwin. Their expertise and perspective in public health greatly contributed to my knowledge and interest in this field.

I thank the current and former members of our research group at Purdue: Jorge Alfaro Murillo, Christina Alvey, Qing Han, Georgi Kapitanov, Katia Vogt and Yiqiang Zheng, it was a pleasure to learn from all of them in our seminars and classes. Sincere

gratitude goes to my former Professors in Mexico and Canada who saw in me the potential to continue my studies, Professors Arturo Erdely, Victor Ibarra and Byron Schmuland among others.

I also want to express my gratitude towards all members of the Department of Mathematics at Purdue for all their support during my studies here. I only have good memories from all the people I met at the department, many of whom became my little family away from home.

Finally I thank my family, parents, brothers, aunts, uncles, cousins, nephew, grandparents and in laws, whose presence in my life gave me strength and motivation to continue pursuing my dreams. Last but not least I thank my collaborator and partner Jonathan Chavez-Casillas, it has been a privilege to have him by my side in this journey.

TABLE OF CONTENTS

LIST OF TABLES

LIST OF FIGURES

ABSTRACT

Hernandez-Ceron, Nancy PhD, Purdue University, May 2015. Discrete Epidemic Models with Arbitrarily Distributed Disease Stages. Major Professor: Zhilan Feng.

The use of discrete-time models (or discrete models) in the field of mathematical epidemiology has been limited while continuous-time models (or continuous models) are often times preferred, particularly because disease dynamics do occur continuously in time and more mathematical tools are available for model analysis. However, discrete models are not only more tractable and easier to understand, but also more directly related to data, particularly when the disease stage distributions are arbitrarily distributed (e.g., when the data cannot be fitted by distributions from a parametric family). Under these circumstances continuous models usually lead to complex system of integral equations.

Deterministic and stochastic epidemic models have commonly assumed that the disease stages, particularly the infectious period, have constant exit rates (continuous models) or constant exit probabilities (discrete models), which correspond to exponential and geometric distributions, respectively. The very property of these distributions that makes models tractable, the memoryless property, is biologically unrealistic for most infectious diseases. In fact, it has been shown that models with these simplifying assumptions may generate biased and possibly misleading evaluations for disease control strategies.

Realistic alternatives considered in the literature are the Gamma and Negative Binomial distributions, a natural generalization due to their relationship with the above mentioned distributions. The "linear chain trick" can be used to reduce a system of integro-differential equations to a system of ordinary differential equations and a similar idea can be applied in stochastic models to allow for the use of Gamma

distribution, while still preserving the Markov property of the process. Few models, however, include distributions beyond these alternatives. The focuses of this thesis is the use of arbitrarily distributed disease stages in discrete models, their formulation and analysis, as well as the study of the impact of a given distribution on model predictions.

Chapter 1 includes a brief review of relevant topics and the motivation for this work. In Chapter 2 several SEIR-type models with arbitrarily distributed infectious period are introduced and analyzed. This chapter focuses on the use of the next generation matrix approach to derive analytic expressions for $\mathcal{R}_0$ and $\mathcal{R}_C$. In Chapter 3 we develop and analyze of a model with quarantine and isolation when arbitrarily distributed disease stages are incorporated. The results obtained in the general framework are then applied to models with specific distributions (e.g., Geometric vs. more realistic distributions), which allow us to investigate the influence of disease stage distributions on the dynamics of single epidemic outbreaks. It is demonstrated that the discrepancies between model predictions can sometimes be substantial.

In Chapter 4 a stochastic discrete-time model with n patches and (random) infectious period T is developed. The results obtained are then used to investigate how the distribution of T may affect model outcomes. Specific distributions analyzed include Geometric, Negative Binomial, Poisson and Uniform. The model predictions are contrasted both numerically and analytically by comparing the corresponding $\mathcal{R}_0$ values as well as the probability of disease extinction. It is shown analytically that for $n = 2$ the $\mathcal{R}_0$ values corresponding to different distributions of T can be ordered based on the probability generating function ϕ_T of T. In addition, numerical simulations are carried out to examine the final epidemic size, duration and peak of the epidemic.

1. INTRODUCTION AND BACKGROUND

The birth of mathematical theory of epidemics can be traced to the work of Daniel Bernoulli in 1760 [1], who developed a *discrete* epidemic model to analyze the mortality of smallpox, and more recently to Sir Ronald Ross [2], Anderson Gray McKendrick [3], and the statistician William Ogilvy Kermack. Sir Ronald Ross, an English physician and Nobel Laureate, developed the first mathematical models for the study of the transmission dynamics of malaria [2]. McKendrick and Kermack published a series of papers, introducing a deterministic epidemiological model and their celebrated threshold theorem [3–5]. In the first paper of this series a discrete-time epidemic model is considered, which leads to a continous-time model as the time steps are taken to the limit.

After the 2003 SARS outbreaks, and more recently the 2009 H1N1 pandemic and the 2014 Ebola epidemics, efforts to connect models to data have increased greatly. Single-outbreak epidemic models are now routinely used to estimate the basic reproduction number $\mathcal{R}_0$ and the effective or control reproduction number $\mathcal{R}_C$, and to evaluate disease control strategies for continuous [6–15] and discrete models [16–23].

In 2004 Y. Zhou, Z. Ma and F. Brauer developed a discrete-time model for SARS [24]. Other epidemics of particular diseases have also been modeled in a discrete framework. These include measles [25], tuberculosis [26], rodent-hantavirus [17, 23], chytridiomycosis in amphibians [17], plant diseases [27], and diseases involving vector-host transmission [28] and vertical transmission [29]. More mathematical results about epidemic models can be found in [30, 31] (permanence and stability of models with delay), [29, 32, 33] (stability analysis), [32, 34, 35] (presence of chaos) and the references therein.

The connection between epidemic models in discrete-time and continuous-time settings has been investigated in the past. For example, Pellis et al. [36] examined

and extended the insights that can be gained from Ludwig's result [37], which specified conditions under which a continuous-time infectious process has the same final size distribution as another discrete-generation contact process. This topic has also been discussed in [8] (see Exercise 1.40) and [22,28,38]. However, it is not the focus of this work to study the relationship between continuous-time and discrete-time models for epidemics.

The focus of this work is on the formulation and analyses of discrete-time models that allow for the inclusion of *arbitrarily distributed* waiting time distributions. Most existing discrete-time models for infectious diseases implicitly assume a geometric distribution for the disease stage durations (e.g., latent or infectious period), which makes the models tractable and easy to analyze. However, this assumption is not realistic for most infectious diseases. Although these simpler models can be very helpful for gaining important insights into disease dynamics, there are many situations in which they may not be appropriate and can generate biased or misleading results, as demonstrated in the following chapters. Therefore, it is important to investigate how the assumptions on disease stages may influence model outcomes. The approach presented in this thesis is to develop a model with an arbitrarily distributed disease durations (latent and/or infectious period). The results can then be used to compare model outcomes when the arbitrary distribution is replaced by various distributions (e.g., geometric, binomial, Poisson, or empirical). The measures used for model comparison include the basic and control reproduction numbers ($\mathcal{R}_0$ and $\mathcal{R}_C$), final epidemic size, probability of major/minor outbreaks, duration and peak of the epidemic.

Chapters 2 and 3 are devoted to deterministic models, while Chapter 4 considers a stochastic model. In order to bring into the context of epidemiological applications, formulas for $\mathcal{R}_0$ and $\mathcal{R}_C$ are derived in all cases. Our detailed derivations help reveal the explicit dependance of $\mathcal{R}_0$ and $\mathcal{R}_C$ on the mean values of the stage distributions, the mean sojourn times, and other distribution-adjusted probabilities. Throughout, we highlight the role that modeling assumptions (a priori selection of distributions for

disease stage durations) have on the qualitative and quantitative assessment of model outcomes. Examples of discrete-time models under different stage-duration distributions are considered to illustrate the discrepancies in model evaluation, particularly when control strategies are present.

The remainder of this chapter is organized as follows. Section 1.1 includes a brief summary of results involving deterministic epidemic models in discrete-time. Section 1.2 includes a discussion about the importance of considering more realistic distributions for disease stages, as well as some drawbacks of using the (commonly assumed) Geometric distribution. Finally, a summary of important results in continous-time stochastic SIR models with arbitrarily distributed infectious period can be found in Section 1.3. These results strongly motivated the work presented in Chapter 4.

1.1 Discrete epidemic models

As pointed out in [32], there are usually two ways to construct a discrete epidemic model. The first approach, used in [34], directly makes use of the property of the epidemic disease, whereas the second approach, used in [31], consists in discretizing a continuous-time model using techniques such as the forward Euler scheme or Mickens non-standard discretization. In this thesis the first approach is used and the discrete-time single-outbreak model introduced and analyzed in [39] is generalized through the inclusion of arbitrary distributed disease stages. The building block to do so is the basic model

$$\begin{aligned} S_{n+1} &= S_n G\left(I_n/T_n\right) \\ I_{n+1} &= S_n\left[1-G\left(I_n/T_n\right)\right]+(1-\gamma)I_n \\ R_{n+1} &= R_n+\gamma I_n, \qquad n=1,2,\ldots \end{aligned} \tag{1.1}$$

depicted in figure 1.1. Here, $T_n = S_n + I_n + R_n$ is the total population size and I_n/T_n is the prevalence, at time n. The proportion of susceptible individuals who become infected at time $n+1$ is given by $1-G$, where $G : [0,1] \to [0,1]$ is a monotone function with $G(0) = 1$, $G'(x) < 0$ and $G''(x) \geqslant 0$, as pointed out by Castillo-Chavez

and Yakubu in [34]. When the population size is assumed to be constant, a customary practice for short term single outbreak models, the dependence of G on T_n can be dropped. This is the case for the models studied in this thesis. Including demographic effects or disease death is straightforward but some results (specially those involving final size relations) might no longer hold if this factor is included.

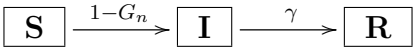

Figure 1.1. Transmission diagram for the discrete SIR model (1.1)

If the time between contacts is assumed to be Exponential with parameter β/N then, at time $n+1$, the number of times a susceptible has been in contact with *any* infective follows a Poisson distribution with parameter $\beta I_n/N$. Thus, the probability of entering in contact with *at least* one infective is $1-e^{\beta I_n/N}$. For this reason, often times it is assumed that

$$G(I_n) = e^{\beta I_n/N}, \tag{1.2}$$

This functional form of G guarantees that the solutions remain nonnegative at all times. Other options for the function G are explored in [34, 40].

One of the main motivations for this thesis comes from the transition from the I to the R class. Under constant exit probability, the proportion of individuals leaving the I class after exactly i days is $(1-\gamma)^{i-1}\gamma$ for $i \in \{1,2,3,\dots\}$, which is the probability mass function of a Geometric distribution with parameter γ. The proportion of individuals who stay *more* that i days in the I class, also called survival probability, is

$$p_i = \sum_{k=i+1}^{\infty} (1-\gamma)^{k-1}\gamma = (1-\gamma)^i, \qquad i \in \{0,1,2\cdots\}$$

In Section 1.2 drawbacks of the use of this distribution are discussed. An interesting discussion of a similar restriction in continuous models (constant exit rate) can be found in [41].

1.1.1 Computations of $\mathcal{R}_0$ and $\mathcal{R}_C$

The most commonly used quantity in the study of epidemiological models is the basic reproduction number $\mathcal{R}_0$ or the control reproduction number $\mathcal{R}_C$. They provide critical measures for designing strategies for disease control and prevention, as well as the evolutionary dynamics of the pathogen. Various approaches have been developed for the derivation of an analytical expression for $\mathcal{R}_0$ ($\mathcal{R}_C$). These studies include both continuous-time models (see, for example, [6–12]) and discrete-time models (see, for example, [16–23, 38])

A commonly used method to compute $\mathcal{R}_0$ and $\mathcal{R}_C$ is the so called next generation matrix method. Let $X_0 = (x_1, \ldots, x_m)^T$ and $X_1 = (x_{m+1}, \ldots, x_n)^T$, where $x_1, \ldots, x_m$ are the infected classes of the epidemic model and $x_{m+1}, \ldots, x_n$ are uninfected. Let

$$X(n+1) = \mathcal{M}(X(n)), \quad n = 0, 1, 2, \ldots \tag{1.3}$$

where $\mathcal{M} : \mathbb{R}^n_+ \to \mathbb{R}^n_+$ is a continuous and differentiable function. Assume there is a unique DFE for which, after linearizing one obtains $Y(n+1) = JY(n)$. Here, J is the $n \times n$ Jacobian matrix at the DFE and has the form

$$J = \begin{bmatrix} F+T & 0 \\ A & C \end{bmatrix} \tag{1.4}$$

The next theorem by Allen and van den Driessche (Thm 2.1 in [17]) gives a formula for $\mathcal{R}_0$ as well as stability conditions. A complete proof and examples can be found in [17, 20, 22, 23].

Theorem 1.1.1 *Suppose the system of difference equations* (1.3) *has a unique DFE and that linearization of the system about the DFE yields* (1.4) *with matrices* F *and*

T nonnegative, $F+T$ is irreducible, and matrices C and T satisfying $\rho(C), \rho(T) < 1$. Then the basic reproduction number is given by

$$\mathcal{R}_0 = \varrho\left(F(I-T)^{-1}\right), \tag{1.5}$$

In addition, the DFE is locally asymptotically stable if $\mathcal{R}_0 < 1$ and unstable if $\mathcal{R}_0 > 1$.

The key point here, is that the model must be written in the form (1.3), for which the Geometric function assumption is key. If a different distribution is used for the transition from I to R then the next generation method cannot be directly applied, as we will see in Chapter 2, Section 2.4

1.2 Why do we need to consider more realistic distributions?

As mentioned in Section 1.1, constant exit probability from the I class carries with it the assumption of Geometric distribution for the infectious period. The memoryless property of the Geometric distribution

$$\mathbb{P}(X > n+m | X > m) = \mathbb{P}(X > n) \tag{1.6}$$

means that the probability of X exceeding the value $n+m$, given that it already has passed m, is the same as X originally exceeding n regardless of the value of m. In other words, every instant is the beginning of a new random period and the past has no bearing on the future behavior of X. The Exponential and Geometric distributions are the *only* memoryless continuous and discrete random variables. The memoryless property explains an important factor of the I equation in the model 1.1: the number of individuals who remain in the I class at time $n+1$ depends only on I_n. For with Geometric distribution, it is not necessary to keep track of the past in order to know the values at the present.

The Geometric distribution however, might be biologically unrealistic for most infectious diseases. Plots of the probability density ($f_i = \mathbb{P}(X = i)$) and survival functions ($p_i = \mathbb{P}(X > i)$), depicted in Figure 1.2, support this claim, as a "bell

shaped" distribution is expected for the duration of the infectious period. The Geometric distribution on the other hand is far too positively skewed.

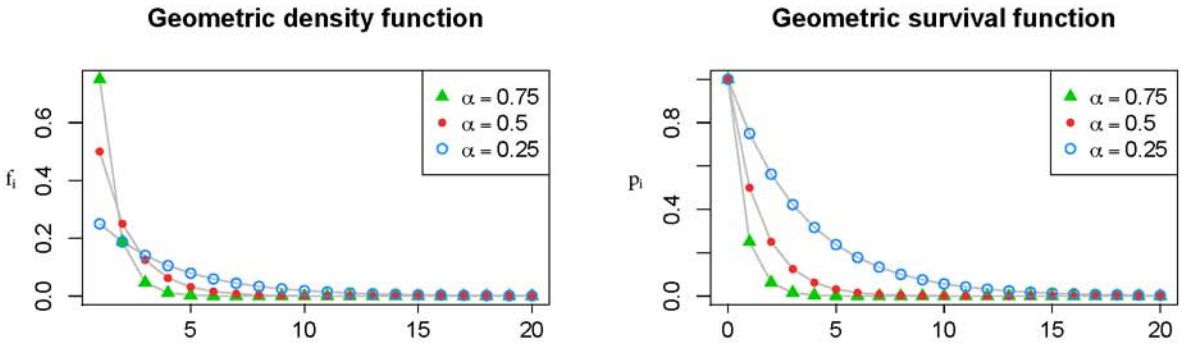

Figure 1.2. Plots of the mass (left) and the survival (right) probability functions of a geometric distribution.

Denote by $\mathcal{M}_X(s)$ the expected remaining time in a stage (latent or infectious) given that s units of time have already elapsed in the given class, this is

$$\mathcal{M}_X(m) = \begin{cases} \sum_{n=0}^{\infty} \mathbb{P}(X > n | X > m) = \sum_{n=0}^{\infty} \frac{\mathbb{P}(X > n+m)}{\mathbb{P}(X > m)} & \text{if} \quad \mathbb{P}(X > m) > 0 \\ 0 & \text{if} \quad \mathbb{P}(X > m) = 0 \end{cases}$$

A desirable property of a distribution used to model infectious periods is that the expected remaining sojourn is considerably shorter than the mean sojourn. For both the Geometric and Exponential distributions this is not the case. Particularly, if $X \sim \text{Geom}(\gamma)$,

$$\mathcal{M}_X(m) = \sum_{n=0}^{\infty} \frac{(1-\gamma)^{n+m}}{(1-\gamma)^m} = \sum_{n=0}^{\infty} (1-\gamma)^n = \mathbb{E}(X) = \mathcal{M}_X(0).$$

Again, by the memoryless property, the expected remaining sojourn after an individual already spent m units of time in the latent stage is independent of m. This may contribute in a significant way to the potentially biased model predictions on the effect of disease control strategies. The use of other distributions may lead to

more reliable assessments because of their ability to capture more accurately the description for the expected remaining sojourns. In Chapter 3 Section 3.4.2 this point is exemplified with specific distributions, for a model with disease control.

A natural and more realistic alternative to the Exponential (Geometric) distribution is the Gamma (Negative Binomial) distribution. In the continuous-time setting the so called "linear chain trick" can be used to reduce the system of integro-differential equations (obtained under Gamma distribution) to a system of ordinary differential equations (for details see, for example, [42–46]). The key idea in this approach is to introduce multiple sub-stages, each of which follows an exponential distribution. For stochastic models a similar idea is applied to allow the use of Gamma distribution, while still preserving the Markov property of the process. Such models were first developed and studied in [47, 48] and more recently in [49–51].

A discrete model with arbitrarily infectious period is considered in [52]. However, the impact of the choice of distribution is not analyzed in this study. More recently there has been an interest in the literature to study this topic. For instance, Castillo-Chavez points out in [53] that the choice of specific distributions in a model is particularly important when the model is used to evaluate disease control strategies such as quarantine and isolation. Moreover, in [54] Wearing et al explain how substantial bias are introduced by (i) neglecting the latent period, and (ii) assuming that the latent and/or infectious periods are exponentially distributed. In short, this unrealistic assumptions give rise to overoptimistic predictions, i.e. underestimation of $\mathcal{R}_0$. It is shown in [55] how parameter estimates depend sensitively on the assumptions made concerning the viral life cycle in within-host models. The assumption of exponential lifespan can lead to underestimates of $\mathcal{R}_0$ and overly optimistic predictions on prevention/eradication of the disease. The results in [45, 56] illustrate how unrealistic assumptions on the distribution of the infection and recovery process may change considerably some dynamical properties of a model. In particular, detailed explanations are provided as to how the inclusion of the more realistic Gamma distribution destabilizes the model and changes persistence. A similar conclusion is reached

in [43, 57, 58] by showing that models with Exponential and Geometric stage distributions may generate misleading assessments on disease control strategies. Thus, it is important to consider more realistic distributions, as less dispersed distributions seem to be more appropriate for modeling diseases with longer latent and infectious periods [54, 59].

1.3 Stochastic SIR models in a closed population

In this section a brief review of stochastic continous-time SIR models with arbitrarily distributed infectious period is included. In Section 1.3.1 the use of branching processes to approximate such models is discussed. Section 1.3.2 is devoted to the computation and interpretation of the probability of a minor and major epidemic. The methods and tools used in this section are modified and adapted to analyze the the discrete-time model developed in Chapter 4.

Two underlying processes define a stochastic SIR model in a closed population: infection and recovery. The infection process has mostly been modeled by a homogeneous Poisson process, i.e., contacts between any two individuals happen at a random time according to an Exponential random variable with fixed rate. Few models allow other transmission structures [60], but in recent years researches have incorporated network structures in the population to make the modeling of infection process more realistic, see for example [61] and the references therein.

The recovery process, on the other hand, has been given more flexibility and several models that allow an arbitrarily distributed infectious period have been developed. In spite of this, the most commonly used assumption is the Exponential distribution with a fixed parameter (see Figure 1.3). This, together with exponentially distributed contact times, makes the process a continuous time Markov chain (CTMC). This explains the popularity of such models, first developed and studied in the 1950s [62, 63].

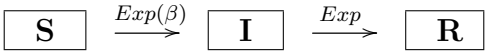

Figure 1.3. Depiction of the typical CTMC model in which contacts are modeled by a Poisson process with an exponential infectious period.

As discussed in Section 1.2, the exponential distribution offers tractable models but this assumption is often times biologically unrealistic. Models with Gamma distributed infectious period have been studied as early as 1964, when the first one appeared in [47]. More recently, such a model was analyzed and extended in [48].

A fully generalized SIR model that imposes no assumption on the infectious period was proposed as early as 1978 in [64], and was further analyzed by Ball in [65, 66]. In this framework individuals recover according to an arbitrary (non negative) random variable with distribution F, for which the first moment exists. A recursive formula for the exact probability mass function of the final size was provided by using the representation developed by Sellke in [67]. Asymptotic results involving the distribution of the final size and severity of an epidemic (area under the trajectory of infective) were also presented in [65]. Furthermore, these results were generalized to epidemics among a heterogeneous population.

1.3.1 Branching process approximation

The early stages of an epidemic is approximated by a properly defined branching process (BP). The "convergence" of the epidemic model to its associated BP has been established previously [68–70]. A less formal but more practical exposition can be found in [28, 50, 51, 71].

In particular, a simple BP can approximate the epidemic when the infectious period is exponential. If the Exponential distribution is replaced by Gamma, then a multi-type BP id used instead of a simple BP [28,50]. More generally, a Crump-Mode-

Jagers BP can be used to approximate the epidemic when the infectious period is not Exponential nor Gamma distributed. Some properties of these processes are studied in [72] (see chapter 6). A Crump-Mode-Jagers BP is generally non Markovian, while simple BP and multi-type BP are.

Figure 1.4. Depiction of an SIR stochastic model in which (i) contacts are modeled by a Poisson process and (ii) infectious period is arbitrarily distributed, according to $X \sim F$.

Let $S(t), I(t), R(t)$ represent the system depicted in Figure 1.4, with constant population size and $I(0)$ initial infectious individuals. On the other hand, let $Y(t)$ represent a Crump-Mode-Jagers BP with $I(0)$ ancestors. In this BP, each individual x has a life span λ_x while the point process $\xi_x(t)$ represents the reproduction (offsprings) of x. To approximate the number of infectious individuals $I(t)$ by $Y(t)$ we let

- $\lambda_x = X$, where X is a random variable with distribution F, and
- $\xi_x(t)$ is a poisson process with constant rate β.

Let ζ be the number of offspring produced by an individual in its entire life. Clearly ζ is equal to the poisson process ξ evaluated at X, thus $\zeta \sim \text{Poisson}(\beta X)$. In particular

$$\mathbb{P}(\zeta = k | X = x) = \frac{(\beta x)^k e^{-\beta x}}{k!} \tag{1.7}$$

It is known that either $Y(t) \to \infty$ or $Y(t) \to 0$ as $t \to \infty$. This asymptotic behavior strongly depends of the mean value of ζ. If $\mathbb{E}(\zeta) < 1$, $Y(t)$ is called *subcritical* and $\mathbb{P}\left(\lim_{t\to\infty} Y(t) = 0\right) = 1$. On the other hand, if $\mathbb{E}(\zeta) > 1$, $Y(t)$ is called *supercritical* and $\mathbb{P}\left(\lim_{t\to\infty} Y(t) = 0\right) < 1$.

Generally speaking, a threshold condition for deterministic models is well known: if $\mathcal{R}_0 < 1$ then there is no epidemic, and if $\mathcal{R}_0 > 1$ then an epidemic can occur.

On the other hand, for stochastic models, is harder to define what is meant by an "epidemic". For instance, unlike the deterministic $\hat{I}(t)$, the stochastic $I(t)$ can (and most of the times will) go up and down several times before converging to zero. This motivated the use of the BP as an approximation for stochastic epidemic processes. In the literature, the probabilities of a minor and major epidemic are defined as

$$\mathbb{P}(\text{major epidemic}) = \mathbb{P}\left(\lim_{t\to\infty} Y(t) = \infty\right), \quad \mathbb{P}(\text{minor epidemic}) = \mathbb{P}\left(\lim_{t\to\infty} Y(t) = 0\right).$$

For ease of notation, let $\mathbb{P}_0 = \mathbb{P}(\text{minor epidemic})$. Notice that, with probability one $Y(t)$ either vanishes or goes to infinity as $t \to \infty$. Therefore, $\mathbb{P}(\text{major epidemic}) = 1 - \mathbb{P}_0$. The following theorem from the theory of branching processes gives an explicit formula to compute $\mathbb{P}_0$

Theorem 1.3.1 *Let ϕ be the moment generating function of the infectious period X*

$$\phi(s) = \mathbb{E}(e^{-sX}) = \begin{cases} \displaystyle\int_0^\infty e^{-sx} f(x)dx & \text{if } X \text{ is continuous,} \\ \displaystyle\sum_{k=1}^{\infty} e^{-sk} p_{x_k} & \text{if } X \text{ is discrete,} \end{cases} \tag{1.8}$$

A major epidemic can only occur if $\mathcal{R}_0 = \beta\mathbb{E}(X) > 1$, in which case this happens with probability $1 - \mathbb{P}_0$. Moreover, $\mathbb{P}_0 = q^{I_0}$, where q is the smallest root of equation

$$\phi(\beta(1-s)) = s. \tag{1.9}$$

A complete proof (not included here) can be found in [66, 68, 72]. Intuition for equation (1.9) comes from the fact that $\mathbb{P}_0$ is the smallest root of the reproduction generating function of the BP $Y(t)$, given by

$$s \mapsto \mathbb{E}(s^\zeta) \qquad s \in [0,1]$$

The key in finding an expression for $\mathbb{E}(s^\zeta)$ is writing

$$\mathbb{P}(\zeta = k) = \mathbb{E}\left(\mathbb{E}\left(\mathbb{I}_{\{\zeta=k\}}|X\right)\right) = \mathbb{E}\left(\frac{(\beta X)^k e^{-\beta X}}{k!}\right).$$

Then, (see 6.4.4 in [73] for details)

$$\begin{aligned}\mathbb{E}(s^{\zeta}) &= \sum_{k=0}^{\infty} s^k \mathbb{P}(\zeta = k) = \sum_{k=0}^{\infty} s^k \mathbb{E}\left(\frac{(\beta X)^k e^{-\beta X}}{k!}\right) = \sum_{k=0}^{\infty} \mathbb{E}\left(\frac{(s\beta X)^k e^{-\beta X}}{k!}\right) \\ &= \mathbb{E}\left(\sum_{k=0}^{\infty} \frac{(s\beta X)^k e^{-\beta X}}{k!}\right) = \mathbb{E}\left(e^{-\beta X} \sum_{k=0}^{\infty} \frac{(s\beta X)^k}{k!}\right) = \mathbb{E}\left(e^{-\beta X} e^{s\beta X}\right) \\ &= \mathbb{E}\left(e^{-\beta(1-s)X}\right).\end{aligned}$$

A generalization of Theorem 1.3.1 is used in Section 4.2.2, Chapter 4 to compute the probability of a minor epidemic for our discrete metapopulation model.

1.3.2 The probability of a minor and major epidemic

An important feature of any BP is the so called extinction probability, i.e. the probability that the process vanishes as $t \to \infty$. This number has been widely studied and its exact value can be computed. For us, this means that it is possible to have an expression for $\mathbb{P}_0$. Theorem 1.3.1 gives a "recipe" to compute $\mathbb{P}_0$ that depends on the distribution F through its mgf ϕ, given by (1.8), and the initial number of infected $I(0)$. From basic probability theory it is known that $\varphi(s) = \phi\big(\beta(1-s)\big)$ is increasing and convex in the interval $[0, 1]$. Also, $\varphi(0) > 0$, $\varphi'(1) = \mathcal{R}_0$ and $\varphi(1) = 1$ (see Fig 1.7). If $\mathcal{R}_0 < 1$ then $s = 1$ is the only root of $\varphi(s) = s$, but if $\mathcal{R}_0 > 1$ then there exist another root, smaller than one. Due to the geometric properties of φ, the iteration method is a perfect candidate to numerically find this root.

Once the parameters β and $\mathbb{E}(X)$ have been chosen, $\mathcal{R}_0$ and $\mathbb{P}_0$ can be computed. If $\mathcal{R}_0 < 1$ then $\mathbb{P}_0 = 1$, but if $\mathcal{R}_0 > 1$ then the value of $\mathbb{P}_0$ depends on the distribution chosen for X. Although possible, it is unlikely that different distributions will produce the same $\mathbb{P}_0$. To investigate how the choice of the distribution F may affect the value of $\mathbb{P}_0$, we compare several models with different distributions F. We consider two models to be *comparable* if they have the same parameters β and $\mathbb{E}(X)$, and thus the same $\mathcal{R}_0$.

Four examples of comparable models are considered bellow. Then, assuming that $\mathcal{R}_0 > 1$, the q value produced for each model, see equation (1.9), are computed. Let q be denoted by $q^{(E)}$, $q^{(G,k)}$, $\underline{q}$ and $q^{(p)}$ in examples **A**–**D**, respectively.

A. $X \sim$ Exponential(γ). In this case, $\mathbb{E}(X) = 1/\gamma$, $\mathcal{R}_0 = \beta/\gamma$, $\phi(s) = \frac{\gamma}{\gamma+s}$ and

$$q^{(E)} = \frac{1}{\mathcal{R}_0}.$$

B. $X \sim$ Gamma($k, k\gamma$). In this case, $\mathbb{E}(X) = 1/\gamma$, $\mathcal{R}_0 = \beta/\gamma$, $\phi(s) = \left(\frac{k\gamma}{k\gamma+s}\right)^k$, and $q^{(G,k)}$ is the smallest root of

$$\frac{1}{\left(1 + \mathcal{R}_0 \frac{1-s}{k}\right)^k} = s, \qquad s \in [0,1].$$

C. $X = 1/\gamma$, i.e. fixed duration. In this case $\mathbb{E}(X) = 1/\gamma$, $\mathcal{R}_0 = \beta/\gamma$, $\phi(s) = e^{-s/\gamma}$ and $\underline{q}$ is the smallest root of the equation

$$e^{-\mathcal{R}_0(1-s)} = s, \qquad s \in [0,1].$$

D. X is discrete with finitely many points and mass function equal to

$$\mathbb{P}(X = x) = \begin{cases} p_k & \text{if } x = x_k, \quad k = 1, 2, \cdots, n \\ 0 & \text{otherwise} \end{cases}$$

Then, from equation (1.8), $\phi(s) = \sum_{k=1}^{n} p_k e^{-s x_k}$, $\phi(\beta(1-s)) = \sum_{k=1}^{n} p_k e^{-\beta(1-s)x_k}$ and q is the smallest root of

$$\sum_{k=1}^{n} p_k e^{-\beta(1-s)x_k} = s, \qquad s \in [0,1]. \tag{1.10}$$

For instance, case **D** represents empiric data, in which case typically $x_k = k$; p_k is equal to the proportion of people who recover after k units of time; and

$$\phi\big(\beta(1-s)\big) = \sum_{k=1}^{n} p_k e^{-\beta(1-s)k}.$$

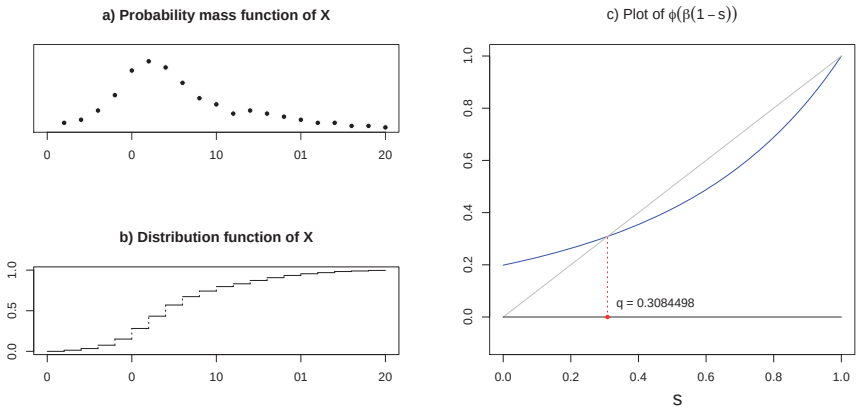

Figure 1.5. Example of X with finite support (**D**) and parameters $\mathcal{R}_0 = 1.946735,\ \beta = 0.25,\ \mathbb{E}(X) = 7.786942$

Figures 1.5 and 1.6 present a "fictitious" examples in which X could be empiric data. Figures 1.5a) and 1.6a) show the probability mass function $\mathbb{P}(X = k)$, while 1.5b) and 1.6b) are plots of the cumulative function $\mathbb{P}(X \leqslant k)$. Notice that the infectious period, X in Figure 1.6 is bimodal. Such X would be extremely difficult to model if we restrict to commonly used families of distributions. In particular, Exponential and Gamma distributions are a terrible fit for a distribution like this.

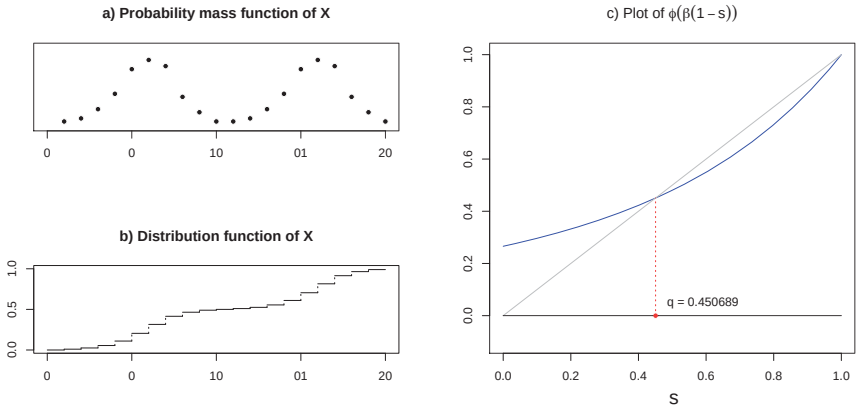

Figure 1.6. Example of bimodal X with finite support (**D**) and $\mathcal{R}_0 = 1.623,\ \beta = 0.15,\ \mathbb{E}(X) = 10.82$

The four examples above illustrate how different the probability of no epidemic can be, even when the models are comparable. The relationship between $q^{(E)}$, $q^{(G,k)}$ and $\underline{q}$ has been studied before, see for example [48]. It is known that if $\mathcal{R}_0 > 1$, then $\forall\ k \geqslant 2$, $k \in \mathbb{Z}$ we have

$$\underline{q} < q^{(G,k+1)} < q^{(G,k)} < q^{(E)} < 1 \qquad \text{and} \qquad \lim_{k\to\infty} q^{(G,k)} = \underline{q}.$$

Figure 1.7 suggest that $\underline{q}$ may be the smallest possible value for q among other comparable models. The following result proves this conjecture.

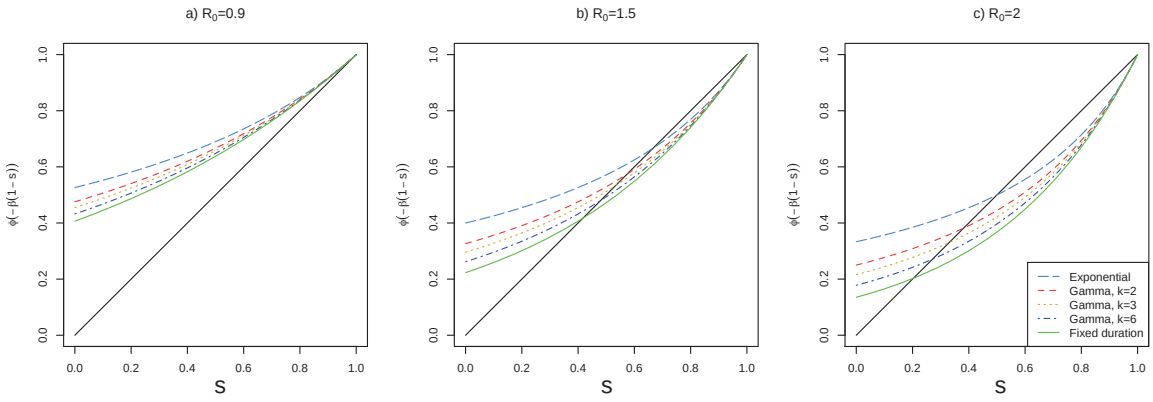

Figure 1.7. Graphic of $\phi\big(-\beta(1-s)\big)$ for comparable models **A**–**C** with: a) $\mathcal{R}_0 = 0.9$, b) $\mathcal{R}_0 = 1.5$ and c) $\mathcal{R}_0 = 2$.

Theorem 1.3.2 *If $\mathcal{R}_0 > 1$ then the model in which X is constant (fixed duration) predicts the smallest probability of minor epidemic.*

Proof Let $\underline{X}$ be the constant m and X be any arbitrary comparable infectious period. This is, $\mathbb{E}(\underline{X}) = \mathbb{E}(X) = m$. Denote by ϕ and $\underline{\phi}(s) = e^{-sm}$ the mgf of X and $\underline{X}$, respectively. Let $\underline{q}, q \in (0,1)$ be the smallest root of $\underline{\phi}\big(\beta(1-s)\big) = s$ and $\phi\big(\beta(1-s)\big) = s$. Apply Jensen's inequality to the convex function $x \mapsto e^{-sx}$ to obtain

$$e^{-s\mathbb{E}(X)} \leqslant \mathbb{E}(e^{-sX}) \qquad \Rightarrow \qquad \underline{\phi}(s) \leqslant \phi(t).$$

This, implies that $\underline{q} \leqslant \phi(\beta(1-\underline{q}))$ and $q \geqslant \underline{\phi}(\beta(1-q))$. Let $\varphi(s) = \underline{\phi}(\beta(1-s)) - s = e^{-\mathcal{R}_0(1-s)} - s$, clearly f is continuous and strictly convex. Since $\varphi(0)\varphi(q) \leqslant 0$, f must vanish at some $s' \in (0, q]$. Finally, since $\underline{q}$ is the smallest zero of f, it follows that $\underline{q} \leqslant q$. ■

Theorem 1.3.2 gives a lower bound for the value of q. It turns out it is also possible to find an upper bound, as shown in the following result

Theorem 1.3.3 *Consider all comparable models for which $\mathbb{E}(X) = m$ (thus $\mathcal{R}_0 = \beta m$) and $Var(X) \leqslant \sigma^2$. The probability of a minor epidemic is bounded above by $\bar{q}$, the smallest root of*

$$\bar{\phi}(s) = \frac{\sigma^2}{m^2+\sigma^2} + \frac{m^2}{m^2+\sigma^2} e^{-\beta(1-s)\frac{m^2+\sigma^2}{m}} = s, \qquad s \in [0,1].$$

This upper bound is attained when the infectious period $\bar{X}$ is the two point r.v.

$$\bar{X} = \begin{cases} 0 & \text{with probability } \frac{\sigma^2}{m^2+\sigma^2}, \\ \frac{m^2+\sigma^2}{m} & \text{with probability } \frac{m^2}{m^2+\sigma^2}. \end{cases}$$

The proof of this theorem, based on a result in [74], is not included here because of the similarities with the proof of Theorem 4.3.3. See details at the end of Section 4.3.2.

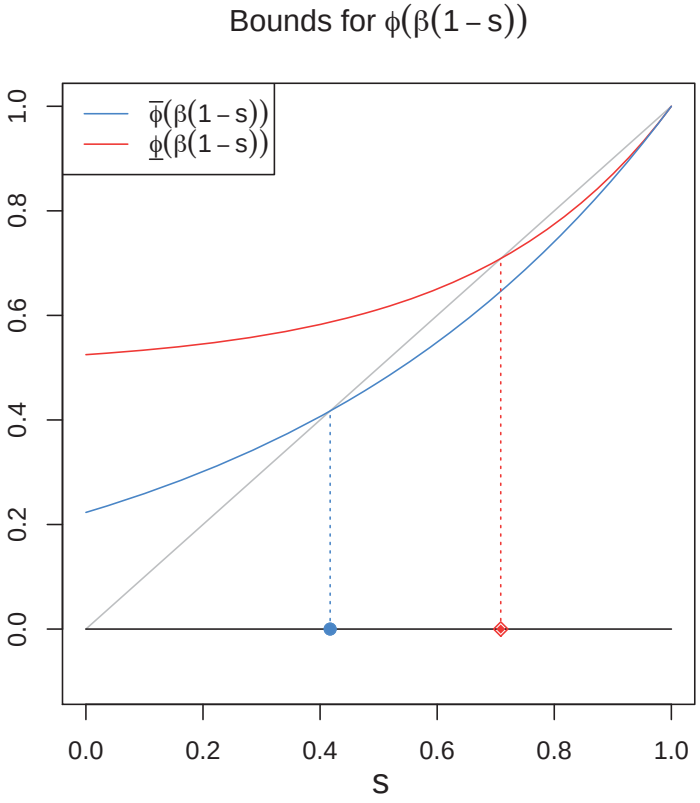

Figure 1.8. Upper and lower bounds for $\phi\big(\beta(1-s)\big)$ as given by Theorems 1.3.2 and 1.3.3. The points • and ◆ contain all possible values for q for comparable models with $\beta = 0.1875$, $\mathcal{R}_0 = 1.5$ and $\mathrm{Var}(X) \leqslant 64$.

2. DISCRETE EPIDEMIC MODELS WITH ARBITRARILY DISTRIBUTED INFECTIOUS PERIOD

The work presented in this chapter was done in collaboration with Feng and van den Driessche. Most of the results and ideas in this chapter were published in the Journal of Difference Equations and Applications [57]. My contribution includes model formulation and analysis as well as the writing of the manuscript. All models considered in this chapter are deterministic and for discrete-time.

2.1 Introduction

In this chapter several SEIR-type of models are introduced and analyzed. We begin by presenting models without control (Sections 2.2 and 2.3) and finish by analyzing a model with a control measure (isolation). The focus of this chapter is on the development of a general framework for formulating and analyzing discrete-time models that allow for the inclusion of *arbitrarily distributed* waiting times.

It is known that the 2.14 property (see equations (1.6) and (2.14)) of the Geometric distribution (an analogue property of the exponential distribution in continuous-time models) may generate biased and possibly misleading evaluations on disease control strategies; see, e.g., [21, 43]. It is also known that less dispersed distributed stages seem to be more appropriate for modeling diseases with longer latent and infectious periods [45, 54–56, 59], see Section 1.2 for a discussion along these lines.

With this is mind, in Section 2.2.2 a model that uses a shifted negative binomial distribution for the infectious period is presented. In Section 2.2.3, we fully generalized the model so that *any* discrete distribution with support in $\{1, 2, 3, \ldots, M\}$ can be used to model the infectious period. At this level of generality, the model is modified to include two strains (Section 2.3.1) or heterosexual transmission (Section

2.3.2). Finally, in Section 2.4, we consider a model with disease control in the form of isolation/hospitalization of infectious individuals. In all models demographic processes, such as birth and death, are ignored and the total population size is assumed to be the constant N.

In order to bring into the context of epidemiological applications, $\mathcal{R}_0$ and $\mathcal{R}_C$ are computed and interpreted. When Geometric distribution is assumed, the next generation matrix approach is straightforward to apply, but when another distribution is used this is no longer the case. In this chapter we explore different ways to modify this approach under those circumstances and show that our formulas are consistent with those obtained from biological considerations.

Throughout these ideas can be extrapolated to allow an arbitrary distribution of the latent period as well, but in this chapter we focus on the infectious period only. In Chapter 3 a model with arbitrary distribution for latent, infectious, quarantine and isolation periods is considered.

2.2 SIER models with various distributions and computation of $\mathcal{R}_0$

In this section SEIR-type of models with several distributions for the infectious period are considered, including the case of a general distribution. All distributions are assumed to have the same mean to allow for the comparison of model results. The outcomes of these models are compared in terms of the reproduction number $\mathcal{R}_0$ (or $\mathcal{R}_C$) or final epidemic size.

2.2.1 A simple SEIR model with Geometric distribution

We begin by presenting a standard SEIR model inspired by the work of Brauer et al in [39]. The distribution used to model the latent and infectious stages is Geometric, which is equivalent to assuming that individuals exit a stage with a constant probability at each time step. This assumption is commonly encounter throughout the literature, as it makes the model easier to formulate and analyze.

Table 2.1.
List of parameters and symbols commonly used in Chapter 2

Symbols	**Definitions**
β	Transmission parameter
β_i	Stage dependent transmission parameter
α	Exit probability of E class, $\alpha \in (0,1)$
γ	Exit probability of I class, $\gamma \in (0,1)$, Geometric model (2.1)
ϕ, ϕ_i	Exit probability of I subclasses, $\phi, \phi_i \in (0,1)$, sNB model (2.6), (2.9)
ρ	Reduction factor of H class (Section 2.4)
Y	Length of the infectious period
Y_w	Length of the infectious period, strain
	$(w = s, r)$ or sex $(w = f, m)$ dependent
W	Age since infection at which an individual is isolated
f_i	Probability mass function of Y
p_i	Survival function of Y
$p_{w,i}$	Survival function Y_w, $w = s, r$ (strain) or $w = f, m$ (sex)
q_i	Survival function of W

In the equations bellow S_n, E_n, I_n and R_n represent the number of susceptible, exposed, infected and recovered at time $n \in \{0, 1, 2, \dots\}$. A complete list of symbols and parameters can be found in Table 3.2.

$$\begin{aligned} S_{n+1} &= S_n G(I_n), \qquad G(I_n) = e^{-\beta I_n/N} \\ E_{n+1} &= S_n[1 - G(I_n)] + (1-\alpha)E_n \\ I_{n+1} &= \alpha E_n + (1-\gamma)I_n \\ R_{n+1} &= R_n + \gamma I_n, \qquad n = 1, 2, \dots \end{aligned} \tag{2.1}$$

Notice that, since the total population is constant, the last compartment can be dropped from the system. In the future, an equation for R will not be included since

we could easily let $R_n = N - S_n - E_n - I_n$. A transition diagram for this model is shown in Figure 2.1.

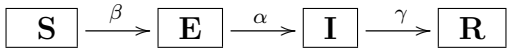

Figure 2.1. Disease transmission diagram for model (2.1). The constant exit probabilities from E and I are α and γ, respectively.

The survival probability of a susceptible individual from being infected, per unit of time, given the per capita infection rate is given by $G(I_n) = e^{-\beta I_n/N}$. See equation (1.2) in Chapter 1, Section 1.1 for details.

Under constant exit probability, the proportion of individuals leaving the I class after exactly i days is $f_i = (1-\gamma)^{i-1}\gamma$ for $i \in \{1, 2, 3, \dots\}$, this is known as the probability mass function. The proportion of individuals who stay *more* that i days in the I class, also called survival probability, is

$$p_i = \sum_{k=i+1}^{\infty} (1-\gamma)^{k-1}\gamma = (1-\gamma)^i, \qquad i \in \{0, 1, 2 \cdots\} \tag{2.2}$$

This is, under constant exit probability the number of days spent in the I compartment follows a Geometric distribution with parameter γ. Figure 2.2.1 depicts the Geometric mass and survival functions corresponding to different parameter values γ. The average time spent in the I class is

$$\frac{1}{\gamma} = \sum_{k=1}^{\infty} i f_i = \sum_{k=0}^{\infty} p_i \tag{2.3}$$

For the computation of $\mathcal{R}_0$, we adopt the method described in [17] (see Chapter 1 Section 1.1.1). To use the approach of next-generation matrix, the disease stages (S, E and I) at time $n+1$ must be written in the form

$$[\ E_{n+1},\ I_{n+1},\ S_{n+1}\ ]^T = \mathcal{M}[\ E_n,\ I_n,\ S_n\ ]^T,$$

Then, F (the matrix associated with new infections) and T (the matrix associated with other transitions) are calculated on the infected variables only evaluated at the

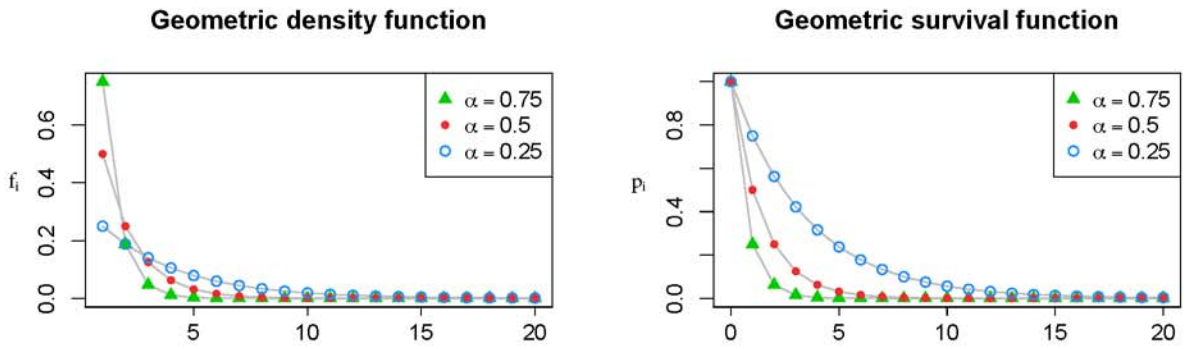

Figure 2.2. Plots of the mass (left) and the survival (right) probability functions of a geometric distribution.

disease-free equilibrium, and the Jacobian on these variables is $F + T$, which is an irreducible matrix. Moreover,

$$\mathcal{R}_0 = \varrho\left(F(I-T)^{-1}\right). \tag{2.4}$$

Under suitable assumptions (see Theorem 1.1.1 in Chapter 1) the reproduction number $\mathcal{R}_0$ gives relevant threshold information about the model. If $\mathcal{R}_0 < 1$, then the disease-free equilibrium (DFE) is locally asymptotically stable; whereas if $\mathcal{R}_0 > 1$, it is unstable.

For the system (2.1), the Jacobian matrix evaluated at the DFE $(E, I, S) = (0, 0, N)$ is given by

$$\begin{bmatrix} 1-\alpha & \beta & 0 \\ \alpha & 1-\gamma & 0 \\ 0 & -\beta & 1 \end{bmatrix}.$$

Then, the matrices associated with new infections and transitions are

$$F = \begin{bmatrix} 0 & \beta \\ 0 & 0 \end{bmatrix} \qquad \text{and} \qquad T = \begin{bmatrix} 1-\alpha & 0 \\ \alpha & 1-\gamma \end{bmatrix},$$

respectively. See that $\varrho(T) = \max\{1-\alpha, 1-\gamma\} < 1$, and

$$(I-T)^{-1} = \begin{bmatrix} \alpha & 0 \\ -\alpha & \gamma \end{bmatrix}^{-1} = \begin{bmatrix} 1/\alpha & 0 \\ 1/\gamma & 1/\gamma \end{bmatrix} \quad \Rightarrow \quad F(I-T)^{-1} = \begin{bmatrix} \frac{\beta}{\gamma} & \frac{\beta}{\gamma} \\ 0 & 0 \end{bmatrix}.$$

Finally,

$$\mathcal{R}_0 = \varrho\left(F(I-T)^{-1}\right) = \frac{\beta}{\gamma}, \tag{2.5}$$

Notice that $\mathcal{R}_0$ is the product of the average number of secondary infections produced per day (β) and the mean infectious period ($1/\gamma$). Since latent individuals do not transmit disease, the latent period plays no role in the final expression of the reproduction number. Because of this, Geometric distribution was used to model the latent period (E class), and focus only on the distribution of the infectious period (transition from I to R).

2.2.2 The case of negative binomial distribution

For continuous-time models, the Gamma distribution is usually considered to be more appropriate to model the infectious period than the Exponential distribution. In fact, the latter is a special case of the former, obtained when the shape parameter is equal to one. A discrete equivalent of the above relation occurs with the Geometric and the shifted Negative Binomial distribution (sNB).

The "linear chain trick" used in continuous time models consists in breaking the infectious class I into subclasses $I^{(k)}$ (see, for example, [42–46, 71]). This relies on the fact that a Gamma is the sum of iid Exponential random variables. Such ideas can also be applied to our discrete mode, so that the I class is separated into k different sub-stages. The idea behind this is to recover the infectious period as a sum of k geometric distributions. The transition diagram for this modified model is given in Figure 2.3. $I^{(i)}$ represents the i^{th} sub-stage corresponding to the i^{th} geometric distribution in the sNB distribution. Individuals in the infectious classes can progress with probability ϕ or satay with probability $1-\phi$. For this model, it is shown that

the structure of $\mathcal{R}_0$ remains the same, although the formula for the mean infectious period can be different.

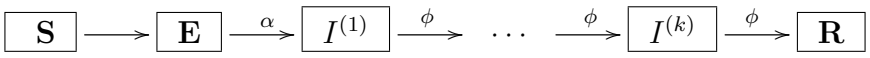

Figure 2.3. A transition diagram for a model with infectious subclasses. With this structure the infectious period follows a sNB. The superscript i represents the i^{th} geometric sub-stage for the negative binomial distribution.

The system

$$\begin{aligned} S_{n+1} &= S_n e^{-\beta[I_n^{(1)} + \cdots + I_n^{(k)}]/N} \\ E_{n+1} &= S_n \left[1 - e^{-\beta[I_n^{(1)} + \cdots + I_n^{(k)}]/N}\right] + (1-\alpha)E_n \\ I_{n+1}^{(1)} &= \alpha E_n + (1-\phi)I_n^{(1)} \\ I_{n+1}^{(j)} &= \phi I_n^{(j-1)} + (1-\phi)I_n^{(j)}, \qquad 2 \leqslant j \leqslant k \end{aligned} \tag{2.6}$$

corresponds to the transition diagram depicted in Figure 2.3. At any given time the exit probability of the class $I^{(i)}$ is ϕ, this restriction is relaxed at the end of this section.

The proportion of population spending exactly i days in the infectious compartments is equal to $f_i = \mathbb{P}(X_1 + \cdots + X_k = i)$, where $X_j \sim \text{Geom}(\phi)$. From basic probability theory [75–77]

$$f_i = \binom{i-1}{i-k} \phi^k (1-\phi)^{i-k}, \qquad i = k, k+1, k+2, \ldots \tag{2.7}$$

See that, an infected individual spends at least k days in the infectious classes (one day per subclass), which explains the ϕ^k factor above. The factor $(1-\phi)^{i-k}$ accounts for the remaining $i-k$ "stay days". Finally, there are $\binom{i-1}{i-k}$ ways to distribute this event. The distribution given in (2.7) corresponds to a shifted Negative Binomial (sNB) with parameters (k, ϕ) and support on $\{k, k+1, \ldots\}$. When $k = 1$ and $\gamma = \phi$ this distribution corresponds to a Geometric with parameter γ. The mean infectious

period with a sNB(k, ϕ) distribution is k/ϕ. Plots of the probability density and survival function for this distribution are presented in Figure 2.4.

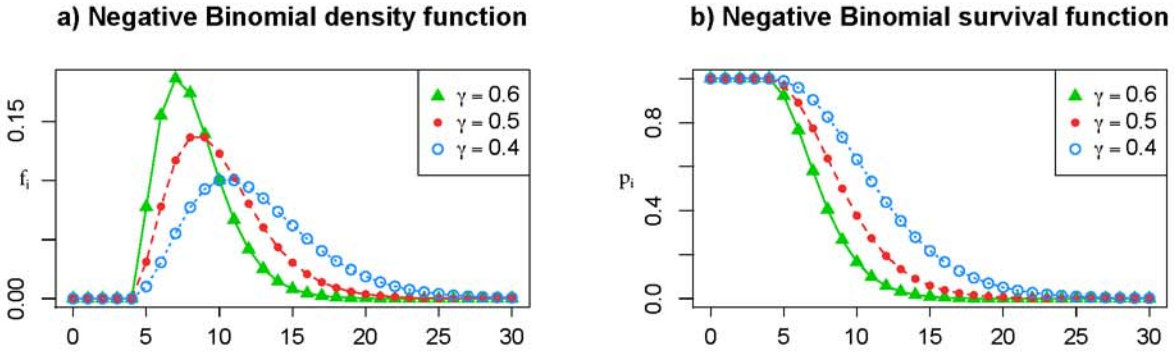

Figure 2.4. Plots of the probability density and survival function of a sNB distribution, described by (2.7), for different values of ϕ and $k = 5$.

For the computation of $\mathcal{R}_0$, note that the $(k+1) \times (k+1)$ infection matrix F and the transition matrix T matrix are given by

$$F = \begin{bmatrix} 0 & \beta & \cdots & \beta & \beta \\ 0 & 0 & \cdots & 0 & 0 \\ 0 & 0 & \cdots & 0 & 0 \\ \vdots & \vdots & & \vdots & \vdots \\ 0 & 0 & \cdots & 0 & 0 \end{bmatrix} \quad \text{and} \quad T = \begin{bmatrix} 1-\alpha & 0 & 0 & \cdots & 0 & 0 \\ \alpha & 1-\phi & 0 & \cdots & 0 & 0 \\ 0 & \phi & 1-\phi & \cdots & 0 & 0 \\ \vdots & \vdots & \vdots & & \vdots & \vdots \\ 0 & 0 & 0 & \cdots & \phi & 1-\phi \end{bmatrix}.$$

Then

$$(I-T)^{-1} = \begin{bmatrix} \frac{1}{\alpha} & 0 & \cdots & 0 & 0 \\ 1/\phi & 1/\phi & \cdots & 0 & 0 \\ \vdots & \vdots & & \vdots & \vdots \\ 1/\phi & 1/\phi & \cdots & 1/\phi & 1/\phi \end{bmatrix} \Rightarrow F(I-T)^{-1} = \begin{bmatrix} \frac{k\beta}{\phi} & \frac{k\beta}{\phi} & \frac{(k-1)\beta}{\phi} & \cdots & \frac{\beta}{\phi} \\ 0 & 0 & 0 & \cdots & 0 \\ \vdots & \vdots & \vdots & & \vdots \\ 0 & 0 & 0 & \cdots & 0 \end{bmatrix}.$$

Thus, the reproduction number is

$$\mathcal{R}_0 = \varrho(F(I-T)^{-1}) = \beta\frac{k}{\phi}, \tag{2.8}$$

once again, the average number of infections per day times the mean infectious period.

Stage dependent transmission and exit probability

If epidemiological data suggest that either the exit probabilities or transmission parameters are stage dependent, the model (2.6) can easily be modified to include this dependance. The system

$$\begin{aligned} S_{n+1} &= S_n e^{-[\beta_1 I_n^{(1)} + \cdots + \beta_n I_n^{(k)}]/N} \\ E_{n+1} &= S_n \left[1 - e^{-[\beta_1 I_n^{(1)} + \cdots + \beta_n I_n^{(k)}]/N}\right] + (1-\alpha)E_n \\ I_{n+1}^{(1)} &= \alpha E_n + (1-\phi_1) I_n^{(1)} \\ I_{n+1}^{(j)} &= \phi_{j-1} I_n^{(j-1)} + (1-\phi_j) I_n^{(j)}, \qquad 2 \leqslant j \leqslant k \end{aligned} \tag{2.9}$$

incorporate this features. The infectious period however is no longer a sNB but a more "general sum" of geometric distributions with different parameters ϕ_i.

The $(k+1) \times (k+1)$ new infection matrix F and the transition matrix T matrix are given by

$$F = \begin{bmatrix} 0 & \beta_1 & \cdots & \beta_{k-1} & \beta_k \\ 0 & 0 & \cdots & 0 & 0 \\ \vdots & \vdots & & \vdots & \vdots \\ 0 & 0 & \cdots & 0 & 0 \end{bmatrix} \quad \text{and} \quad T = \begin{bmatrix} 1-\alpha & 0 & 0 & \cdots & 0 & 0 \\ \alpha & 1-\phi_1 & 0 & \cdots & 0 & 0 \\ 0 & \phi_1 & 1-\phi_2 & \cdots & 0 & 0 \\ 0 & 0 & \phi_2 & \cdots & 0 & 0 \\ \vdots & \vdots & \vdots & & \vdots & \vdots \\ 0 & 0 & 0 & \cdots & \phi_{k-1} & 1-\phi_k \end{bmatrix}.$$

Simple calculations yield

$$\mathcal{R}_0 = \sum_{i=1}^{k} \frac{\beta_i}{\phi_i}. \tag{2.10}$$

If $\beta_i = \beta$ and $\phi_i = \phi$, then equation (2.10) reduces to (2.8).

2.2.3 A general model with arbitrary distribution

In this section we develop a discrete $SEIR$ model with arbitrarily distributed infectious period and compute $\mathcal{R}_0$ using the next generation matrix approach. Several

models of this nature have been developed and analyzed in a continuous time framework (see for example [43]). These models however, are rather complex even without control measures like isolation or hospitalization, involving a set of integral-differential equations

$$\begin{aligned} S' &= -\tfrac{\beta}{N} SI \\ E' &= \tfrac{\beta}{N} SI - \alpha E \\ I(t) &= \int_0^t \alpha E(s) P(t-s) ds \end{aligned}$$

The discrete counterpart of the model above is much simpler, easy to understand and interpret, giving it an edge over continuous-time models. If we take under consideration the fact that data is collected at most daily, we see that discrete models offer an advantage for biologists and public health researchers.

Consider an arbitrary discrete distribution on $\mathbb{N}$ with compact support. In other words, if Y represents the length of the infectious period of and average individual in the population, let

$$f_i = \mathbb{P}(Y = i) \quad \text{and} \quad p_i = \mathbb{P}(Y > i), \qquad i \in \{1, 2, \ldots, M\}.$$

By definition $f_i \in [0,1]$, $p_0 = 1$, $p_M = 0$, $\sum_{i=1}^{M} f_i = 1$ and $p_i = \sum_{k=i+1}^{\infty} f_i = \sum_{k=i+1}^{M} f_i$. The mean infectious period is given by

$$\mathbb{E}(Y) = \sum_{i=1}^{M} i f_i = \sum_{i=0}^{M} p_i = \sum_{i=0}^{M-1} p_i \tag{2.11}$$

The discrete-time model with survival function $\{p_i\}$ for the infectious period, depicted in Figure 2.5 is given by the set of difference equations

$$\begin{aligned} S_{n+1} &= S_n e^{-\frac{\beta}{N} I_n}, \\ E_{n+1} &= S_n (1 - e^{-\frac{\beta}{N} I_n}) + (1-\alpha) E_n \\ I_{n+1} &= i_{n+1} + i_n p_1 + \cdots + i_1 p_n, \qquad i_k = \alpha E_{k-1} \end{aligned} \tag{2.12}$$

with initial conditions $S_0 = N - E_0$, $E_0 > 0$, $I_0 = 0$. Here, i_k is the input to the I class at time k and $i_{n+1-j} p_j$ is the number of individuals who entered the I class j

time units ago and are still in I at time $n+1$. The biological interpretation of the reproduction number $\mathcal{R}_0$ leads once again to the formula

$$\mathcal{R}_0 = \beta \mathbb{E}(Y). \tag{2.13}$$

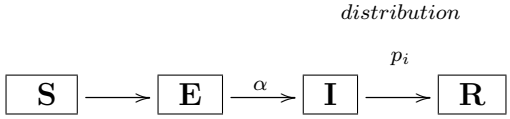

Figure 2.5. Disease transmission diagram with an arbitrarily distributed infectious period.

Computing $\mathcal{R}_0$ using the next generation matrix approach for this system presents some challenges since, without the memoryless property

$$\mathbb{P}(Y > n+m | Y > m) = \mathbb{P}(Y > n) \tag{2.14}$$

of the geometric distribution, it is necessary to keep track of the past in order to know the values at the present. Since the disease stages S, E and I, at time $n+1$ cannot be written in the form

$$[\ E_{n+1},\ I_{n+1},\ S_{n+1}\ ]^T = \mathcal{M}\left([\ E_n,\ I_n,\ S_n\ ]^T\right), \quad \mathcal{M} : \mathbb{R}^3 \to \mathbb{R}^3$$

it is impossible to use the next-generation matrix method directly, see Chapter 1 Section 1.1.1 . To overcome this difficulty we can consider multiple I stages, an approach similar to the "linear chain trick". To the best of our knowledge, this technique has not been used in discrete models.

Since I_n in (2.12) depends on other variables besides I_n and E_n, the subclasses $I^{(1)}, \ldots, I^{(M)}$ are introduced, see Figure 2.6. The superscript i corresponds to the age-since-infection. Notice that these subclasses are different from those in the sNB model (2.6) and (2.9), because an individual can only stay in $I^{(i)}$ for *one* unit of time, and must either progress to $I^{(i+1)}$ or recover.

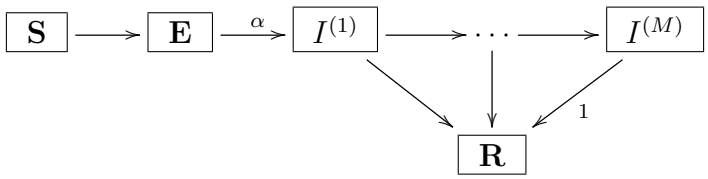

Figure 2.6. A transition diagram for a model with arbitrarily distributed infectious period. The superscript i in $I^{(i)}$ represents age since infection.

An equivalent system for (2.12) is given by

$$\begin{aligned} S_{n+1} &= S_n e^{-\beta(I_n^{(1)}+\cdots+I_n^{(M)})/N}. \\ E_{n+1} &= S_n\left[1-e^{-\beta(I_n^{(1)}+\cdots+I_n^{(M)})/N}\right]+(1-\alpha)E_n \\ I_{n+1}^{(1)} &= \alpha E_n, \qquad I_{n+1}^{(2)} = p_1 I_n^{(1)} \\ I_{n+1}^{(j)} &= \frac{p_{j-1}}{p_{j-2}} I_n^{(j-1)}, \qquad 3 \leqslant j \leqslant M \end{aligned} \tag{2.15}$$

Notice that the transition probability from the $(j-1)^{th}$ class to the j^{th} class is given by the probability that an infectious individual is still infectious j time units after acquiring the disease ($\mathbb{P}(Y > j-1) = p_{j-1}$) given that the person remained infectious $j-1$ time units ago, ($\mathbb{P}(Y > j-2) = p_{j-2}$). Thus, the proportion of individuals in the $(j-1)^{th}$ class that progress to j^{th} class is p_{j-1}/p_{j-2}, while the remaining proportion, $(1-p_{j-1}/p_{j-2})$, go to the R compartment. A disease diagram for (2.15) is depicted in Figure 2.6.

The computation of $\mathcal{R}_0$ in this case is more challenging. Although the next generation matrix method cannot be applied to the system (2.12), it can be used to compute $\mathcal{R}_0$ for the system (2.15). The $(M+1)\times(M+1)$ matrices F and T are

$$F = \begin{bmatrix} 0 & \beta & \cdots & \beta \\ 0 & 0 & \cdots & 0 \\ \vdots & \vdots & & \vdots \\ 0 & 0 & \cdots & 0 \end{bmatrix} \qquad \text{and} \qquad T = \begin{bmatrix} 1-\alpha & 0 & 0 & \cdots & 0 & 0 \\ \alpha & 0 & 0 & \cdots & 0 & 0 \\ 0 & p_1 & 0 & \cdots & 0 & 0 \\ 0 & 0 & \frac{p_2}{p_1} & \cdots & 0 & 0 \\ \vdots & \vdots & \vdots & & \vdots & \vdots \\ 0 & 0 & 0 & \cdots & \frac{p_{M-1}}{p_{M-2}} & 0 \end{bmatrix}.$$

Thus,

$$F(I-T)^{-1} = \begin{bmatrix} \beta \sum_{i=1}^{M} \beta_i p_{i-1} & \beta \sum_{i=1}^{M} p_{i-1} & \cdots & \beta \\ 0 & 0 & \cdots & 0 \\ \vdots & \vdots & & \vdots \\ 0 & 0 & \cdots & 0 \end{bmatrix}.$$

Therefore

$$\mathcal{R}_0 = \varrho(F(I-T)^{-1}) = \beta \sum_{i=1}^{M} p_{i-1} = \beta \mathbb{E}(Y) \tag{2.16}$$

which is consistent with the formula given in (2.13).

Stage dependent transmission

Just like in the second part of Section 2.2.2, transmission parameters can depend on age since infection. Let β_i be the transmission parameter for the substage $I^{(i)}$. In this case (2.15) becomes

$$\begin{aligned} S_{n+1} &= S_n e^{-(\beta_1 I_n^{(1)} + \cdots + \beta_n I_n^{(M)})/N}. \\ E_{n+1} &= S_n \left[1 - e^{-(\beta_1 I_n^{(1)} + \cdots + \beta_n I_n^{(M)})/N}\right] + (1-\alpha) E_n \\ I_{n+1}^{(1)} &= \alpha E_n, \qquad I_{n+1}^{(2)} = p_1 I_n^{(1)} \\ I_{n+1}^{(j)} &= \tfrac{p_{j-1}}{p_{j-2}} I_n^{(j-1)}, \qquad 3 \leqslant j \leqslant M \end{aligned} \tag{2.17}$$

In this case,

$$F = \begin{bmatrix} 0 & \beta_1 & \beta_2 & \cdots & \beta_M \\ 0 & 0 & 0 & \cdots & 0 \\ \vdots & \vdots & \vdots & & \vdots \\ 0 & 0 & 0 & \cdots & 0 \end{bmatrix} \qquad \text{and} \qquad T = \begin{bmatrix} 1-\alpha & 0 & 0 & \cdots & 0 & 0 \\ \alpha & 0 & 0 & \cdots & 0 & 0 \\ 0 & p_1 & 0 & \cdots & 0 & 0 \\ 0 & 0 & \frac{p_2}{p_1} & \cdots & 0 & 0 \\ \vdots & \vdots & \vdots & & \vdots & \vdots \\ 0 & 0 & 0 & \cdots & \frac{p_{M-1}}{p_{M-2}} & 0 \end{bmatrix}.$$

Therefore,

$$F(I-T)^{-1} = \begin{bmatrix} \sum_{i=1}^{M} \beta_i p_{i-1} & \sum_{i=1}^{M} \beta_i p_{i-1} & \cdots & \beta_M \\ 0 & 0 & \cdots & 0 \\ \vdots & \vdots & & \vdots \\ 0 & 0 & \cdots & 0 \end{bmatrix}$$

and

$$\mathcal{R}_0 = \varrho(F(I-T)^{-1}) = \sum_{i=1}^{M} \beta_i p_{i-1}. \tag{2.18}$$

If $\beta_i = \beta$, then formula (2.18) reduces to (2.16).

To interpret (2.18), recall that that for a given function h

$$\sum_{m=1}^{M} \mathbb{P}(Y=m)h(m) = \mathbb{E}[h(Y)].$$

This follows from the definition of expectation and the fact that Y has an upper bound M. In particular, let $h(m) = \sum_{i=1}^{m} \beta_i$, to obtain

$$\begin{aligned} \mathcal{R}_0 &= \sum_{i=0}^{M-1} \beta_{i+1} p_i = \sum_{i=0}^{M-1} \beta_{i+1} \sum_{m=i+1}^{M} \mathbb{P}(Y=m) = \sum_{i=0}^{M-1} \sum_{m=i+1}^{M} \beta_{i+1} \mathbb{P}(Y=m) \\ &= \sum_{m=1}^{M} \sum_{i=0}^{m-1} \beta_{i+1} \mathbb{P}(Y=m) = \sum_{m=1}^{M} \left[\mathbb{P}(Y=m) \sum_{i=1}^{m} \beta_i \right] = \mathbb{E}\left(\sum_{i=1}^{Y} \beta_i \right). \end{aligned}$$

In plane words, $\mathcal{R}_0$ is the average of adding the transmission parameters for as long as the individual is infectious.

2.3 Models with more complexities and computation of $\mathcal{R}_0$

For the models considered in the previous section, the computation of $\mathcal{R}_0$ is relatively easier due to the fact that the next generation matrix has rank 1. When models involve more complexities, the next generation matrix may have rank greater than 1. a couple of such examples are presented in this section.

2.3.1 A two-strain pathogen model

Building from the equivalent models (2.12) and (2.15), we now consider two parasite strains (e.g., drug-sensitive and drug-resistant strains) that compete for a single susceptible population. Assume that the infectious periods for both strains follow arbitrary discrete (bounded) distributions denoted by Y_s and Y_r, respectively. Here the subscript s stands for the sensitive strain and the subscript r stands for resistant strain. Suppose that M_w for $w = s, r$ are the maximum length of the infectious period Y_w. Let

$$p_{s,i} = \mathbb{P}(Y_s > i) \qquad \text{and} \qquad p_{r,i} = \mathbb{P}(Y_r > i).$$

The model equations under this circumstances are

$$\begin{aligned}
S_{n+1} &= S_n e^{-\left[\sum_{i=1}^{M_s}\beta_{s,i}I_{s,n}^{(i)} + \sum_{i=1}^{M_r}\beta_{r,i}I_{r,n}^{(i)}\right]/N}. \\
E_{w,n+1} &= S_n\left[1 - e^{-\sum_{i=1}^{M_w}\beta_{w,i}I_{w,n}^{(i)}/N}\right] + (1-\alpha_w)E_{w,n} \\
I_{w,n+1}^{(1)} &= (1-\alpha_w)E_{w,n} \\
I_{w,n+1}^{(2)} &= p_{w,1}I_{w,n}^{(1)} \\
I_{w,n+1}^{(j)} &= \frac{p_{w,j-1}}{p_{w,j-2}}I_{w,n}^{(j-1)} \qquad 3 \leqslant j \leqslant M_w, \qquad w = s, r
\end{aligned} \tag{2.19}$$

Notice that the transmission parameter depend on the age since infection, and the exit probability of the latent class, α_w, is strain dependent. A transition diagram is illustrated in Figure 2.7.

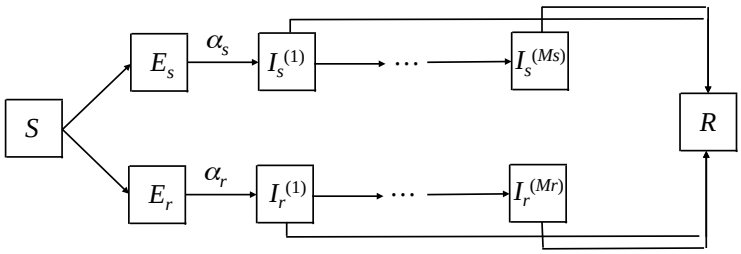

Figure 2.7. A transition diagram for the model with two strains. The subscripts s and r denote drug-sensitive and drug-resistant strains, respectively.

The corresponding F and T matrices for model (2.19) are

$$F = \begin{bmatrix} F_s & 0 \\ 0 & F_r \end{bmatrix} \qquad \text{and} \qquad T = \begin{bmatrix} T_s & 0 \\ 0 & T_r \end{bmatrix},$$

where F_w and T_w $(w = s, r)$ are the $(M_w + 1) \times (M_w + 1)$ matrices

$$F_w = \begin{bmatrix} 0 & \beta_{w,1} & \beta_{w,2} & \cdots & \beta_{w,M_w} \\ 0 & 0 & 0 & \cdots & 0 \\ 0 & 0 & 0 & \cdots & 0 \\ 0 & 0 & 0 & \cdots & 0 \\ \vdots & \vdots & \vdots & & \vdots \\ 0 & 0 & 0 & \cdots & 0 \end{bmatrix}, \qquad T_w = \begin{bmatrix} 1-\alpha_w & 0 & 0 & \cdots & 0 & 0 \\ \alpha_w & 0 & 0 & \cdots & 0 & 0 \\ 0 & p_{w,1} & 0 & \cdots & 0 & 0 \\ 0 & 0 & \frac{p_{w,2}}{p_{w,1}} & \cdots & 0 & 0 \\ \vdots & \vdots & \vdots & & \vdots & \vdots \\ 0 & 0 & 0 & \cdots & \frac{p_{w,M_w-1}}{p_{w,M_w-2}} & 0 \end{bmatrix}.$$

Then

$$F(I-T)^{-1} = \begin{bmatrix} F_s(I-T_s)^{-1} & 0 \\ 0 & F_r(I-T_r)^{-1} \end{bmatrix},$$

where

$$F_w(I-T_w)^{-1} = \begin{bmatrix} \sum_{i=1}^{M_w} \beta_{w,i} p_{w,i-1} & \sum_{i=1}^{M_w} \beta_{w,i} p_{w,i-1} & \cdots & \beta_{w,M_w} \\ 0 & 0 & \cdots & 0 \\ \vdots & \vdots & & \vdots \\ 0 & 0 & \cdots & 0 \end{bmatrix}, \quad w = s, r.$$

Since $F_w(I-T_w)^{-1}$ reduces to a block diagonal matrix, with each of the two blocks having one positive eigenvalue, it follows that

$$\begin{aligned}\mathcal{R}_0 &= \varrho(F(I-T)^{-1}) = \max\left\{\sum_{i=1}^{M_s}\beta_{s,i}\ p_{s,i-1}\ ,\ \ \sum_{i=1}^{M_r}\beta_{r,i}\ p_{r,i-1}\right\}\\ &= \max\left\{\mathbb{E}\left(\sum_{i=1}^{Y_s}\beta_{s,i}\right),\ \mathbb{E}\left(\sum_{i=1}^{Y_r}\beta_{r,i}\right)\right\}\end{aligned}$$

2.3.2 A two-gender model for sexually transmitted infections

In this section we introduce a system that includes two sub-populations, female and male, with heterosexual mixing (i.e., no sexual contacts between individuals of the same sex). Assume that the infectious periods for female and male populations follow arbitrary discrete (bounded) distributions denoted by Y_f and Y_m, respectively. The subscripts f and m stand for female and male, respectively. Let

$$p_{f,i} = \mathbb{P}(Y_f > i) \quad \text{and} \quad p_{m,i} = \mathbb{P}(Y_m > i).$$

Denoted by M_w (for $w = f, m$) the maximum length of the infectious period. The model equations are

$$\begin{aligned}S_{w,n+1} &= S_{w,n}e^{-\sum_{i=1}^{M_{\tilde{w}}}\beta_{\tilde{w},i}I^{(i)}_{\tilde{w},n}/N},\\ E_{w,n+1} &= S_{w,n}\left[1-e^{-\sum_{i=1}^{M_{\tilde{w}}}\beta_{\tilde{w},i}I^{(i)}_{\tilde{w},n}/N}\right]+(1-\alpha_w)E_{w,n}\\ I^{(1)}_{w,n+1} &= \alpha_w E_{w,n}\\ I^{(2)}_{w,n+1} &= p_{w,1}I^{(1)}_{w,n}\\ I^{(j)}_{w,n+1} &= \tfrac{p_{w,j-1}}{p_{w,j-2}}I^{(j-1)}_{w,n}, \qquad 3\leqslant j\leqslant M_w, \quad w=f,m.\end{aligned} \tag{2.20}$$

Here, $\tilde{w}$ represents the opposite sex of w. The constant $\beta_{\tilde{f},i}$ ($\beta_{\tilde{m},i}$) is the transmission parameter to a female (male) by infectious male (female) individuals with age since infection i.

The corresponding F and T matrices for (2.20) are

$$F=\begin{bmatrix}0 & F_m\\ F_f & 0\end{bmatrix},\quad T=\begin{bmatrix}T_f & 0\\ 0 & T_m\end{bmatrix},$$

where F_w and T_w $(w = f, m)$ are the $(M_w + 1) \times (M_w + 1)$ matrices

$$F_w = \begin{bmatrix} 0 & \beta_{w,1} & \beta_{w,2} & \cdots & \beta_{w,M_w} \\ 0 & 0 & 0 & \cdots & 0 \\ \vdots & \vdots & \vdots & & \vdots \\ 0 & 0 & 0 & \cdots & 0 \end{bmatrix}, \quad T_w = \begin{bmatrix} 1-\alpha_w & 0 & 0 & \cdots & 0 & 0 \\ \alpha_w & 0 & 0 & \cdots & 0 & 0 \\ 0 & p_{w,1} & 0 & \cdots & 0 & 0 \\ 0 & 0 & \frac{p_{w,2}}{p_{w,1}} & \cdots & 0 & 0 \\ \vdots & \vdots & \vdots & & \vdots & \vdots \\ 0 & 0 & 0 & \cdots & \frac{p_{w,M_w-1}}{p_{w,M_w-2}} & 0 \end{bmatrix}.$$

Then,

$$F(I-T)^{-1} = \begin{bmatrix} 0 & F_m(I-T_m)^{-1} \\ F_f(I-T_f)^{-1} & 0 \end{bmatrix}$$

where

$$F_w(I-T_w)^{-1} = \begin{bmatrix} \sum_{i=1}^{M_w} \beta_{w,i} p_{w,i-1} & \sum_{i=1}^{M_w} \beta_{w,i} p_{w,i-1} & \cdots & \beta_{w,M_w} \\ 0 & 0 & \cdots & 0 \\ \vdots & \vdots & & \vdots \\ 0 & 0 & \cdots & 0 \end{bmatrix}, \quad w = f, m.$$

The matrix $F(I-T)^{-1}$ has rank 2 and the only two non-zero eigenvalues are

$$\pm\sqrt{\left(\sum_{i=1}^{M_f} \beta_{f,i}\ p_{f,i-1}\right)\left(\sum_{i=1}^{M_m} \beta_{m,i} p_{m,i-1}\right)}.$$

It follows that

$$\begin{aligned} \mathcal{R}_0 &= \varrho(F(I-T)^{-1}) = \sqrt{\left(\sum_{i=1}^{M_f} \beta_{f,i}\ p_{f,i-1}\right)\left(\sum_{i=1}^{M_m} \beta_{m,i} p_{m,i-1}\right)} \\ &= \sqrt{\mathbb{E}\left(\sum_{i=1}^{Y_f} \beta_{f,i}\right)\mathbb{E}\left(\sum_{i=1}^{Y_m} \beta_{m,i}\right)} \end{aligned}$$

Secondary infections need to be computed from one female (male) to other females (males) through the male (female) population. This is the reason behind the square root in the formula above. Let

$$\mathcal{R}_0^{(fm)} = \mathbb{E}\left(\sum_{i=1}^{Y_f} \beta_{f,i}\right), \qquad \mathcal{R}_0^{(mf)} = \mathbb{E}\left(\sum_{i=1}^{Y_m} \beta_{m,i}\right).$$

These quantities describe the average number of secondary infections an infectious female (male) individual can produce in a susceptible male (female) population during her(his) infectious period. Thus, $\mathcal{R}_0$ is the geometric mean of $\mathcal{R}_0^{(fm)}$ and $\mathcal{R}_0^{(mf)}$.

2.4 SEIR models with disease control and derivation of $\mathcal{R}_C$

In this section, the system (2.15) in Section 2.2.3 is modified to include disease control in the form of isolation/hospitalization. Continuous-time models with arbitrarily distributed disease stages and control have been studied before, consider for example

$$\begin{aligned}
S' &= -\tfrac{\delta}{N} S[I + (1-\rho)H] \\
E' &= \tfrac{\delta}{N} S[I + (1-\rho)H] - (1-\alpha)E \\
I(t) &= \int_0^t \underbrace{(1-\alpha)E(s)}_{\text{input to } I \text{ at time } s} \cdot \underbrace{P(t-s)Q(t-s)}_{\text{still in } I \text{ at time } t} ds \\
H(t) &= \int_0^t \underbrace{\int_0^\tau (1-\alpha)E(s)[-P(\tau-s)Q'(\tau-s)ds}_{\text{input to } H \text{ at time } \tau} \underbrace{P(t-\tau|\tau-s)}_{\text{still in } H \text{ at time } t} d\tau \\
&= \int_0^t (1-\alpha)E(s)P(t-s)[1-Q(t-s)]ds.
\end{aligned}$$

This model allows the use of distributions P and Q for the infectious period and isolation time, respectively. Unless P and Q are Exponential or Gamma distributions, we are left with a set of integral-differential equations that a might be hard to interpret implement. Models along this lines are presented in [41] and [43]. Several findings of the latter study suggest that the use of more realistic assumptions on the distribution of the infectious period can be critical when isolation/hospitalization of infectious individuals is included in the model.

With this in mind, a discrete model capturing such features is developed in this section. A transition diagram is described in Figure 2.8. The isolated (or hospitalized)

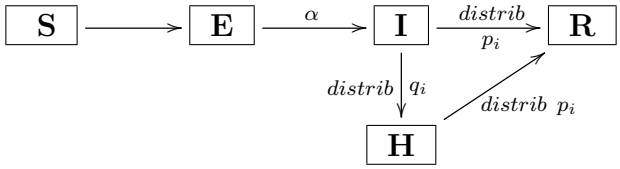

Figure 2.8. A transition diagram for the model with isolation and an arbitrary bounded distribution for the infectious period.

class is denoted by H. As before, let Y be the length of the infectious period and, in addition, let W be the age since infection at which an individual is isolated, then

$$p_i = \mathbb{P}(Y > i) \qquad \text{and} \qquad q_i = \mathbb{P}(W > i).$$

Denote by M the upper bound of Y and W, i.e., $p_m = q_m = 0$ for all $m \geqslant M$. Assume that isolated individuals have a reduced transmission factor $\rho \in (0, 1)$ so that the force of infection can be written as

$$\lambda(I_n, H_n) = \frac{\beta}{N}[I_n + (1 - \rho)H_n].$$

The model equations read

$$\begin{aligned} S_{n+1} &= S_n e^{-\lambda(I_n,H_n)}, \\ E_{n+1} &= S_n(1 - e^{-\lambda(I_n,H_n)}) + (1 - \alpha)E_n \\ I_{n+1} &= i_{n+1} + i_n p_1 q_1 + i_{n-1} p_2 q_2 + \cdots + i_1 p_n q_n \\ H_{n+1} &= i_n p_1(1 - q_1) + i_{n-1} p_2(1 - q_2) + \cdots + i_1 p_n(1 - q_n), \end{aligned} \tag{2.21}$$

where $i_{j+1} = \alpha E_j$ is the input from the E class to the I class at time $j + 1$. Initial conditions are given by $S_0 = N - E_0, E_0 > 0$ and $I_0 = H_0 = 0$.

As for (2.12) in Section 2.2.3, the classes S, E, I and H at time $n + 1$ cannot be written in the form

$$[\ E_{n+1},\ I_{n+1},\ H_{n+1},\ S_{n+1}\ ]^T = \mathcal{M}\left([\ E_n,\ I_n,\ H_n,\ S_n\ ]^T\right),$$

where $\mathcal{M} : \mathbb{R}^4 \to \mathbb{R}^4$. Therefore, in order to compute $\mathcal{R}_C$ using the next generation matrix method, the set of equations (2.21) must be reformulated. Consider substages

for the I and H classes, as shown in Figure 2.9. The substage $I^{(i)}$ represents individuals who have been infected for i units of time without being isolated, and $H^{(i)}$ represents isolated individuals infected for i units of time. Note that $H^{(1)} = 0$ as isolations occurs after becoming infectious. All of the I and H sub-stages are connected to R, representing the fact that infectious individuals may recover at any time. All individuals will be recovered by M units of time after becoming infectious. Then, the system (2.21) can be replaced by the following equations:

$$\begin{aligned}
S_{n+1} &= S_n \exp\left(-\tfrac{\beta}{N}\sum_{i=1}^{M}[I_n^{(i)} + (1-\rho)H_n^{(i)}]\right),\\
E_{n+1} &= S_n\left[1 - \exp\left(-\tfrac{\beta}{N}\sum_{i=1}^{M}[I_n^{(i)} + (1-\rho)H_n^{(i)}]\right)\right] + (1-\alpha)E_n,\\
I_{n+1}^{(1)} &= \alpha E_n, \qquad I_{n+1}^{(2)} = p_1 q_1 I_n^{(1)},\\
I_{n+1}^{(j)} &= \frac{p_{j-1}q_{j-1}}{p_{j-2}q_{j-2}} I_n^{(j-1)},\\
H_{n+1}^{(2)} &= p_1(1-q_1)I_n^{(1)},\\
H_{n+1}^{(j)} &= \frac{p_{j-1}(q_{j-2}-q_{j-1})}{p_{j-2}q_{j-2}} I_n^{(j-1)} + \frac{p_{j-1}}{p_{j-2}} H_n^{(j-1)}, \qquad 3 \leqslant j \leqslant M.
\end{aligned} \tag{2.22}$$

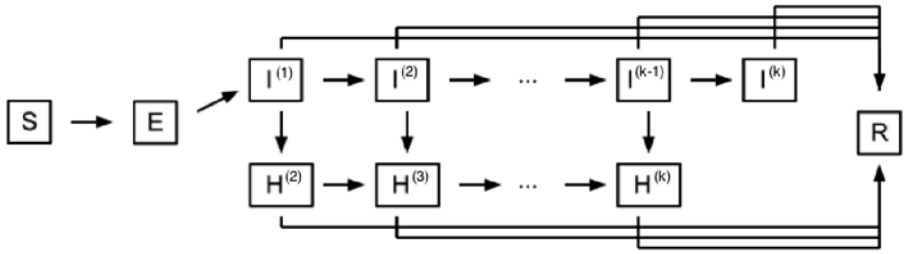

Figure 2.9. A detailed diagram for a reformulated model, equivalent to (2.21)

Derivation of the control reproduction number $\mathcal{R}_C$

We now present the derivation of $\mathcal{R}_C$. The detailed derivation and biological explanations help reveal the explicit dependance of $\mathcal{R}_C$ on the mean values of the

stage distributions and the 'isolation-adjusted' mean sojourn time. From the set of equations (2.22) the $2M \times 2M$ matrix F associated with new infections is

$$F = \begin{bmatrix} 0 & \beta & \cdots & \beta & (1-\rho)\beta & \cdots & (1-\rho)\beta \\ 0 & 0 & \cdots & 0 & 0 & \cdots & 0 \\ \vdots & \vdots & \vdots & \vdots & \vdots & & \vdots \\ 0 & 0 & \cdots & 0 & 0 & \cdots & 0 \end{bmatrix}.$$

As before, T denotes the $2M \times 2M$ block matrix associated with transitions. Then $I - T = \begin{bmatrix} A & 0 \\ C & D \end{bmatrix}$, where the matrices A of dimension $(M+1) \times (M+1)$; C of dimension $(M+1) \times (M-1)$; and D of dimension $(M-1) \times (M-1)$ are

$$A = \begin{bmatrix} \alpha & 0 & 0 & \cdots & 0 & 0 \\ \alpha & 1 & 0 & \cdots & 0 & 0 \\ 0 & -p_1 q_1 & 1 & \cdots & 0 & 0 \\ 0 & 0 & -\frac{p_2 q_2}{p_1 q_2} & \cdots & 0 & 0 \\ \vdots & \vdots & \vdots & & \vdots & \vdots \\ 0 & 0 & 0 & \cdots & 1 & 0 \\ 0 & 0 & 0 & \cdots & -\frac{p_{M-1} q_{M-1}}{p_{M-2} q_{M-2}} & 1 \end{bmatrix}, \quad D = \begin{bmatrix} 1 & 0 & 0 & \cdots & 0 & 0 \\ -\frac{p_2}{p_1} & 1 & 0 & \cdots & 0 & 0 \\ 0 & -\frac{p_3}{p_2} & 1 & \cdots & 0 & 0 \\ \vdots & \vdots & \vdots & & \vdots & \vdots \\ 0 & 0 & 0 & \cdots & 1 & 0 \\ 0 & 0 & 0 & \cdots & -\frac{p_{M-1}}{p_{M-2}} & 1 \end{bmatrix},$$

$$C = \begin{bmatrix} 0 & -p_1(1-q_1) & 0 & \cdots & 0 & 0 & 0 \\ 0 & 0 & -\frac{p_2(q_1-q_2)}{p_1 q_1} & \cdots & 0 & 0 & 0 \\ \vdots & \vdots & \vdots & & \vdots & \vdots & \vdots \\ 0 & 0 & 0 & \cdots & 0 & -\frac{p_{M-1}(q_{M-2}-q_{M-1})}{p_{M-2} q_{M-2}} & 0 \end{bmatrix}.$$

The inverse of $I - T$ is given by $\begin{bmatrix} A^{-1} & 0 \\ -D^{-1}CA^{-1} & D^{-1} \end{bmatrix}$, where

$$A^{-1} = \begin{bmatrix} \frac{1}{1-\alpha} & 0 & 0 & \cdots & 0 & 0 \\ 1 & 1 & 0 & \cdots & 0 & 0 \\ p_1q_1 & p_1q_1 & 1 & \cdots & 0 & 0 \\ p_2q_2 & p_2q_2 & \frac{p_2q_2}{p_1q_1} & \cdots & 0 & 0 \\ \vdots & \vdots & \vdots & & \vdots & \vdots \\ p_{M-1}q_{M-1} & p_{M-1}q_{M-1} & p_{M-1}q_{M-1} & \cdots & \frac{p_{M-1}q_{M-1}}{p_{M-2}q_{M-2}} & 1 \end{bmatrix},$$

$$D^{-1} = \begin{bmatrix} 1 & 0 & 0 & \cdots & 0 & 0 \\ \frac{p_2}{p_1} & 1 & 0 & \cdots & 0 & 0 \\ \frac{p_3}{p_1} & \frac{p_3}{p_2} & 1 & \cdots & 0 & 0 \\ \vdots & \vdots & \vdots & & \vdots & \vdots \\ \frac{p_{M-2}}{p_1} & \frac{p_{M-2}}{p_2} & \frac{p_{M-2}}{p_3} & \cdots & 1 & 0 \\ \frac{p_{M-1}}{p_1} & \frac{p_{M-1}}{p_2} & \frac{p_{M-1}}{p_3} & \cdots & \frac{p_{M-1}}{p_{M-2}} & 1 \end{bmatrix},$$

and

$$-D^{-1}CA^{-1} = \begin{bmatrix} p_1(1-q_1) & * & \cdots & * \\ \frac{p_2}{p_1}p_1(1-q_1) + p_2(q_1-q_2) = p_2(1-q_2) & * & \cdots & * \\ \frac{p_3}{p_1}p_1(1-q_1) + \frac{p_3}{p_2}p_2(q_1-q_2) + p_3(q_2-q_3) = p_3(1-q_3) & * & \cdots & * \\ \vdots & & \vdots & \\ \frac{p_{M-1}}{p_1}p_1(1-q_1) + \cdots + p_{M-1}(q_{M-2}-q_{M-1}) = p_{M-1}(1-q_{M-1}) & * & \cdots & * \end{bmatrix}.$$

Notice that only the first column of the previous matrix is relevant for computing the eigenvalues of the next generation matrix since F has rank 1 and

$$
\begin{aligned}
F(I-T)^{-1} &= \begin{bmatrix} 0 & \beta & \cdots & \beta & (1-\rho)\beta & \cdots & (1-\rho)\beta \\ 0 & 0 & \cdots & 0 & 0 & \cdots & 0 \\ 0 & 0 & \cdots & 0 & 0 & \cdots & 0 \\ \vdots & \vdots & \vdots & \vdots & \vdots & & \vdots \\ 0 & 0 & \cdots & 0 & 0 & \cdots & 0 \end{bmatrix} \begin{bmatrix} A^{-1} & 0 \\ -D^{-1}CA^{-1} & D^{-1} \end{bmatrix} \\
&= \begin{bmatrix} \beta \sum_{i=0}^{M-1} p_i q_i + \beta(1-\rho) \sum_{i=0}^{M-1} p_i(1-q_i) & * & \cdots & * \\ 0 & 0 & \cdots & 0 \\ \vdots & \vdots & & \vdots \\ 0 & 0 & \cdots & 0 \end{bmatrix}
\end{aligned}
$$

To interpret $\mathcal{R}_0$ in biologically relevant terms, see that

$$
\sum_{i=0}^{M-1} p_i q_i = \mathbb{E}\left(\min\{Y, W\}\right) \quad \text{and} \quad \sum_{i=0}^{M-1} p_i(1-q_i) = \mathbb{E}(Y) - \mathbb{E}\left(\min\{Y, W\}\right).
$$

$\mathbb{E}(Y)$ represents the mean time spent in compartments I and H, $\mathbb{E}\left(\min\{Y, W\}\right)$ is the mean time spent in I ('isolation-adjusted' mean sojourn time) and $\mathbb{E}(Y) - \mathbb{E}\left(\min\{Y, W\}\right)$ is the mean time spent in H. Using this expressions, a formula for $\mathcal{R}_C$ is given by

$$
\mathcal{R}_C = \underbrace{\beta\mathbb{E}\left(\min\{Y, W\}\right)}_{\mathcal{R}_I} + \underbrace{\beta(1-\rho)\left[\mathbb{E}(Y) - \mathbb{E}\left(\min\{Y, W\}\right)\right]}_{\mathcal{R}_H}. \tag{2.23}
$$

Here, $\mathcal{R}_I$ represents the number of secondary infections produced in a susceptible population by an individual in the I class, during his/her infectious period. Similarly, $\mathcal{R}_H$ is the number of secondary infections produced by an individual in the H class.

If $\rho = 0$, i.e., isolation does not reduce the transmission rate, this model is comparable to the systems (2.12) and (2.15). Clearly, $\mathcal{R}_C\big|_{\rho=0} = \beta\mathbb{E}(Y)$, which is identical to $\mathcal{R}_0$ obtained in (2.16), Section 2.2.3. On the other hand, if $\rho > 0$ then $\mathcal{R}_C < \mathcal{R}_0$, as expected.

2.4.1 Effect of disease stage distribution on $\mathcal{R}_C$

Equation (2.23) provides a simple way to asses the effect that our choice on the distributions p_i, q_i has on the value of $\mathcal{R}_C$. To illustrate this effect, consider the following distributions for the infectious period Y.

(i) *Shifted Binomial.* Let $Y_1 - 1 \sim$ Binomial $\left(19, \frac{4}{19}\right)$, then $Y_1 \in \{1, 2, 3, \cdots, 20\}$, $\mathbb{E}(Y_1) = 5$ and $1 = p_0 > p_1 > \cdots > p_{19} > p_{20} = 0$. The probability mass function of Y_1 is

$$\mathbb{P}(Y_1 = i) = p_{i-1} - p_i = \binom{19}{i-1} \left(\frac{4}{19}\right)^{i-1} \left(1 - \frac{4}{19}\right)^{19-i+1}, \qquad i = 1, 2, \cdots, 20$$

and its survival function is recursively given by $p_0 = 1$ and

$$p_i = p_{i-1} - \binom{19}{i-1} \left(\frac{4}{19}\right)^{i-1} \left(1 - \frac{4}{19}\right)^{19-i+1}, \qquad i = 1, 2, \cdots, 20$$

A graph of both functions can be found in Figure 2.10a and 2.10b.

(ii) *Truncated Geometric.* Let Y_2 be a truncated Geometric with parameter $\psi = 0.197548$, and $Y_2 \in \{1, 2, 3, \cdots, 20\}$. The value for ψ has been chosen so that $E(Y_2) \approx 5$. The survival function is given by $p_i = 0.802452^i$ for $i = 0, 1, \cdots, 19$ and $p_{20} = 0$. The plots of its mass and survival functions are shown in Figures 2.10a and 2.10b, respectively.

(iii) *"Artificial".* Y_3 is a distribution that does not belong to any family of discrete distribution. Our goal here is to show that *any* distribution (particularly empirical distributions obtained directly from data) can be used in (2.21) and (2.22). The made up distribution has probability mass function

$$\mathbb{P}(Y_3 = i) = p_{i-1} - p_i = \begin{cases} a & \text{if } i = 1, 2, 3, \\ b & \text{if } i = 4, 5, 6, \\ 0.01 & \text{if } i = 7, \cdots, 20, \\ 0 & \text{otherwise.} \end{cases}$$

The values for a and b are chosen so that $\mathbb{E}(Y_3) = 5$. Since $\mathbb{E}(Y_3) = 6a+15b+1.89$ and $3a+3b+0.14 = 1$, we chose $a = \frac{1.19}{9}$ and $b = \frac{1.39}{9}$. The density and survival functions are shown in Figures 2.10a and 2.10b.

These three distributions are comparable, as they all have the same support $\{1, \cdots, 20\}$ and mean $\mathbb{E}(Y_1) = \mathbb{E}(Y_2) = \mathbb{E}(Y_3) = 5$.

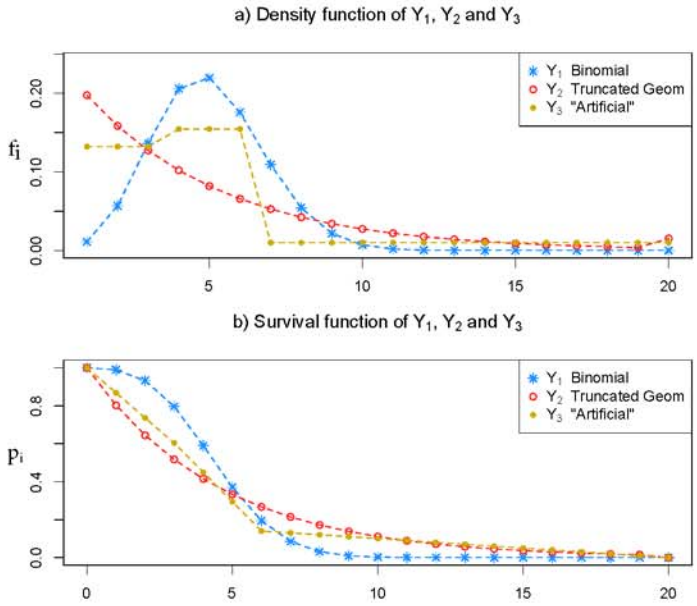

Figure 2.10. Plots of the probability mass (a) and survival functions (b) of the distributions of Y_j, $j = 1, 2, 3$. These potential distributions for the infectious period have the same support and mean value.

To allow comparison, assume that the distribution W is a shifted Binomial with parameter θ (see the definition of Y_1) taking values on the set $\{1, \cdots, 20\}$. Let W_θ denote the dependence on W on θ. Figure 2.11 shows the density and survival functions of W_θ for $\theta = 0.05, 0.4$ and 0.75. The average time spent before isolation is given by $\mathbb{E}(W) = 19\theta + 1$. Notice that $\mathbb{E}(W_\theta) \geqslant 1$ because at least one unit of time has to elapse before the transition from I to H, see the transition diagram in Figures 2.8 and 2.9. Smaller values of θ (close to zero) imply that isolation occurred very soon after entering the infectious class. Larger values of θ (close to 1) imply a longer stay

in the infectious class before isolation occurs. In this case more individuals in I will move to the R class than to the H class. Thus, θ is a parameter that determines the timing of isolation.

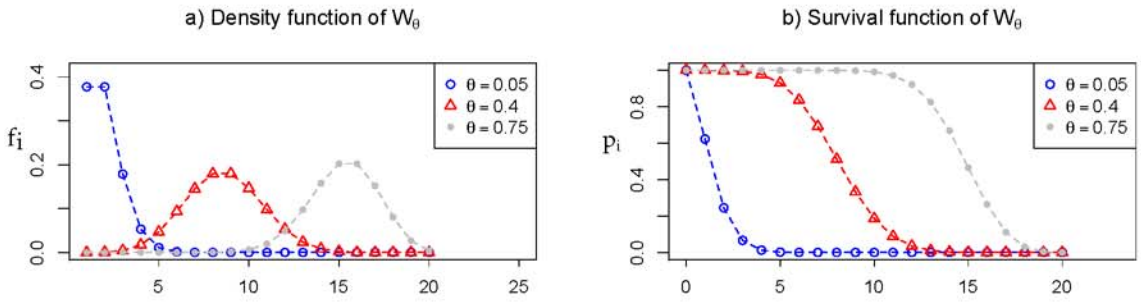

Figure 2.11. Plots of the probability mass (a) and the survival functions (b) of W_θ for three different values of θ. A small value of θ represents early isolation whereas a larger θ (close to one) represents delayed isolation, in which case most infectious individuals will recover before being moved to the H class.

The numeric values of $\mathbb{E}\left(\min\{Y_j, W_\theta\}\right)$, for $j = 1, 2, 3$ and $\theta \in (0, 1)$, can be easily computed and are shown in Figure 2.12. Let $\mathcal{R}_C(\theta, j)$ be the control reproduction number of a model with $Y = Y_j$ and $W = W_\theta$. Using equation (2.23), we obtain

$$\begin{aligned} \mathcal{R}_C(\theta, j) &= \beta\left[\mathbb{E}\left(\min\{Y_j, W_\theta\}\right) + (1-\rho)(5 - \mathbb{E}\left(\min\{Y_j, W_\theta\}\right))\right] \\ &= \beta\left[\rho\mathbb{E}\left(\min\{Y_j, W_\theta\}\right) + 5(1-\rho)\right]. \end{aligned} \tag{2.24}$$

The formula (2.24) can be used to examine the influence of distributions Y_j on the assessment of control strategies W_θ (isolation), as measured by $\mathcal{R}_C(\theta, j)$. As expected, the effect of isolation on the reduction of $\mathcal{R}_C(\theta, j)$ also depends on the isolation efficiency (ρ) and transmission rate (β).

A plot of $\mathcal{R}_C(\theta, j)$ for $j = 1, 2, 3$, $\theta \in [0, 1]$ and various values of ρ and β is shown in Figure 2.13. The threshold values of θ, below which $\mathcal{R}_C < 1$ (no disease outbreak), are marked for the three distributions Y_j. The following observations can be made:

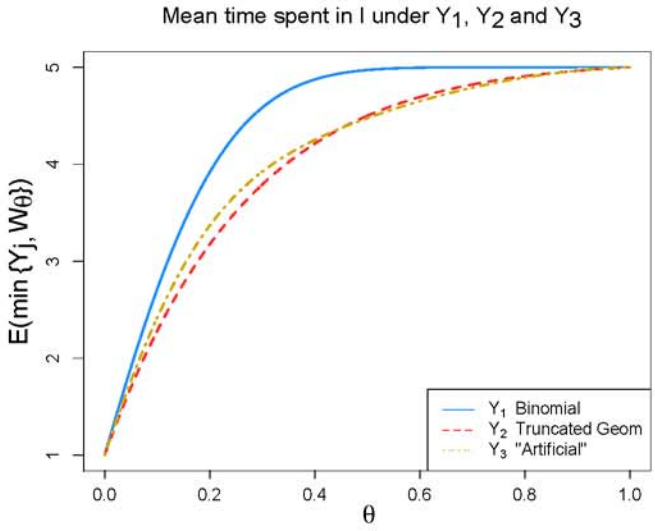

Figure 2.12. Plot of the mean time spent in I, $\mathbb{E}\left(\min\{Y_j, W_\theta\}\right)$, under three scenarios given by Y_j, $j = 1, 2, 3$.

(i) Y_1 (Binomial distribution) always generates the lowest threshold (earlier isolations) than Y_2 and Y_3. This suggest that the Truncated Geometric and the Artificial distributions tend to provide more optimistic evaluations;

(ii) the discrepancy between the three distributions is larger for lower transmission rate β (see figure 2.13b) than for higher β (see figure 2.13c)

(iii) the discrepancy between the three distributions is smaller for lower isolation efficiency ρ (see figures 2.13a,c) than for higher ρ (see figures 2.13b,d).

Our results suggest that the choice of distribution for the infectious period plays a crucial role in outcomes of the model with isolation.

2.5 Conclusion and future directions

The results in this chapter provide a systematic derivation for the reproduction numbers of various discrete-time epidemic models under various assumptions on the distribution of the infectious period, including an arbitrarily distributed (bounded)

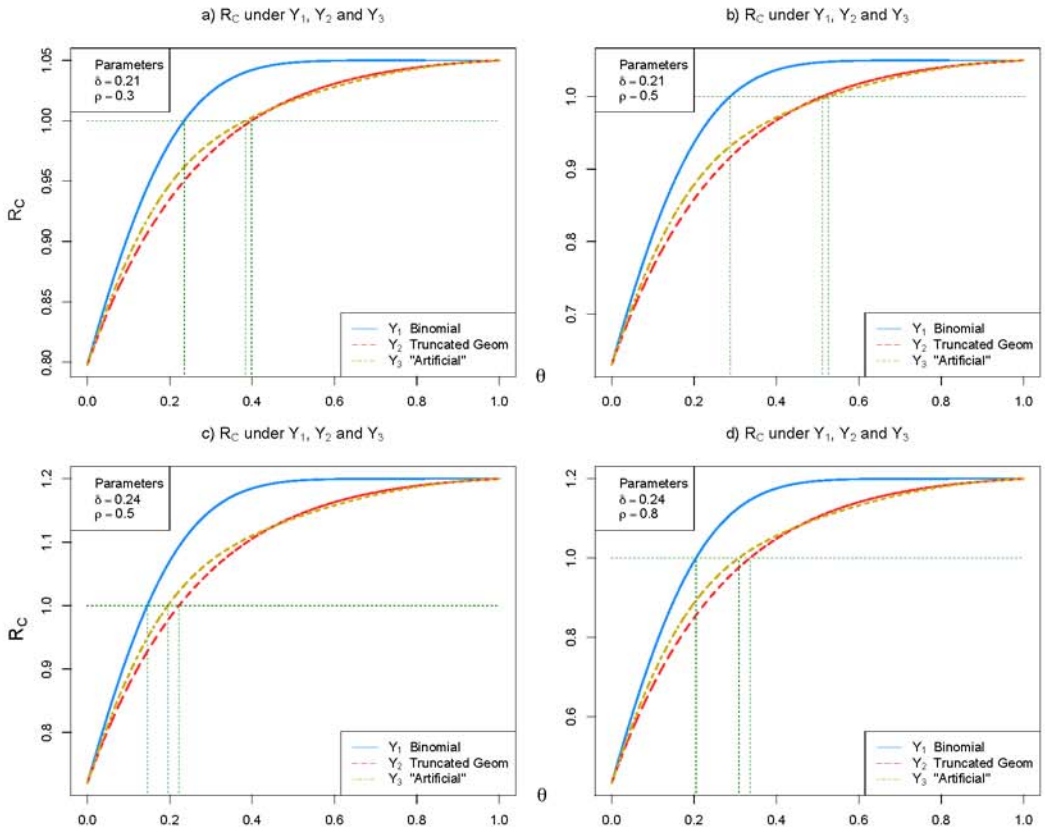

Figure 2.13. Plot of $\mathcal{R}_C(\theta, j)$. The vertical lines show a threshold value for θ, under which $\mathcal{R}_C(\theta, j) < 1$. The interval between these vertical lines mark an interval for θ in which the models predict different results when analyzing whether or not there is an epidemic.

infectious period. For models without disease control (Sections 2.2 and 2.3), we presented the derivation for reproduction numbers by using the next generation matrices. The resulting formulas for $\mathcal{R}_0$ are shown to be consistent with biological considerations.

To facilitate the use of the next generation matrix approach on the models with negative binomial and arbitrary distribution (Sections 2.2.2, 2.2.3), we introduced multiple infectious stages; a technique that we believe is novel for discrete systems. We also demonstrated other innovative ideas of analyzing discrete models in Section 2.3 where the I stages represent the age-since-infection. Similar techniques were

also used in the analyses of other models including multiple strains or structured populations (e.g., structured by sex), as well as for a model with isolation.

For the model with isolation (Section 2.4), $\mathcal{R}_C$ was also computed using the next generation matrix approach. It is shown that the control reproduction number $\mathcal{R}_C$ depends, among other factors, on the mean infectious period $\mathbb{E}(Y)$ and the isolation-adjusted mean sojourn time $\mathbb{E}(\min\{Y, W\})$ (see equation (2.23)). This formula is particularly useful for model applications as it works for general distributions, and can be applied to a particular disease or population for which a specific stage distribution can be identified. $\mathcal{R}_C$ depends both on the parameters related to the infectious stage distribution and on the distribution associated with isolation probability during the infectious period. To control the disease it is necessary to decrease $\mathcal{R}_C$ below one and having an explicit formula of $\mathcal{R}_C$ makes it easier to identify the most effective control strategies, based on specific probability distributions associated with the disease. More importantly, the choice of distributions may have significant influence on the applications of the model in evaluating control strategies (see Figure 2.13 and the related discussion in Section 2.4.1).

Previous studies have shown that epidemiological models with different assumptions on the distribution of disease stage durations can generate dramatically different conclusions. In this chapter we show that for discrete models, the use of a geometric distribution (the analogue of an exponential distribution in continuous models) can lead to biased evaluations on disease control strategies when compared with models with other disease stage distributions [21]. These findings suggest that it is important to study models with more realistic assumptions on disease stage distributions.

For future directions, some interesting problems include the uses of the results for the study of specific diseases for different regions and populations, the application of the formulas for $\mathcal{R}_C$ when particular distributions are suggested by epidemiological data, and the computations of $\mathcal{R}_C$ for discrete-time models that incorporate more complex factors.

3. INFLUENCE OF STAGE DISTRIBUTIONS ON MODEL PREDICTIONS

The work presented in this chapter was done in collaboration with Feng and Castillo-Chavez. Most of the results and ideas in this chapter were published in Bulletin of Mathematical Biology [21]. My contribution includes model formulation and analysis as well as the writing of the paper. All models considered in this chapter are deterministic and for discrete-time.

3.1 Introduction

In this chapter, we expand on the discrete-time single-outbreak models introduced and analyzed in Chapter 2 through the inclusion of (1) two control measures: quarantine (of latent individuals) and isolation (of infectious individuals); and (2) arbitrary distributions of the latent and infectious periods. The main goal of this chapter is to evaluate the impact of alternative stage-duration distributions on model predictions. To do so, a single epidemic outbreak model built on geometric period distributions, which is the baseline model in our analyses and discussion, is introduced and analyzed. Results from the geometric distribution model will provide the reference frame for comparisons with models with more realistic distributions.

Throughout, we highlight the role that modeling assumptions (a priori selection of disease stage duration distributions) have on the quantitative assessment of disease control strategies. Examples of models under different stage-duration distributions are considered to illustrate the discrepancies in model evaluations of disease control strategies. Similar discrepancies in model evaluations of disease control strategies under different distribution assumptions have also been observed in continuous-time models (see [43]).

One of the main contributions of this chapter is to develop an epidemic model with arbitrarily distributed stage durations in a discrete setting, as well as to derive analytical formulas for the reproduction number $\mathcal{R}_C$ and the final epidemic size. Such formulas depend on the characteristics of these arbitrary distributions and allow for comparison between distribution. Compared with continuous time models, when arbitrary stage distributions and disease control are included (which will lead to complex system of integral equations as in Feng et al. [43]), our discrete models are not only more tractable and more directly related to data (particularly when the disease stage distributions cannot be fitted well by continuous probability distributions), but also easier to analyze and adopt by biologists.

The organization of this chapter is as follows. In section 3.2, we develop a general discrete-time model with arbitrarily distributed disease stages. Formulas for $\mathcal{R}_C$ and the final size relation are also included. In Sections 3.3 and 3.4 the general model is analyzed under specific distributions. Particularly, we compare model outcomes when the disease durations follow classical distributions (Geometric, Poisson, or Binomial). A discussion of model results and final thoughts are included in Section 3.5.

3.2 A general model with quarantine and isolation

In this section we present a general single-outbreak model involving arbitrarily distributed stage-durations for disease stages. This model is a discrete-time analogue of the continuous-time epidemiological model in [43]. The model is derived following the approach taken in Chapter 2, with an added probabilistic perspective.

As usual, let n denote time (time step or generation time), S_n, E_n, I_n and E_n represent the number of susceptible, exposed but not yet infectious, infectious, and recovered at time n. In addition, let Q_n and H_n be the number of quarantined and isolated individuals at time (generation) n. It is also assumed that only individuals in the I and H classes are capable of transmitting the disease. Let β denote the

transmission coefficient and ρ the isolation efficiency, i.e. $\rho = 0$ represents no isolation and $\rho = 1$ perfect isolation. Define

$$\begin{aligned} p_i^L &= \text{ proportion of individuals that remain latent } i \text{ steps after infection;} \\ p_i^I &= \text{ proportion of individuals that remain infectious } i \text{ steps after becoming infectious;} \\ k_i^Q &= \text{ proportion of individuals who are not quarantined } i \text{ steps after infection;} \\ k_i^H &= \text{ proportion of individuals who are not isolated } i \text{ steps after becoming infectious.} \end{aligned} \tag{3.1}$$

The applications of our framework is extremely flexible because the probabilities p_i, q_i, k_i, and l_i do not have to come from a particular parametric family of discrete distributions. Model (3.5) can in fact incorporate directly empirically estimated (from the raw data) probabilities. That is, no specific assumptions on the shape of the duration-stage distribution of latent and infectious stages or on the waiting-time distributions in quarantine and/or isolation classes are required within the framework of this chapter.

Making use of probabilistic terminology facilitates the interpretation and applicability of our deterministic model results. For this reason let X and Y represent the time an individual spends in latent (E, Q) and infectious (I, H) classes, respectively. Similarly, denote by Z the time at which an exposed individual is quarantined (transition from E to Q), and W the time at which an infected individual is isolated (transition from I to H). X, Y, Z and W must take values on $\{1, 2, 3, \dots\}$ and have survival probability functions $\{p_i^L\}$, $\{p_i^I\}$ $\{k_i^Q\}$ and $\{k_i^H\}$. Under this notation,

$$p_i^L = \mathbb{P}(X > i), \quad p_i^I = \mathbb{P}(Y > i), \quad k_i^Q = \mathbb{P}(Z > i) \quad \text{and} \quad k_i^H = \mathbb{P}(W > i)$$

By definition $p_i^L \geqslant p_{i+1}^L$, $\mathbb{P}(X = i) = p_{i-1}^L - p_i^L$ and $\mathbb{E}(X) = \sum_{i=0}^{\infty} p_i^L$, where $\mathbb{E}(X)$ is the mean or expectation of X. Similar equalities hold for p_i^I, k_i^Q and k_i^H. Assume that

$$p_0^L = p_0^I = k_0^Q = k_0^H = 1, \tag{3.2}$$

meaning that the latency, infectious, quarantine and isolation periods last at least one time step. For ease of presentation, we introduce the following notation:

e_n input to E at time n (new infections),
i_n input to I at time n,
q_n input to Q at time n,
h_n input to H from Q at time n,

A transition diagram using the above notation is shown in Figure 3.1.

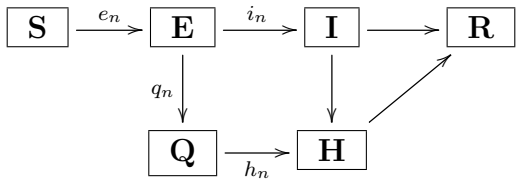

Figure 3.1. Transmission diagram for the discrete model with arbitrarily distributed stage durations.

The equation related to susceptible is given by

$$S_{n+1} = S_n G_n, \quad n = 0, 1, 2, 3, \cdots, \tag{3.3}$$

where $G_n = G(I_n, H_n)$ is the force of infection at generation n. It is commonly assumed in the literature that the functional form of G is given by $G(I_n, H_n) = e^{-\frac{\beta}{N}[I_n + (1-\rho)H_n]}$, which follows from an argument that assumes that contacts between individuals in a population happened after an exponential amount of time. For details, see equation 1.2 in Section 1.1, Chapter 1.

The input to E at time n, e_n, is recursively defined by

$$e_0 = E_0, \quad e_{n+1} = S_n - S_{n+1} = S_n(1 - G_n), \quad n \geqslant 0.$$

An expression for E_n is formulated in terms of e_n and p_n^L following this argument: individuals who entered the E compartment j units of time ago (e_{n+1-j}) and have

Table 3.1.
List of parameters and symbols commonly used in Chapter 3

Symbols	**Definitions**
β	Transmission parameter
α, γ	Exit probability of latent and infectious class (GDM)
θ_Q, θ_H	Quarantine and Isolation probability (GDM, PDM, BDM)
e_n	input to E at time n (new infections)
i_n	input to I at time n
q_n	input to Q at time n
h_n	input to H from Q at time n
X	Latent period, time spent in latent (E, Q) classes
Y	Infectious period, time spent in infectious (I, H) classes
Z	Time at which an exposed individual is quarantined $(E \to Q)$
W	Time at which an infected individual is isolated $(I \to H)$
p_i^L	Survival probability function of X, $\mathbb{P}(X > i)$
p_i^I	Survival probability function of Y, $\mathbb{P}(Y > i)$
k_i^Q	Survival probability function of Z, $\mathbb{P}(Z > i)$
k_i^H	Survival probability function of W, $\mathbb{P}(W > i)$
$\mathcal{D}_E$	Mean sojourn time in the exposed stage
$\mathcal{D}_{E*}$	'Quarantine adjusted' mean sojourn time in the exposed stage
$\mathcal{D}_I$	Mean sojourn time in the infectious stage
$\mathcal{D}_{I*}$	'Isolation adjusted' mean sojourn time in the infectious stage
$\mathcal{P}_{E\to I}$	Proportion of individuals in the E class who enter the I class
$\mathcal{P}_{E\to Q}$	Proportion of individuals in the E class who enter the Q class
$\mathcal{M}_U$	Expected remaining sojourn $(U = X, Y)$

not been quarantined (k_j^Q) no have become infectious (p_j^L) are still in E time $n+1$, therefore

$$E_{n+1} = e_{n+1} + e_n p_1^L k_1^Q + \cdots + e_1 p_n^L k_n^Q + e_0 p_{n+1}^L k_{n+1}^Q.$$

To obtain an equation for Q_n, notice that the total number of latent individuals at time $n+1$ ($E_{n+1}+Q_{n+1}$) consists of individuals who became infected j units of time ago (e_j), whose latent period has not ended q_j^L. Therefore

$$E_{n+1}+Q_{n+1}=e_{n+1}+e_np_1^L+\cdots+e_1p_n^L+e_0p_{n+1}^L.$$

Combine the last two equations to obtain

$$Q_{n+1}=e_np_1^L(1-k_1^Q)+\cdots+e_1p_n^L(1-k_n^Q)+e_0p_{n+1}^L(1-k_{n+1}^Q).$$

The input to the I compartment at time $n+1$ (i_{n+1}) include all individuals who were infected at time j (e_j), remained in E after $n-j$ steps (k_{n-j}^Q) and whose latent period was over after $n-j+1$ time units ($\mathbb{P}(X=n+1-j)$). This yields

$$\begin{aligned} i_{n+1} &= e_n\mathbb{P}(X=1)+e_{n-1}k_1^Q\mathbb{P}(X=2)+\cdots+e_0k_n^Q\mathbb{P}(X=n+1) \\ &= e_n(1-p_1^L)+e_{n-1}(p_1^L-p_2^L)k_1^Q+\cdots+e_0(p_n^L-p_{n+1}^L)k_n^Q. \end{aligned}$$

The I compartment at time n consists of individuals who entered at time j (i_j) and after $n+1-j$ steps, have not recovered (p_{n+1-j}^I) nor have they been isolated (k_{n+1-j}^H). Therefore,

$$I_{n+1}=i_{n+1}+i_np_1^Ik_1^H+\cdots+i_1p_n^Ik_n^H. \tag{3.4}$$

An expression for q_{n+1}, the input to Q at time $n+1$, can be useful to find a formula for H_{n+1}. Clearly

$$q_{n+1}=E_n-E_{n+1}+e_{n+1}-i_{n+1},$$

because individuals who leave the E class enter either I or Q, thus $E_n-(E_{n+1}-e_{n+1})=i_{n+1}+q_{n+1}$. On the other hand the input into H from Q, h_{n+1}, is given by the recursive relationship

$$h_{n+1}=Q_n-(Q_{n+1}-q_{n+1}).$$

Finally, since the total number of infectious at time $n+1$ ($I_{n+1}+H_{n+1}$) include all individuals who became infectious at time j (i_j+h_j) and did not recover after $n+1-j$ units of time (p_{n+1-j}^I), then

$$I_{n+1}+H_{n+1}=(i_{n+1}+h_{n+1})+(i_n+h_n)p_1^I+\cdots+(i_1+h_1)p_n^I,$$

Collecting all of the above formulas, we are now ready to formulate a model with arbitrarily distributed stage duration. The set of difference equations is given by

$$\begin{aligned} S_{n+1} &= S_n G_n, \qquad G_n = e^{-\frac{\beta}{N}[I_n+(1-\rho)H_n]} \\ E_{n+1} &= e_{n+1} + e_n p_1^L k_1^Q + \cdots + e_1 p_n^L k_n^Q + e_0 p_{n+1}^L k_{n+1}^Q \\ Q_{n+1} &= e_n p_1^L (1-k_1^Q) + \cdots + e_1 p_n^L (1-k_n^Q) + e_0 p_{n+1}^L (1-k_{n+1}^Q) \\ I_{n+1} &= i_{n+1} + i_n p_1^I k_1^H + \cdots + i_1 p_n^I k_n^H. \\ H_{n+1} &= (i_{n+1}+h_{n+1}) + (i_n+h_n)p_1^I + \cdots + (i_1+h_1)p_n^I - I_{n+1}, \end{aligned} \tag{3.5}$$

with initial conditions S_0, $E_0 > 0$, $I_0 = Q_0 = H_0 = R_0 = 0$ and inputs

$$\begin{aligned} e_{n+1} &= S_n - S_{n+1} = S_n(1-G_n), \\ q_{n+1} &= E_n - E_{n+1} + e_{n+1} - i_{n+1}, \\ i_{n+1} &= e_n(1-p_1^L) + e_{n-1}(p_1^L - p_2^L)k_1^Q + \cdots + e_0(p_n^L - p_{n-1}^L)k_n^Q, \\ h_{n+1} &= Q_n - (Q_{n+1} - q_{n+1}). \end{aligned} \tag{3.6}$$

Initial conditions for the inputs are $e_0 = E_0 > 0$ and $q_0 = i_0 = h_0 = 0$. Since a constant population size (N) is assumed, the number of recovered can be computed by $R_n = N - S_n - E_n - Q_n - I_n - H_n$.

Theorem 3.2.1 *All the variables in the system given by* (3.5) *and* (3.6) *are non negative.*

Proof Since $1 - G_n \in [0,1]$ for all n, then $0 \leqslant S_{n+1} \leqslant S_n$ and $e_n \geqslant 0$ for all $n \in \mathbb{N}$. Since $p_j^L, p_j^Q \in [0,1]$ then $E_n \geqslant 0$ and $Q_n \geqslant 0$. The inequality $i_n \geqslant 0$ follows from the fact that $p_j^L \geqslant p_{j+1}^L$ and $k_j^Q \geqslant 0$. As a consequence $I_n \geqslant 0$. See that $q_{n+1} = E_n - E_{n+1} + e_{n+1} - i_{n+1}$ reduces to

$$\begin{aligned} q_{n+1} &= \sum_{j=0}^{n} e_j p_{n-j}^L k_{n-j}^Q - \sum_{j=0}^{n+1} e_j p_{n+1-j}^L k_{n+1-j}^Q + e_{n+1} - \sum_{j=0}^{n} e_j (p_{n-j}^L - p_{n+1-j}^L) k_{n-j}^Q \\ &= \sum_{j=0}^{n} e_j \left(p_{n-j}^L k_{n-j}^Q - p_{n+1-j}^L k_{n+1-j}^Q - (p_{n-j}^L - p_{n+1-j}^L) k_{n-j}^Q \right) \\ &= \sum_{j=0}^{n} e_j p_{n+1-j}^L \left(k_{n-j}^Q - k_{n+1-j}^Q \right), \end{aligned}$$

which means that $q_n \geqslant 0$. Finally, $h_{n+1} = Q_n - Q_{n+1} + q_{n+1}$ reduces to

$$\begin{aligned} h_{n+1} &= \sum_{j=0}^{n-1} e_j p_{n-j}^L (1-k_{n-j}^Q) - \sum_{j=0}^{n} e_j p_{n+1-j}^L (1-k_{n+1-j}^Q) + \sum_{j=0}^{n} e_j p_{n+1-j}^L \left[k_{n-j}^Q - k_{n+1-j}^Q\right] \\ &= \sum_{j=0}^{n-1} e_j \left[p_{n-j}^L (1-k_{n-j}^Q) - p_{n+1-j}^L (1-k_{n+1-j}^Q) + p_{n+1-j}^L \left(k_{n-j}^Q - k_{n+1-j}^Q\right)\right] \\ &\quad -e_n p_1^L (1-k_1^Q) + e_n p_1^L \left(k_0^Q - k_1^Q\right) \\ &= \sum_{j=0}^{n-1} e_j \left[p_{n-j}^L (1-k_{n-j}^Q) - p_{n+1-j}^L (1-k_{n-j}^Q)\right] = \sum_{j=0}^{n-1} e_j (p_{n-j}^L - p_{n+1-j}^L)(1-k_{n-j}^Q) \end{aligned}$$

which implies $h_n \geqslant 0$, $h_n + i_n \geqslant 0$ and $H_n \geqslant 0$ for all $n \in \mathbb{N}$. ■

3.2.1 Computation of $\mathcal{R}_C$

In this section we study the control reproduction number $\mathcal{R}_C$. It is proven that the structural form of the $\mathcal{R}_C$ formulae remains the same no matter the distribution assumed for disease stages. In order to find this expression, the following notation is introduced.

$\mathcal{D}_E$	mean sojourn time in the exposed stage
$\mathcal{D}_{E*}$	"quarantine adjusted" mean sojourn time in the exposed stage
$\mathcal{D}_I$	mean sojourn time in the infectious stage
$\mathcal{D}_{I*}$	"isolation adjusted" mean sojourn time in the infectious stage
$\mathcal{P}_{E\to I}$	proportion of individuals in the E class who enter the I class
$\mathcal{P}_{E\to Q}$	proportion of individuals in the E class who enter the Q class

Formulas for these quantities are given by

$$\begin{aligned} \mathcal{D}_E = \mathbb{E}(X) = \sum_{j=0}^{\infty} p_j^L, \qquad \mathcal{D}_{E*} = \mathbb{E}(\min\{X,Z\}) = \sum_{j=0}^{\infty} p_j^L k_j^Q, \\ \mathcal{D}_I = \mathbb{E}(Y) = \sum_{j=0}^{\infty} p_j^I, \qquad \mathcal{D}_{I*} = \mathbb{E}(\min\{Y,W\}) = \sum_{j=0}^{\infty} p_j^I k_j^H. \end{aligned} \tag{3.7}$$

and

$$\begin{aligned} \mathcal{P}_{E\to I} &= \mathbb{P}(X \leqslant Z) = \sum_{j=1}^{\infty} \mathbb{P}(X=j, j \leqslant Z) = \sum_{j=1}^{\infty} \mathbb{P}(X=j)\mathbb{P}(j-1 < Z) \\ &= \sum_{j=1}^{\infty} (p_{j-1}^L - p_j^L) k_{j-1}^Q, \qquad (3.8) \\ \mathcal{P}_{E\to Q} &= 1 - \mathcal{P}_{E\to I} \end{aligned}$$

Remark. An expression for $\mathcal{D}_{E*}$ and $\mathcal{D}_{I*}$ was found using (3.2) and the fact that

$$\mathbb{P}(\min\{X, Z\} > j) = \mathbb{P}(X > j)\mathbb{P}(Z > j) = p_j^L k_j^Q.$$

$$\mathbb{P}(\min\{Y, W\} > j) = \mathbb{P}(Y > j)\mathbb{P}(W > j) = p_j^I k_j^H.$$

Making use of the above defined notation, we introduce the term

$$\mathcal{R}_I = \beta \mathcal{P}_{E\to I} \mathcal{D}_{I*}, \tag{3.9}$$

which represents the number of secondary infections produced in a susceptible population by an individual in the I class during his/her infectious period. Individual in the H class, on the other hand, can be classified as (i) those who entered H from I; and (ii) those who entered H from Q. Again, using terminology from (3.7) and (3.8), the average time spent in H is given by $\mathcal{D}_I - \mathcal{D}_{I*}$ for type (i) individuals and $\mathcal{D}_I$ for type (ii) individuals. The proportions of type (i) and type (ii) individuals are $\mathcal{P}_{E\to I}$ and $\mathcal{P}_{E\to Q}$, respectively. Considering the isolation efficiency determined by ρ, we know that the average numbers of secondary infections produced by type (i) and type (ii) individuals are

$$\mathcal{R}_{IH} = \beta(1-\rho)\mathcal{P}_{E\to I}(\mathcal{D}_I - \mathcal{D}_{I*}) \quad \text{and} \quad \mathcal{R}_{QH} = \beta(1-\rho)\mathcal{P}_{E\to Q}\mathcal{D}_I. \tag{3.10}$$

The above arguments prove the following

Theorem 3.2.2 *The control reproduction number $\mathcal{R}_C$ for the model* (3.5) *can be expressed in terms of the mean $\mathcal{D}_I$, the isolation-adjusted mean $\mathcal{D}_{l*}$, and the quarantine-adjusted probability of disease progressions $\mathcal{P}_{E\to I}$, $\mathcal{P}_{E\to Q}$. That is,*

$$\mathcal{R}_C = \mathcal{R}_I + \mathcal{R}_{IH} + \mathcal{R}_{QH} \tag{3.11}$$

where $\mathcal{R}_I$, $\mathcal{R}_{IH}$ and $\mathcal{R}_{QH}$ are the stage-specific reproduction numbers defined in (3.9) *and* (3.10).

The usefulness of the $\mathcal{R}_C$ formula given in (3.11) emerges from the fact that it was derived for general stage distributions. This expression for $\mathcal{R}_C$ allows for the

investigation of its dependence on the means and control-adjusted means (e.g., $\mathcal{D}_I$, $\mathcal{D}_{I*}$ etc.) of the stage distributions. It also allow us to explore the role of control measures (quarantine and isolation) in reducing $\mathcal{R}_C$ as a function of pre-selected stage distributions (see Section 3.4). For simpler epidemic models, the reproduction number can be derived using the next generation matrix approach presented in [17].

3.2.2 Final epidemic size

In this section, the final size of the epidemic ($\lim_{n\to\infty} S_n$) is explored, and an expression for S_∞ is derived. This expression includes $\mathcal{R}_C$ as one of its main components.

Theorem 3.2.3 *The final epidemic size generated by the dynamics of Model* (3.5) *satisfies the following final size relationship*

$$\ln \frac{S_0}{S_\infty} = \left(1 - \frac{S_\infty}{N}\right) \mathcal{R}_C. \tag{3.12}$$

Proof The E and Q equations in (3.5) together with (3.7) yield

$$\begin{aligned}
\sum_{n=0}^{\infty} E_n &= \sum_{n=0}^{\infty} \left(\sum_{j=0}^{n} e_{n-j} p_j^L k_j^Q \right) = \sum_{j=0}^{\infty} \sum_{n=j}^{\infty} e_{n-j} p_j^L k_j^Q = \sum_{j=0}^{\infty} \left(p_j^L k_j^Q \sum_{n=0}^{\infty} e_n \right) \\
&= (N - S_\infty) \left(\sum_{j=0}^{\infty} p_j^L k_j^Q \right) = (N - S_\infty) \mathcal{D}_{E*}
\end{aligned}$$

and

$$\begin{aligned}
\sum_{n=1}^{\infty} Q_n &= \sum_{n=1}^{\infty} \sum_{j=1}^{n} e_{n-j} p_j^L (1 - k_j^Q) = \sum_{j=1}^{\infty} \sum_{n=j}^{\infty} e_{n-j} p_j^L (1 - k_j^Q) \\
&= \sum_{j=1}^{\infty} \left[(p_j^L - p_j^L k_j^Q) \sum_{n=0}^{\infty} e_n \right] = (N - S_\infty) \left(\sum_{j=1}^{\infty} p_j^L - \sum_{j=1}^{\infty} p_j^L k_j^Q \right) \\
&= (N - S_\infty)[\mathbb{E}(X) - \mathcal{D}_{E*}].
\end{aligned}$$

Since $E_n \geqslant 0$ and $\sum_{n=1}^{\infty} E_n < \infty$, then $E_\infty = 0$. Similarly, Q_n, i_n, I_n, h_n and H_n converge to zero as $n \to \infty$. By definition of i_n (see (3.6)) we get

$$\begin{aligned}\sum_{n=1}^{\infty} i_n &= \sum_{n=1}^{\infty}\sum_{j=1}^{n} e_{n-j}(p_{j-1}^L - p_j^L)k_{j-1}^Q = \sum_{j=1}^{\infty}\left((p_{j-1}^L - p_j^L)k_{j-1}^Q \sum_{n=j}^{\infty} e_{n-j}\right) \\ &= (N - S_\infty)\sum_{j=1}^{\infty}(p_{j-1}^L - p_j^L)k_{j-1}^Q = (N - S_\infty)\mathcal{P}_{E\to I}.\end{aligned}$$

Thus,

$$\begin{aligned}\sum_{n=1}^{\infty} I_n &= i_1 + \sum_{n=2}^{\infty}\left(i_n + \sum_{j=1}^{n-1} i_{n-j}p_j^I k_j^H\right) = \sum_{n=1}^{\infty} i_n + \sum_{j=1}^{\infty}\left(p_j^I k_j^H \sum_{n=j+1}^{\infty} i_{n-j}\right) \\ &= \left(\sum_{n=1}^{\infty} i_n\right)\left(1 + \sum_{j=1}^{\infty} p_j^I k_j^H\right) = (N - S_\infty)\mathcal{P}_{E\to I}\mathcal{D}_{I*}.\end{aligned} \tag{3.13}$$

In addition (see (3.6)),

$$\begin{aligned}\sum_{n=1}^{\infty}(i_n + h_n) &= \sum_{n=1}^{\infty} i_n + \sum_{n=1}^{\infty}(Q_{n-1} - Q_n + q_n) = \sum_{n=1}^{\infty} i_n + Q_0 + \sum_{n=1}^{\infty} q_n \\ &= \sum_{n=1}^{\infty} i_n + \sum_{n=1}^{\infty}(E_{n-1} - E_n + e_n - i_n) = E_0 + \sum_{n=1}^{\infty} e_n \\ &= N - S_\infty.\end{aligned}$$

By the above equation, (3.13), (3.13) and the H equation (in (3.5)) we have that

$$\begin{aligned}\sum_{n=1}^{\infty} H_n &= i_1 + h_1 - I_1 + \sum_{n=2}^{\infty}\left(i_n + h_n + \sum_{j=1}^{n-1}(i_{n-j} + h_{n-j})p_j^I - I_n\right) \\ &= \sum_{n=1}^{\infty}(i_n + h_n) + \sum_{j=1}^{\infty}\left[p_j^I \sum_{n=1}^{\infty}(i_n + h_n)\right] - \sum_{n=1}^{\infty} I_n \\ &= \left[\sum_{n=1}^{\infty}(i_n + h_n)\right]\sum_{j=0}^{\infty} p_j^I - \sum_{n=1}^{\infty} I_n = (N - S_\infty)\mathbb{E}(Y) - \sum_{n=1}^{\infty} I_n \\ &= (N - S_\infty)(\mathcal{D}_I - \mathcal{P}_{E\to I}\mathcal{D}_{I*}).\end{aligned} \tag{3.14}$$

Finally, from the S equation in (3.5), it follows that

$$\begin{aligned}\ln\tfrac{S_0}{S_\infty} &= \tfrac{\beta}{N}\left[\sum_{n=1}^{\infty} I_n + (1-\rho)\sum_{n=1}^{\infty} H_n\right] \\ &= \left(1 - \tfrac{S_\infty}{N}\right)\left[\beta\mathcal{P}_{E\to I}\mathcal{D}_{I*} + \beta(1-\rho)(\mathcal{D}_I - \mathcal{P}_{E\to I}\mathcal{D}_{I*})\right] \\ &= \left(1 - \tfrac{S_\infty}{N}\right)\mathcal{R}_C.\end{aligned}$$

■

It is worth noticing that each term involved in $\mathcal{R}_C$ is expresses in terms of quantities associated with specific probability distributions (expectations, etc.). It can also be observed that the usual final size relation is *robust* under the distribution assumed for disease stages [78–81]. However, changes in p_k^L, p_k^I, k_k^Q, and k^H will lead to quantitatively distinct results.

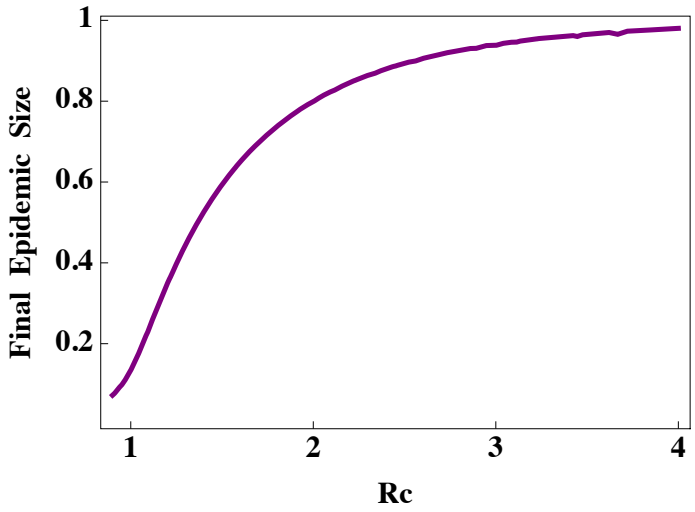

Figure 3.2. A contour plot of the function $\ln S_0/(N(1-y)) = y\mathcal{R}_C$, where $y = 1 - S_\infty/N$ represents the final epidemic size

The final size relation in (3.12) can be rewritten using the proportional size of the final epidemic $y = 1 - S_\infty/N$ as follows:

$$\ln S_0/(N(1-y)) = y\mathcal{R}_C.$$

A contour plot of the equation above expression as a function of $\mathcal{R}_C$ is shown in Figure 3.2. Although this equation cannot be solved analytically for y, the relation between $\mathcal{R}_C$ and the final size y can, from the above expression, be numerically determined.

3.3 Application of the general model in the case of Geometric distribution

In this section we study the general model given in (3.5) and (3.6), under the assumption that p_j^L p_j^I k_j^Q k_j^H are geometric distributions. The diagram in Figure

3.3, shows the model with constant exit probabilities corresponding to the geometric assumption. The set of difference equations is given by

$$\begin{aligned} S_{n+1} &= S_n G_n, \qquad G_n = e^{-\frac{\beta}{N}[I_n+(1-\rho)H_n]} \\ E_{n+1} &= (1-G_n)S_n + (1-\alpha)(1-\theta_Q)E_n \\ Q_{n+1} &= (1-\alpha)\theta_Q E_n + (1-\alpha)Q_n \\ I_{n+1} &= \alpha E_n + (1-\gamma)(1-\theta_H)I_n \\ H_{n+1} &= \alpha Q_n + (1-\gamma)(\theta_H)I_n + (1-\gamma)H_n, \quad n = 0,1,2,3,\cdots, \end{aligned} \tag{3.15}$$

with initial conditions $S_0, E_0 > 0$ and $I_0 = Q_0 = H_0 = R_0 = 0$.

In the E_{n+1} equation, the first term represents the new infection and the second term denotes those individuals who were infected in the previous step (at time n) and have not become infectious $(1-\alpha)$ or been quarantined $(1-\theta_Q)$ at time $n+1$. Other equations can be explained in a similar way. In this model we have assumed that quarantine only captures latent individuals, but not susceptible individuals, which is reasonable if quarantined individuals are much fewer than the susceptible population.

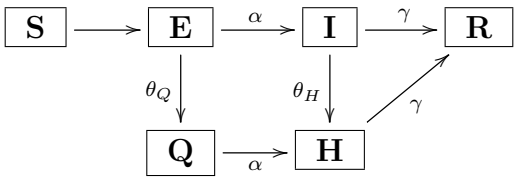

Figure 3.3. Disease transmission diagram for the discrete model (3.15) with constant transition probabilities.

In what follows we show that the system (3.15) is a particular case of (3.5), obtained when Geometric distribution is assumed for X, Y, Z and W. The geometric distribution is a discrete probability distribution supported on $\{1, 2, 3, \dots\}$. It represents the number of independent Bernoulli trials needed to get a single success. Properties of this distribution can be found in (see [75–77]). Assume X follows a Geometric

distribution with parameter α ($X \sim \text{Geom}(\alpha)$), in this case $\mathbb{P}(X = i) = (1-\alpha)^{i-1}(\alpha)$ for $i = 1, 2, \cdots$ and

$$p_i^L = \mathbb{P}(X > i) = (1-\alpha)^i \quad \text{for } i = 0, 1, 2, \ldots$$

Graphics of the above functions can be seen in Figures 1.2 (Section 1.2) and 2.2 (Section 2.2.1). Like its continuous analogue (exponential distribution) the geometric distribution is memoryless, i.e. for any $i, j \in \mathbb{N}$,

$$\mathbb{P}(X > i + j | X > i) = \mathbb{P}(X > j).$$

Theorem 3.3.1 *Assuming that $X \sim$ Geom(α), $Y \sim$ Geom(γ), $Z \sim$ Geom(θ_Q) and $W \sim$ Geom(θ_H), then the general model* (3.5) *becomes the Geometric model given by* (3.15)*. The control reproduction number for this model is $\mathcal{R}_C = \mathcal{R}_I + \mathcal{R}_{IH} + \mathcal{R}_{QH}$, where*

$$\begin{aligned} \mathcal{R}_I &= \beta \frac{\alpha}{\alpha + \theta_Q - \alpha\theta_Q} \cdot \frac{1}{\gamma + \theta_H - \gamma\theta_H}, \\ \mathcal{R}_{IH} &= \beta(1-\rho) \frac{\alpha}{\alpha + \theta_Q - \alpha\theta_Q} \left(\frac{1}{\gamma} - \frac{1}{\gamma + \theta_H - \gamma\theta_H} \right), \\ \mathcal{R}_{QH} &= \beta(1-\rho) \frac{(1-\alpha)\theta_Q}{\alpha + \theta_Q - \alpha\theta_Q} \cdot \frac{1}{\gamma}. \end{aligned} \tag{3.16}$$

and

$$\ln \frac{S_0}{S_\infty} = \left(1 - \frac{S_\infty}{N}\right) \mathcal{R}_C.$$

Proof Under these Geometric distribution assumptions (3.1) becomes

$$\begin{aligned} p_i^L &= (1-\alpha)^i, & p_i^H &= (1-\gamma)^i, \\ k_i^Q &= (1-\theta_Q)^i, & k_i^H &= (1-\theta_H)^i. \qquad i = 0, 1, 2, \ldots \end{aligned}$$

Then the E_{n+1} equation in (3.5), $e_n p_1^L k_1^Q + \cdots + e_1 p_n^L k_n^Q + e_0 p_{n+1}^L k_{n+1}^Q$, simplifies to

$$e_n(1-\alpha)(1-\theta_Q) + \cdots + e_1(1-\alpha)^n(1-\theta_Q)^n + e_0(1-\alpha)^{n+1}(1-\theta_Q)^{n+1} = (1-\alpha)(1-\theta_Q)E_n.$$

Therefore,

$$E_{n+1} = (1 - G_n)S_n + (1-\alpha)(1-\theta_Q)E_n.$$

The i_{n+1} and h_{n+1} equations in (3.6) can be written as

$$i_{n+1} = e_n\alpha + e_{n-1}\alpha(1-\alpha)(1-\theta_Q) + \cdots + e_0\alpha(1-\alpha)^n(1-\theta_Q)^n = \alpha E_n.$$

and

$$\begin{aligned} q_{n+1} &= E_n - E_{n+1} + e_{n+1} - i_{n+1} \\ &= E_n - (1-G_n)S_n - (1-\alpha)(1-\theta_Q)E_n + (1-G_n)S_n - \alpha E_n \\ &= E_n - (1-\alpha)(1-\theta_Q)E_n - \alpha E_n = (1-\alpha)\theta_Q E_n \end{aligned}$$

This yields

$$Q_{n+1} = (1-\alpha)(\theta_Q)E_n + (1-\alpha)Q_n \quad \text{and} \quad I_{n+1} = (\alpha)E_n + (1-\gamma)(1-\theta_H)I_n.$$

Hence $h_{n+1} = \alpha Q_n$ and $H_{n+1} = \alpha Q_n + (1-\gamma)\theta_H I_n + (1-\gamma)H_n$. This shows that the Geometric model (3.15) is a particular case of the general model (3.5), obtained with Geometric distribution assumptions.

Theorem 3.2.2 can now be used to find an expression for $\mathcal{R}_C$. We begin by computing the mean of X

$$\mathbb{E}(X) = \sum_{i=0}^{\infty} p_i^L = \sum_{i=0}^{\infty}(1-\alpha)^i = \frac{1}{\alpha} > 1, \qquad \alpha \in (0,1).$$

Similarly $\mathbb{E}(Y) = \frac{1}{\gamma}$, $\mathbb{E}(Z) = \frac{1}{\theta_Q}$ and $\mathbb{E}(W) = \frac{1}{\theta_H}$. Moreover, $\mathbb{P}(\min\{X,Z\} > i) = (1-\alpha)^i(1-\theta_Q)^i$, so that $\mathbb{E}(X \wedge Z) = \frac{1}{1-(1-\alpha)(1-\theta_Q)} = \frac{1}{\alpha+\theta_Q-\alpha\theta_Q}$. Therefore (see (3.7))

$$\mathcal{D}_E = \frac{1}{\alpha}, \quad \mathcal{D}_{E^*} = \frac{1}{\alpha+\theta_Q-\alpha\theta_Q}, \quad \mathcal{D}_I = \frac{1}{\gamma}, \quad \mathcal{D}_{I^*} = \frac{1}{\gamma+\theta_H-\gamma\theta_H}. \tag{3.17}$$

Similarly,

$$\begin{aligned} \mathbb{P}(X \leqslant Z) &= \sum_{j=1}^{\infty}(p_{j-1}^L - p_j^L)k_{j-1}^Q = \sum_{j=1}^{\infty}\alpha(1-\alpha)^{j-1}(1-\theta_Q)^{j-1} \\ &= \frac{\alpha}{1-(1-\alpha)(1-\theta_Q)} = \frac{\alpha}{\alpha+\theta_Q-\alpha\theta_Q}. \end{aligned} \tag{3.18}$$

Finally, replacing (3.17) and (3.18) in (3.11), expressions for $\mathcal{R}_I$, $\mathcal{R}_{IH}$ and $\mathcal{R}_{QH}$ are obtained

$$\begin{aligned} \mathcal{R}_I &= \beta\mathcal{P}_{E\to I}\mathcal{D}_{I^*} &&= \beta\frac{\alpha}{\alpha+\theta_Q-\alpha\theta_Q}\cdot\frac{1}{\gamma+\theta_H-\gamma\theta_H}, \\ \mathcal{R}_{IH} &= \beta(1-\rho)\mathcal{P}_{E\to I}(\mathcal{D}_I - \mathcal{D}_{I^*}) &&= \beta(1-\rho)\frac{\alpha}{\alpha+\theta_Q-\alpha\theta_Q}\cdot\left(\frac{1}{\gamma} - \frac{1}{\gamma+\theta_H-\gamma\theta_H}\right), \\ \mathcal{R}_{QH} &= \beta(1-\rho)\mathcal{P}_{E\to Q}\mathcal{D}_I &&= \beta(1-\rho)\frac{(1-\alpha)\theta_Q}{\alpha+\theta_Q-\alpha\theta_Q}\cdot\frac{1}{\gamma}, \end{aligned}$$

and by $\mathcal{R}_C = \mathcal{R}_I + \mathcal{R}_{IH} + \mathcal{R}_{QH}$. Finally, by Theorem 3.2.3, the final size relation

$$\ln \frac{S_0}{S_\infty} = \left(1 - \frac{S_\infty}{N}\right) \mathcal{R}_C.$$

holds for this model. ■

3.4 Other applications of the general model

The control reproduction number and final epidemic size are important measures, which are often used to compare the effectiveness of control strategies like quarantine and/or isolation. In our framework, $\mathcal{R}_C$ can also be used to examine the impact of the shape of the latent and infectious period time distributions. In this section, the role of three classical discrete distributions in the modeling process is compared. The Geometric model (GDM) developed in Section 3.3 will be compared to (i) PDM, a Poisson distribution model; and (ii) BDM, a Binomial distribution model.

For simplicity, the quarantine and isolation period distributions (described by Z and W, respectively) are assumed to follow Geometric distributions with

$$k_i^Q = (1-\theta_Q)^i, \quad k_i^H = (1-\theta_H)^i \quad \text{and} \quad \mathbb{E}(Z) = \frac{1}{\theta_Q}, \quad \mathbb{E}(W) = \frac{1}{\theta_H}.$$

3.4.1 Examples of specific stage distributions

Our baseline model GDM, together with PDM and BDM are introduced in this section, followed by a comparison among models. Our goal here is to explore the role that distributions of the latent (X) and infectious period (Y) have on control strategies. To do so, the associated values of $\mathcal{R}_C$ will be computed, compared and contrasted. Figure 3.4 shows a diagram for the three models mentioned above. In order to make these models *comparable* we fix an average latent and infectious period, say

$$\mathbb{E}(X) = \mu_1, \quad \mathbb{E}(Y) = \mu_2.$$

The parameters of the distributions mentioned below have been chosen to match these fixed average times.

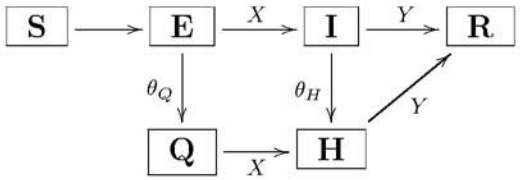

Figure 3.4. Disease transmission diagram for the GDM, PDM and BDM. The difference consists on the distributions used to model X and Y.

GDM. Linked to this model, consider $X_g \sim \text{Geom}(\alpha)$ and $Y_g \sim \text{Geom}(\gamma)$. Parameter values $\frac{1}{\alpha} = \mu_1 > 1$ and $\frac{1}{\gamma} = \mu_2 > 1$ are chosen. See Section 3.3 for more details and properties of the Geometric distribution.

PDM. Linked to this model, we have X_p and Y_p following a shifted Poisson distribution with support in $\{1, 2, 3, \dots\}$. This is, $X_p - 1 \sim \text{Poisson}(\mu_1 - 1)$ and $Y_p - 1 \sim \text{Poisson}(\mu_2 - 1)$. The probability mass function for X_p and Y_p are

$$\mathbb{P}(X_b = i) = e^{-(\mu_1 - 1)} \frac{(\mu_1 - 1)^{i-1}}{(i-1)!}, \qquad \mathbb{P}(Y_b = i) = e^{-(\mu_2 - 1)} \frac{(\mu_2 - 1)^{i-1}}{(i-1)!} \tag{3.19}$$

Figure 3.5 displays the probability mass and survival functions of Poisson distributions for different parameter values.

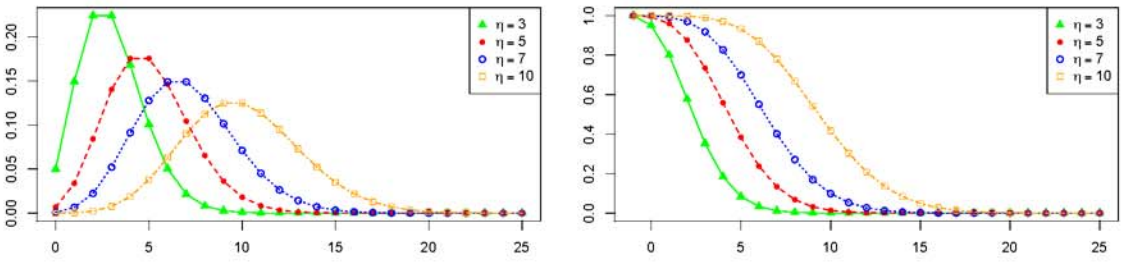

(a) Probability mass function

(b) Survival function

Figure 3.5. Plots of the probability mass and survival functions of Poisson distributions with parameters $\eta = 3, 5, 7, 10$.

BDM. Linked to this model, we have X_b and Y_b following a shifted Binomial distribution with support in $\{1, 2, \ldots, n+1\}$. This is, $X_b \sim \text{Binomial}(n_1, a)$ and $Y_b \sim \text{Binomial}(n_2, b)$. Notice that $n_1 + 1$ $(n_2 + 1)$ is the maximum length of the latent (infectious) period. The parameters n_1, n_2, a and b must satisfy $(n_1 - 1)a + 1 = \mu_1$, $(n_2 - 1)b + 1 = \mu_2$. The probability mass function for X_p and Y_p are

$$\mathbb{P}(X_b = i) = \binom{n_1}{i-1} a^{i-1}(1-a)^{m-i-1}, \quad \mathbb{P}(Y_b = i) = \binom{n_2}{i-1} b^{i-1}(1-b)^{m-i-1}. \tag{3.20}$$

Figure 3.6 displays the probability mass and survival functions of Binomial distributions for different parameter values.

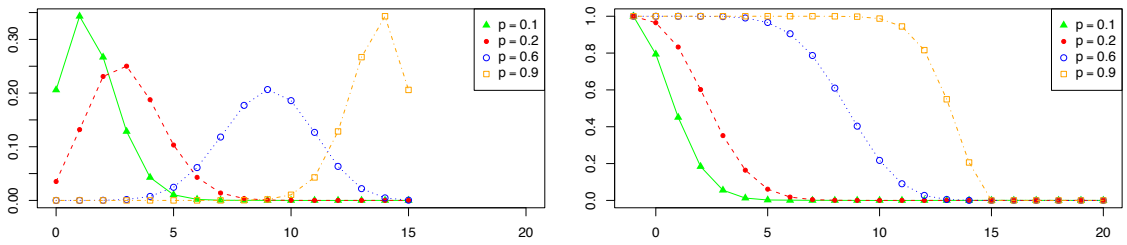

(a) Probability mass function

(b) Survival function

Figure 3.6. Plots of the probability mass and survival functions of Binomial distributions with parameters $m = 15$ and $p = 0.1, 0.2, 0.6, 0.9$.

3.4.2 Expected remaining sojourns

The analysis on the role of exponential and gamma distributed stage durations distributions in continuous-time models was carried out using expected remaining sojourns in [43]. In the case of exponential distributions, the mean sojourn and the expected remaining sojourn are identical (memoryless property) whereas in the case of the gamma distribution the expected remaining sojourn can be much shorter than the mean sojourn. Hence, it is not surprising to see that the use of distinct distributions

leads to discrepancies as well when uses discrete-time models to make predictions. We follow the philosophy in the above mentioned study as we proceed to document stage-distribution generated model discrepancies.

Denote by $\mathcal{M}_U(s)$ $(U = X, Y)$ the expected remaining sojourn, which represents the expected remaining time in a stage (latent or infectious) given that s units of time have already elapsed in the given class. A formula for $\mathcal{M}_U(s)$ is given by

$$\mathcal{M}_U(s) = \begin{cases} \sum_{n=0}^{\infty} \mathbb{P}(U > n | U > s) = \sum_{n=0}^{\infty} \frac{\mathbb{P}(U > n+s)}{\mathbb{P}(U > s)} & \text{if} \quad \mathbb{P}(U > s) > 0 \\ 0 & \text{if} \quad \mathbb{P}(U > s) = 0 \end{cases}$$

For instance, if U is bounded by M, then $\mathcal{M}_U(m) = 0$ for all $m \geqslant M$. Clearly $\mathcal{M}_U(0) = \mathbb{E}(U)$ for $U = X, Y$. In GDM, $X_g \sim \text{Geom}(\alpha)$, thus $p_{i,g} = (1-\alpha)^j$ and

$$\mathcal{M}_{X_g}(s) = \sum_{n=0}^{\infty} \frac{(1-\alpha)^{n+s}}{(1-\alpha)^s} = \sum_{n=0}^{\infty} (1-\alpha)^n = \mathbb{E}(X_g) = \mathcal{M}_{X_g}(0).$$

In plain words, the expected remaining sojourn after an individual already spent s units of time in the latent stage is independent of s. This may contribute in a significant way to the potentially biased model predictions on the effect of disease control strategies (See Chapter 1 Section 1.2). The use of PDM and BDM may lead to more reliable assessments because of their ability to capture more accurately the description for the expected remaining sojourns. Figure. 3.7 illustrates the difference among the three distribution assumptions (GDA, PDA, and BDA) by plotting the expected remaining sojourn as a function of s (the time elapsed after entering the latent stage). This figure shows that the function is constant under GDA, while the functions correspond to PDA and BDA decreases with s. Since the Binomial random variable X is bounded, $\mathcal{M}_X(s) = 0$ after its upper bound.

3.4.3 $\mathcal{R}_C$ under specific distributions

In this section the control reproduction numbers $\mathcal{R}_{C,g}$, $\mathcal{R}_{C,p}$ and $\mathcal{R}_{C,b}$ associated to the GDM, PDM and BCM are computed. A formula for $\mathcal{R}_{C,p}$ has already been

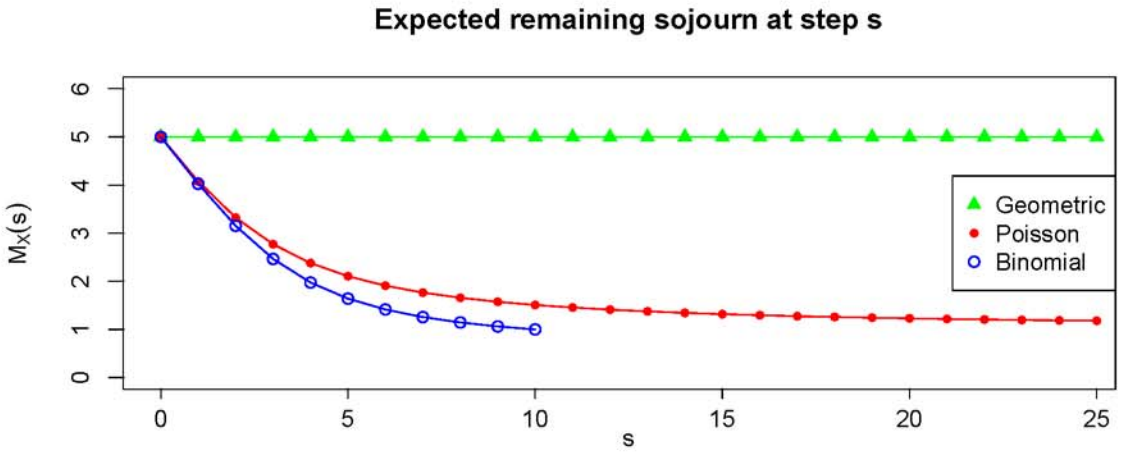

Figure 3.7. Plots of the expected remaining sojourn time, $\mathcal{M}_X(s)$, in a disease stage (latent or infectious) when s units of time have elapsed after entering the stage.

provided in (3.16), Theorem 3.3.1. The first step to find an expression for $\mathcal{R}_{C,p}$, is computing $\mathcal{P}_{E\to I,p}$ and $\mathcal{D}_{I^*,p}$. From (3.7) and (3.19),

$$\begin{aligned}
\mathcal{P}_{E\to I,p} &= \sum_{i=1}^{\infty}\mathbb{P}(X_p=i)\mathbb{P}(Z>i-1) = e^{-(\mu_1-1)}\sum_{i=1}^{\infty}\frac{(\mu_1-1)^{i-1}}{(i-1)!}\cdot(1-\theta_Q)^{i-1}\\
&= e^{-(\mu_1-1)\theta_Q}
\end{aligned}$$

$$\begin{aligned}
\mathcal{D}_{I^*,p} &= 1+\sum_{i=1}^{\infty}p_{i,p}^I k_i^H = 1+\sum_{i=1}^{\infty}\left(1-e^{-(\mu_2-1)}\sum_{j=1}^{i}\tfrac{(\mu_2-1)^{j-1}}{(j-1)!}\right)(1-\theta_H)^i\\
&= 1+\tfrac{1-\theta_H}{\theta_H}-e^{-(\mu_2-1)}\sum_{i=1}^{\infty}\sum_{j=0}^{i-1}\tfrac{(\mu_2-1)^j}{j!}(1-\theta_H)^i = \tfrac{1}{\theta_H}-e^{-(\mu_2-1)}\sum_{j=0}^{\infty}\sum_{i=j+1}^{\infty}\tfrac{(\mu_2-1)^j}{j!}(1-\theta_H)^i\\
&= \tfrac{1}{\theta_H}-e^{-(\mu_2-1)}\sum_{j=0}^{\infty}\tfrac{(\mu_2-1)^j}{j!}\tfrac{(1-\theta_H)^{j+1}}{\theta_H} = \tfrac{1}{\theta_H}-e^{-(\mu_2-1)}\tfrac{1-\theta_H}{\theta_H}\sum_{j=0}^{\infty}\tfrac{[(\mu_2-1)(1-\theta_H)]^j}{j!}\\
&= \tfrac{1-(1-\theta_H)e^{-(\mu_2-1)\theta_H}}{\theta_H}.
\end{aligned}$$

Since, at $\theta_H=0$, $\mathcal{D}_{I^*}=\mathcal{D}_I$ then form PDM, equations (3.9)-(3.11) yield

$$\mathcal{R}_{C,p}=\begin{cases}\beta\left[(1-\rho)\mu_2+\rho e^{-(\mu_1-1)\theta_Q}\cdot\dfrac{1-(1-\theta_H)e^{-(\mu_2-1)\theta_H}}{\theta_H}\right] & \text{if}\quad 0\leqslant\theta_H<1,\\ \beta\mu_2\left[1-\rho\left(1-e^{-(\mu_1-1)\theta_Q}\right)\right] & \text{if}\quad \theta_H=0.\end{cases}$$

Although, computationally easy, obtaining an expression for $\mathcal{R}_{C,b}$ in the BDM is not simple. For instance, for X_b, $q^L_{i,b}$ is a simple sum with no more than n_1+1 terms

$$q^L_{i,b} = \mathbb{P}(X_b > i) = \sum_{k=i+1}^{n_1+1} \mathbb{P}(X=k) = \sum_{k=i+1}^{n_1+1} \binom{n_1}{k-1} a^{k-1}(1-a)^{n_1-k+1}.$$

Therefore $\mathcal{P}_{E\to I,b}$, $\mathcal{P}_{E\to Q,b}$ and $\mathcal{D}_{I*,b}$ consist of finite sums that can not be simplified. For this reason an explicit formula for $\mathcal{R}_{C,b}$ is not included.

The derivatives of $\mathcal{R}_C$ with respect to the control parameters (e.g., θ_Q and θ_H) can provide useful information about the effect of controls on the reduction of $\mathcal{R}_C$. Recall that the average time elapsed before quarantine and isolation are $1/\theta_Q$ and $1/\theta_H$, respectively. Thus, and increment in either θ_Q or θ_H represent a higher control effort. This motivates the following

Theorem 3.4.1 *In the GDM and PDM the control measures, quarantine and isolation, have a positive impact on $\mathcal{R}_C$. More specifically,*

$$\frac{\partial \mathcal{R}_{C,g}}{\partial \theta_Q},\ \frac{\partial \mathcal{R}_{C,g}}{\partial \theta_H},\ \frac{\partial \mathcal{R}_{C,p}}{\partial \theta_Q} \quad \textit{and} \quad \frac{\partial \mathcal{R}_{C,p}}{\partial \theta_H} \quad \leqslant \quad 0.$$

Proof We begin by computing the partial derivatives of $\mathcal{R}_{C,g}$ with respect to both control parameters. Keeping in mind that $\beta > 0$, and $\alpha, \rho, \gamma, \theta_Q, \theta_H \in (0,1)$

$$\frac{\partial \mathcal{R}_{C,g}}{\partial \theta_Q} = -\frac{\beta\rho\alpha(1-\alpha)}{(\alpha+\theta_Q-\alpha\theta_Q)^2(\gamma+\theta_H-\gamma\theta_H)} \leqslant 0,$$

$$\frac{\partial \mathcal{R}_{C,g}}{\partial \theta_H} = -\frac{\beta\rho\alpha(1-\gamma)}{(\alpha+\theta_Q-\alpha\theta_Q)(\gamma+\theta_H-\gamma\theta_H)^2} \leqslant 0,$$

For the PDM,

$$\frac{\partial \mathcal{R}_{C,p}}{\partial \theta_Q} = -\beta\rho(\mu_1-1)\cdot e^{-(\mu_1-1)\theta_Q}\cdot \frac{1-(1-\theta_H)e^{-(\mu_2-1)(\theta_H)}}{\theta_H} \leqslant 0,$$

and

$$\frac{\partial \mathcal{R}_{C,p}}{\partial \theta_H} = -\frac{\beta\rho e^{-(\mu_1-1)\theta_Q}\left[e^{-(\mu_2-1)\theta_H}\left[(\mu_2-1)\theta_H^2-\theta_H(\mu_2-1)-1\right]+1\right]}{\theta_H^2}$$

Notice that $\frac{\partial \mathcal{R}_{C,p}}{\partial \theta_H} \leqslant 0$ if and only if, for all $\theta_H \in (0,1)$

$$\begin{aligned} f(\theta_H) &= e^{-(\mu_2-1)\theta_H}\left[(\mu_2-1)\theta_H^2 - \theta_H(\mu_2-1) - 1\right] + 1 \\ &= e^{-(\mu_2-1)\theta_H}\left[(\mu_2-1)(\theta_H^2-\theta_H) - 1\right] + 1 \ > \ 0. \end{aligned}$$

In order to prove this, compute

$$\begin{aligned} f'(\theta_H) &= e^{-(\mu_2-1)\theta_H}\left[(\mu_2-1)(2\theta_H-1)\right] - (\mu_2-1)e^{-(\mu_2-1)\theta_H}\left[(\mu_2-1)(\theta_H^2-\theta_H) - 1\right] \\ &= e^{-(\mu_2-1)\theta_H}(\mu_2-1)\left[(2\theta_H-1) - (\mu_2-1)(\theta_H^2-\theta_H) + 1\right] \\ &= e^{-(\mu_2-1)\theta_H}(\mu_2-1)\theta_H\left[2 - (\mu_2-1)(\theta_H-1)\right] \end{aligned}$$

Since $\mu_2 > 1$ it is easy to see that $f'(\theta_H) = 0$ if and only if $\theta_H = 0$ or $\theta_H = \frac{\mu_2+1}{\mu_2-1}$. This implies that f is strictly monotone in the interval $\left[0, \frac{\mu_2+1}{\mu_2-1}\right]$, and particularly in $(0,1)$. Finally, since $f(0) = 0$ and $f(1) = 1 - e^{-(\mu_2-1)} > 0$ then $f(\theta_H) > 0$, for all $\theta_H \in (0,1)$. In conclusion $\frac{\partial \mathcal{R}_{C,p}}{\partial \theta_H} \leqslant 0$. ■

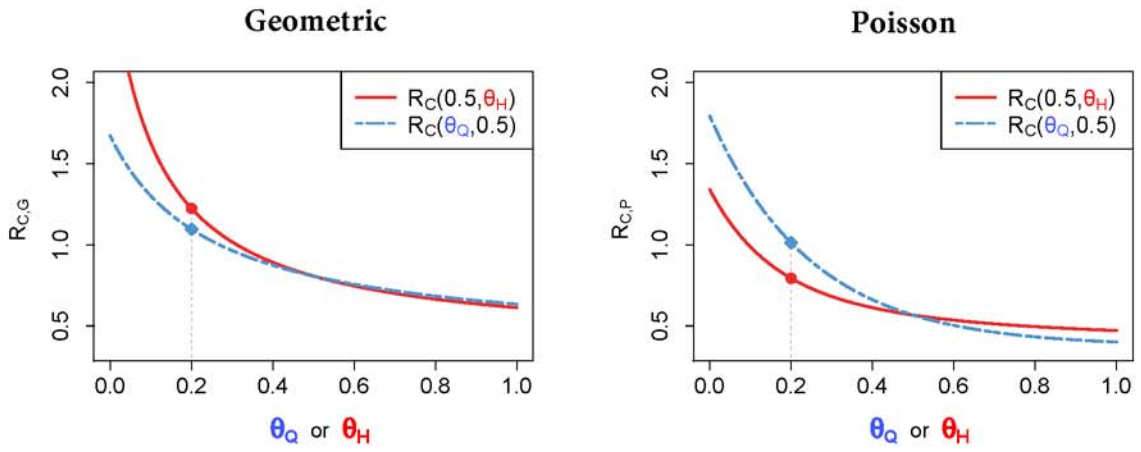

Figure 3.8. Comparison of the GDM and PDM in terms of their evaluations on various control measures. Two control strategies are considered: $(\theta_Q, \theta_H) = (0.5, 0.2)$ (see the solid circle •) and by $(\theta_Q, \theta_H) = (0.2, 0.5)$ (see the solid diamond ◆). Inconsistent assessments are obtained from the GDM (left figure) and PDM (right figure).

The sensitivity of $\mathcal{R}_C$ to the variations of control parameters can be evaluated by examining how $\mathcal{R}_C$, as function of θ_Q and θ_H, change with variations on these

parameters. Two examples are illustrated in Figure 3.8 for the GDM (left) and the PDM (right). The solid line represents $\mathcal{R}_C(0.5, \theta_H)$, while the dashed curve shows $\mathcal{R}_C(\theta_Q, .05)$. The parameter values used to produce this figure are $\beta = 0.75$, $\rho = 0.95$, $\mu_1 = 5$ and $\mu_2 = 10$.

Figure 3.8 also shows reduction in $\mathcal{R}_C$ under two control strategies: Strategy I corresponds to $(\theta_Q, \theta_H) = (0.5, 0.2)$, represented by a circle • on the solid (red) curve. Strategy II, on the other hand, corresponds to $(\theta_Q, \theta_H) = (0.2, 0.5)$ and is represented by a diamond ◆ on the dashed curves. According to the left figure (GDM), Strategy II is more effective than Strategy I, because it leads to larger reductions in $\mathcal{R}_{c,g}$. However, it the right figure (PDM), Strategy I is more effective than Strategy II. This shows that the two models distributions (GDM and PDM) generate contradictory assessments.

Table 3.2.
Components of $\mathcal{R}_C$ determined by the GDM and PDM corresponding to Figure 3.8.

	• Strategy 1: $(\theta_Q, \theta_H) = (0.5, 0.2)$		◆ Strategy 2: $(\theta_Q, \theta_H) = (0.2, 0.5)$	
	GDM	PDM	GDM	PDM
$\mathcal{P}_{E\to I}$	0.33	0.14	0.56	0.45
$\mathcal{D}_{I^*}$	3.57	4.34	1.82	1.99
$\mathcal{R}_I$	0.893	0.44	0.758	0.67
$\mathcal{R}_{IH}$	0.08	0.029	0.171	0.135
$\mathcal{R}_{QH}$	0.25	0.324	0.167	0.207
$\mathcal{R}_C$	1.223	**0.793**	**1.095**	1.011

It is not clear what is the underlying reason for the difference between GDM and PDM presented in Figure 3.8. To better understand how the distributions may affect $\mathcal{R}_C$, we list in Table 3.2 the values of some components of $\mathcal{R}_C$ corresponding to these two scenarios. We observe that for strategy 2, which corresponds to a lower quarantine

(θ_Q) and a higher isolation (θ_H), $\mathcal{P}_{E\to I}$ is higher while $\mathcal{D}_{I*}$ is lower than strategy 1 for both the GDM and PDM. Consequently, $\mathcal{R}_{QH} = \beta(1-\rho)\mathcal{P}_{E\to I}(\mathcal{D}_I - \mathcal{D}_{I*})$ and $\mathcal{R}_{IH} = \beta(1-\rho)\mathcal{P}_{E\to Q}\mathcal{D}_I$ have larger values under strategy 2 than strategy 1 for both distributions. However, for $\mathcal{R}_I = \beta\mathcal{P}_{E\to I}\mathcal{D}_I$, the GDM generates a smaller value under strategy 2 than strategy 1 whereas the PDM generates a larger value under strategy 2 than strategy 1. As a result, GDM produced a smaller $\mathcal{R}_C$ under strategy 2 (1.095 vs. 1.223) while GDM produced a larger $\mathcal{R}_C$ under strategy 2 (1.011 vs. 0.793). From this set of parameter values, it seems that the most significant difference between the distributions or strategies is the lower value of $\mathcal{R}_{IH} + \mathcal{R}_I$ for the PDM when quarantine is relatively high (strategy 1). This may be due to a lower $\mathcal{P}_{E\to I}$ value for the PDM with high quarantine. This suggests that the GDM may underestimate the role of quarantine in reducing the control reproduction number $\mathcal{R}_C$.

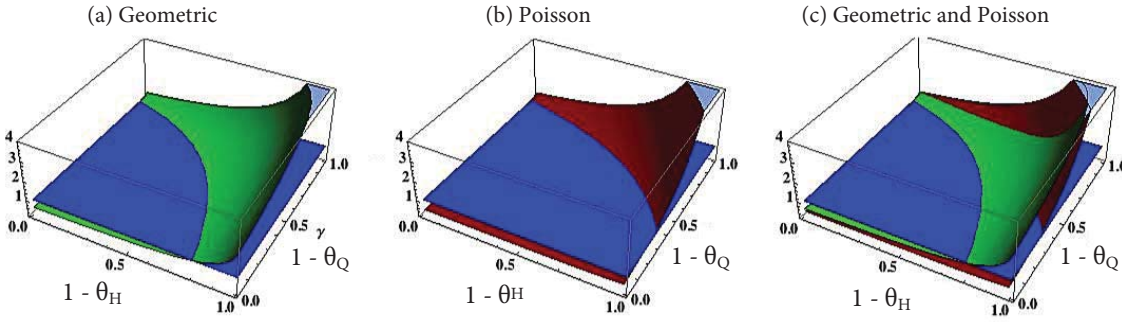

Figure 3.9. Joint effect of quarantine (θ_Q) and isolation (θ_H) on the reduction of $\mathcal{R}_C$. The two surfaces correspond to the GDM and PDM, while the plane indicates $\mathcal{R}_C = 1$.

In Figure 3.9, the joint effect of quarantine (θ_Q) and isolation (θ_H) on the reduction of $\mathcal{R}_C$ is illustrated. (A) shows the surface under GDA and (B) shows the same surface but under PDA. The plane corresponds to $\mathcal{R}_C = 1$ and (C) collects the graphs of both surfaces. The parameter values used are the same as in the previous figure. We observe that for this set of parameter values, PDA provides a lower estimate of $\mathcal{R}_C$ for most values of θ_Q and θ_H, except when either θ_Q is small (less quarantine) or θ_H is small (less isolation). We also observe that within PDM is possible to increase θ_Q

so that $\mathcal{R} < 1$ for each fixed θ_H (including the case when $\theta_H = 0$, i.e., no isolation), while this is not possible in the GDM case.

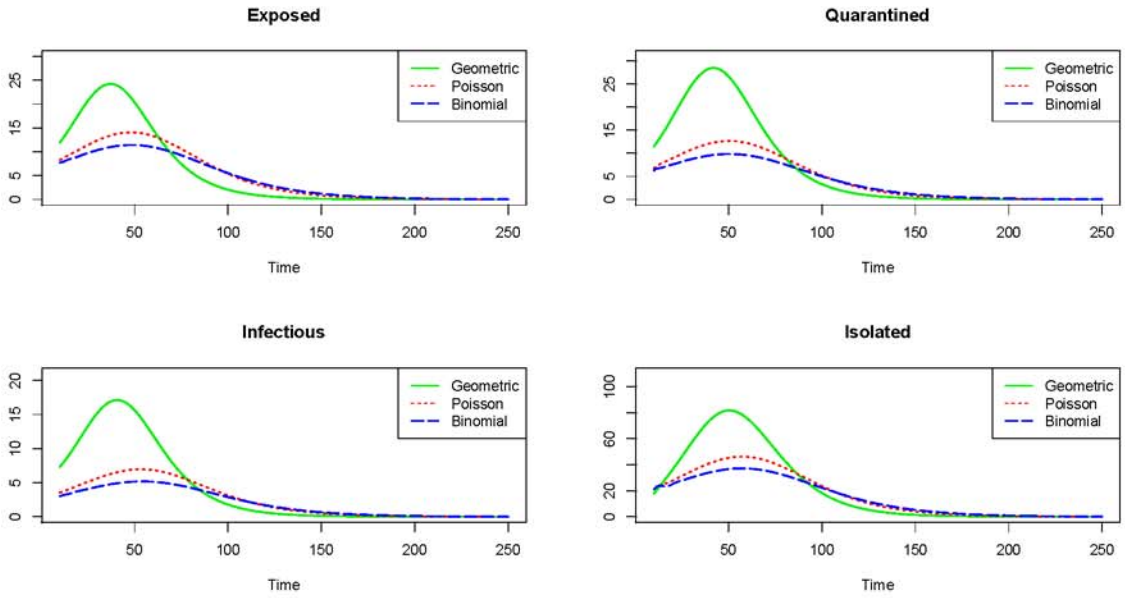

Figure 3.10. Numerical simulations showing the epidemic curves generated by the three models: GDA, PDA, and BDA from time $n = 10$ to $n = 250$. Control parameters are $\theta_Q = 0.3$ and $\theta_H = 0.2$. In this case, the GDM generates a much higher epidemic peak than the other two models.

In addition to the reproduction number and final epidemic size, we can also examine some of the characteristics of epidemic curves generated by the three models (GDM, PDM, and BDM) and the influence on these characteristics of quarantine and isolation, as shown in Figure 3.10. The values for the control parameters are $\theta_Q = 0.3, \theta_H = 0.2$, the initial condition is $S = 980, E_0 = 20, I_0 = Q_0 = H_0 = R_0 = 0$, and $\beta = .75., \rho = .95$. We observe that the GDM predicts a much higher peak for the initial epidemic than the other two models. However, it is not the case that the epidemic peak generated by the GDM is always higher. As seen in Figure 3.11, for different parameter values, the epidemic peak from the GDM may be lower than that generated by the other two models. Figure 3.11 was produced with the same initial conditions as Figure 3.10 and $\beta = .4., \rho = .95$, $\theta_Q = 0.1$, $\theta_H = 0.2$.

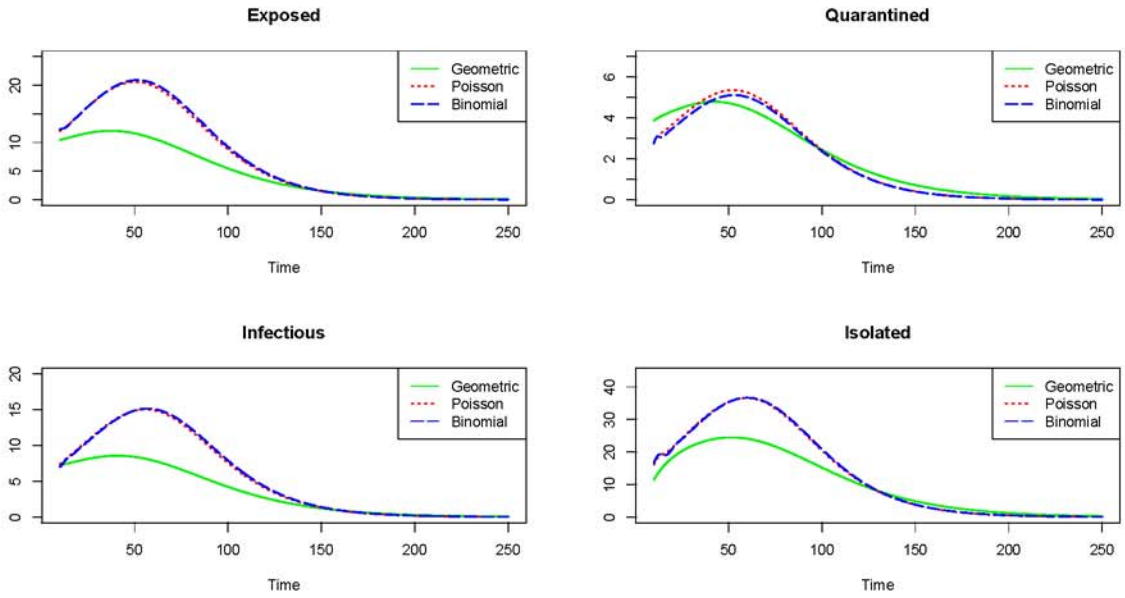

Figure 3.11. Contrasting with Figure 3.10, GDM generates a much lower epidemic peak than the other two models. All parameter values used for this figure are consistent with Figure 3.10, except $\theta_Q = 0.05$, (low quarantine effort).

Finally, to conclude our analysis of the GDM and PDM, the general formulas for for $\mathcal{R}_{C,g}$ and $\mathcal{R}_{C,p}$ (see Theorem 3.4.1) allow further examination of the role of its additive components, $\mathcal{R}_I$, $\mathcal{R}_{IH}$ and $\mathcal{R}_{QH}$. These effects are illustrated in the GDM (left) and the PDM (right) plots of Figure 3.12.

Figure 3.12 plots $\mathcal{R}_{I,w}$, $\mathcal{R}_{IH,w}$ and $\mathcal{R}_{QH,w}$ $(w = g, p)$ as a function of the infectious period. The thin solid curve corresponds to $\mathcal{R}_C$. The parameter values used for in Figure 3.12 are $\beta = 0.75$, $\rho = 0.7$, $\theta_Q = 0.4$, $\theta_H = 0.1$. We observe that $\mathcal{R}_{I,w}$ and $\mathcal{R}_{IH,w}$ have a much bigger impact on $\mathcal{R}_C$ than $\mathcal{R}_{IQ,w}$. Moreover, the contributions from $\mathcal{R}_{I,w}$ and $\mathcal{R}_{IH,w}$ are different for both distributions. Particularly, these effects are observed in the case of the geometric distribution where $\mathcal{R}_{I,g} > \mathcal{R}_{IH,g}$ for small infectious periods but $\mathcal{R}_{I,g} < \mathcal{R}_{IH,g}$ for larger infectious periods (and they are very close). In the case of the Poisson distribution, $\mathcal{R}_{IH,p}$ turns out to be significantly larger than $\mathcal{R}_{I,p}$ for all values of the infectious period in the range displayed. This

suggests that reducing $\mathcal{R}_{IH,p}$ (e.g., by increasing isolation efficiency ρ) might be more effective for reducing $\mathcal{R}_C$. Hence, the use of the PDM is more likely to emphasize the importance of isolation efficiency.

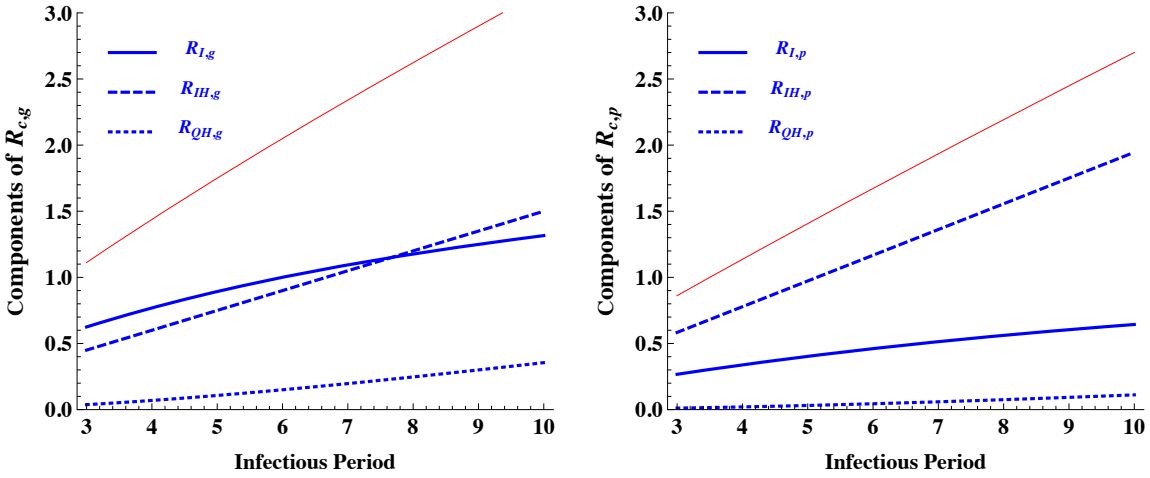

Figure 3.12. Plots of the components of $\mathcal{R}_C$ ($\mathcal{R}_I$, $\mathcal{R}_{IH}$, and $\mathcal{R}_{QH}$) as functions of the control parameters (θ_Q and θ_H). The two models considered are the GDM and the PDM.

3.5 Conclusions and observations

This chapter focuses primarily on the evaluation of the impact of epidemiological and control stage-duration distributions on the quantitative dynamics of discrete-time single-outbreak epidemiological models. The analyses presented here allow the evaluation of the final epidemic size and the role of stage-duration distributions on the additive components in the control reproduction number. The models considered are discrete-time SEIR-type single-outbreak epidemic models with build in control strategies (quarantine and isolation). The results are discussed in particular within the context of three classical discrete parametric distributions: Geometric, Poisson and Binomial. General model results suggest for example, that the use of distinct parametric distributions can lead to contradictory predictions, see Figure 3.8. *Some* of the consequences that arise from the use of selected distributions in the context

of particular intervention efforts were analyzed. A comprehensive evaluation requires the use of data sets and model validation approaches, topics left for future work. Fortunately, the framework introduced in this chapter allows for the incorporating of empirical stage-duration distributions. The use of data-generated stage-duration distributions directly provides an approach that some may consider satisfactory, particularly when model results turned out to be highly sensitive to distribution shape parameters.

We remark that the main contribution of this study is the construction and analysis of a discrete-time epidemic model that allows an arbitrarily distributed duration for the infectious period. This can provide an important advantage of using data in the application of the model than models that assume a specific parametric distribution of the disease stage. Indeed, if we were going to try to fit exponentially waiting times there would not be an advantage in the use of geometric times, but if the data was just collected and the duration of times was arbitrary then this model has an advantage as one could just use the data. If one were to fit a model then one may feel tempted, lets say to use a gamma or generalized gamma distribution (for continuous-time model) or to use a negative binomial (for discrete-time models), but as it was shown in the case of HIV/AIDS by the late Stephen Lagakos and Marcelo Pagano, the use of a parametric distribution [53], is simply not good. They found a "perfect" fit with incubation period distributions of 10 years and 100 years. In our modeling framework, using a discrete model allows the use of the data somewhat closer to what those using non-parametric methods tend to use. Yes, the results from the discrete-time model are not unexpected but the level of arbitrariness incorporated allow us for the use of the data which is similar to the distribution-free approaches that have been argued by the statisticians involved in HIV as most effective and realistic (discrete distributions). Again, the goal here is not to fit data but to use the data directly.

To the best of our knowledge, no discrete-time epidemic models have been developed and analyzed that include quarantine and isolation while the disease durations

are allowed to have arbitrary distributions. Thus, the construction and analysis of a such discrete-time model provided in this study can contribute to the applicability of epidemic models in public health policymaking. As mentioned earlier a discrete-time model is more tractable than continuous-time model, specially when an arbitrary distribution is used to model waiting times in disease stages.

Another major contribution of this study is the derivation of the analytic formulas for the reproduction numbers and final epidemic sizes for models with arbitrarily distributed disease durations, see Theorem 3.2.3 in Section 3.2.2 for details. The general formula for $\mathcal{R}_C$ allows further examination of the role of its additive components $\mathcal{R}_I$, $\mathcal{R}_{IH}$ and $\mathcal{R}_{QH}$. In particular, for the analysis of Geometric vs Poisson distributions, these effects are illustrated in Figure 3.12. It can be observed that the use of the PDM is more likely to emphasize the importance of isolation efficiency.

Finally, the question of what stage distribution(s) is (are) more appropriate depends on what we actually know about the epidemiological process. The specifics of each disease provide the most critical information. Researchers involved in the study of the dynamics of infectious diseases seem to prefer to work with models that make use of geometric stage-duration distributions. Needless to say, the latent or infectious stage distributions may be fit better alternative distributions, for a great number of infectious diseases. Does the general use of geometric distributions matter? In the goal is to carry out a qualitative study within single-outbreak epidemic models then no, but if the goal is to assess quantitatively the efficacy of control measures for specific diseases then the answer is, most likely yes.

4. MULTI-PATCH MODEL WITH ARBITRARILY DISTRIBUTED INFECTIOUS PERIOD

The work presented in this chapter was done in collaboration with Chavez-Casillas and Feng. Most of the results and ideas in this chapter were published in Mathematical Biosciences [82]. My contribution includes model development and analysis as well as the writing of the paper. All models considered in this chapter are stochastic and for discrete-time.

4.1 Introduction

Historically, some of the first stochastic models with arbitrarily distributed infectious period were considered in [64, 68, 83], but Sellke's construction [67] helped derive stronger results such as those in [65, 66]. In general, mathematical formulations of continuous-time models are complicated when an arbitrarily distributed infectious period is included [64–66, 68, 83–85]. In contrast, analogous discrete-time models can be formulated in a way that is much easier to understand and analyze (see, for example, [21, 28, 57]). Discrete models also have the capability of incorporating distributions directly from empirical data, whereas for continuous-time models the parameters for a standard distribution have to be estimated via data fitting. In spite of this, little attention has been given to discrete models in a stochastic framework.

In this chapter, a stochastic discrete-time model is developed to study the spread of an infectious disease in an n-patch environment. The model includes an arbitrary distribution of the (random) infectious period T, and the results are used to investigate how the distribution of T may influence the model outcomes. Although discrete, the model developed in this chapter goes one step further than the model discussed in Section 1.3. As a result of this added complexity the formulas for both $\mathcal{R}_0$ and

$\mathbb{P}_0$ are significantly more complicated (compare Theorem 1.3.1 vs Theorem 4.2.1 and 4.2.2).

In Section 4.2, a general model with n patches and Markov displacement is described. For an infected individual, the infectious period (T) is assumed to be a discrete random variable with an arbitrary distribution and finite mean. We derive a formula for the basic reproduction number $\mathcal{R}_0$, which is given by the spectral radius of the mean offspring matrix, a matrix that depends on D and the probability generating function (pgf) of T. An equation for the probability of minor epidemic (extinction probability) $\mathbb{P}_0$ is also derived. Our model was inspired by the work of P. Neal, presented in [85].

In Section 4.3, the general results are applied to the case $n = 2$ patches. In addition to an exact formula, lower and upper bounds for $\mathcal{R}_0$ are also identified. To examine the effect that the distribution of T has on $\mathcal{R}_0$, we consider three specific distributions: shifted Geometric, shifted Negative Binomial, and shifted Poisson. The reproduction numbers corresponding to these distributions have a specific order relation. Numerical simulations for the two-patch model are carried out to explore the influence of the T distribution on the final epidemic size ($\mathcal{F}$), duration of epidemic ($\mathcal{D}$), as well as the probability of disease extinction ($\mathbb{P}_0$).

4.2 Formulation and analysis of the general model

We adopt the approach used in [84, 85] for continuous models to develop a *discrete* stochastic SIR metapopulation model, in a closed population, for an epidemic outbreak with an arbitrarily distribution for the infectious period (IP). The main objective of this study is to investigate how the distribution of IP may affect the model outcomes, particularly the basic reproduction number $\mathcal{R}_0$ and the probability of major epidemic ($1 - \mathbb{P}_0$).

Consider a metapopulation with n sub-populations (patches). Let $N_i(t)$ denote the size of population i at time t for $i = 1, 2, \cdots, n$. Assume that the total population

Table 4.1.
List of parameters and symbols commonly used in Chapter 4

Symbols	**Definitions**
$N_i,\ N$	Population sizes, $N = N_1 + \cdots + N_n$
T	Random infectious period
U	Markov Chain that controls movement between patches
D	$= (\sigma_{ij})$, Markov matrix associated of U
π_i	Stationary probability of U
β_i	Number of effective contacts per unit of time in population i (Poisson)
m_{ij}	Average number of offsprings (secondary infections) generated in population j by an individual from population i during the lifetime (T)
M	$= (m_{ij})$, Mean offspring matrix
$G(\vec{s})$	pgf of the offspring distribution
$\phi(s)$	pgf of T
$\mathcal{F}$	Final size of the epidemic
$\mathcal{D}$	Duration of the epidemic
$\mathcal{P}$	Peak of the epidemic
$\mathbb{P}_0$	Probability of disease extinction, Probability of minor epidemic
Model with $n = 2$ populations	
a	Probability of staying in population 1 per time unit, (σ_{11})
b	Probability of staying in population 2 per time unit (σ_{22})
λ	Smaller eigenvalue of D
$\mathcal{R}_{0i}$	Basic reproduction number for population $i = 1, 2$
$\overline{\mathcal{R}}_0$	Weighted average of $\mathcal{R}_{01}$ and $\mathcal{R}_{02}$ according to π_1 and π_2

size $N = \sum_{i=1}^{n} N_i(t)$ remains constant for all time. Individuals can move between any

two patches, this movement is determined by a *discrete* time Markov chain U, which is described by the transition matrix $D = (\sigma_{ij})$. The entry σ_{ij} represents the probability of moving from population i to population j, at each time step.

Effective contacts by individual in population i, per unit of time, is modeled by a Poisson random variable with parameter β_i. In the early stages of the epidemic most effective contacts will produce an infection because most individuals are susceptible. The disease transmission dynamics within each sub-population is governed by an SIR model. It is assumed that individuals become immune after recovery. Let T denote the random variable for the IP (the time until recovery), which is assumed to be the same for all sub-populations. Here, we place no restriction on the T distribution, other than T is discrete, non negative and has a finite mean. All variables and parameters are listed in Table 4.1. Figure 4.1 provides a graphical representation of the model described above.

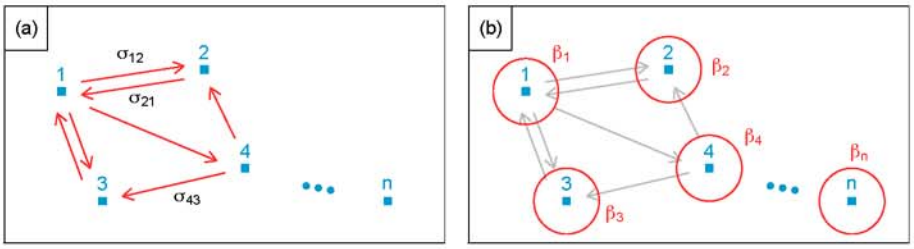

Figure 4.1. **(a)** Individuals move from patch to patch at time $t \in \mathbb{N}$ according to the Markov chain U. **(b)** Once the infection process has started in one patch, the disease can spread to other patches. Contacts by an infected individual, per unit of time in patch i, is described by Poisson(β_i).

New infections are produced between time steps in the interval $(t, t+1)$, while recovery and geographical displacement (governed by the discrete random variables T and U) occur at integer time points. This simplification assumption accompanies discrete models and not their continuous counterpart. However, the assumption is biologically reasonable for different situations, including (i) commuters traveling at

peak hours from city to city or (ii) domestic animals who are transported from farm to farm at night.

Assume that, at time $t = 0$, $N_i(0) \approx N\pi_i$ $(i = 1, 2, \cdots, n)$, where $\pi = (\pi_i)_{i=1}^n$ is the stationary probability (i.e. $\pi D = \pi$). Thus, although random, the subpopulation $N_i(t)$ will remain close to its initial value throughout time. Some of the properties of the model are described in the following sections.

4.2.1 Computation of $\mathcal{R}_0$

In this section, we follow the approach presented by Neal in [85]. The early stages of an epidemic is approximated by a properly defined multi-type branching process, see Section 1.3.1 for a discussion on the use branching process on the computation of the basic reproduction number $\mathcal{R}_0$.

To facilitate the derivation of a formula for $\mathcal{R}_0$ the following notation is introduced:

$\zeta_{ij} =$ random time spent in patch j (before recovery) by an infectious individual from patch i;

$m_{ij} =$ average number of "offspring" (i.e., secondary infections) that an individual, from patch i, can produce in patch j during the entire "life span" (i.e. the random infectious period modeled by T);

$M =$ (m_{ij}), the mean offspring matrix.

Then, $\mathcal{R}_0$ is given by the spectral radius of the matrix M [16, 17, 68, 71, 86], which entries m_{ij} can be written as

$$m_{ij} = \beta_j \mathbb{E}(\zeta_{ij}). \tag{4.1}$$

By conditional expectation $\mathbb{E}(\zeta_{ij}) = \sum_{t=0}^{\infty} \mathbb{E}(\zeta_{ij}|T = t)\mathbb{P}(T = t)$ and

$$\mathbb{E}(\zeta_{ij}|T = t) = \mathbb{E}\left(\sum_{k=0}^{t-1} \mathbb{I}_{U_i(k)=j}\right) = \sum_{k=0}^{t-1} \mathbb{P}(U_i(k) = j) = \sum_{k=0}^{t-1} \sigma_{ij}^{(k)},$$

where $\sigma_{ij}^{(k)}$ denotes the $ij-$th entry of the matrix D^k, $U_i(k)$ the state of the Markov chain at time k given that $U_i(0) = i$, and $\mathbb{I}_{U_i(k)=j}$ the indicator function of the event

$U_i(k) = j$. Notice that new infections at time t are generated by infective individuals at time $t-1$, which is why the sum above has been taken from 0 to $t-1$. Combining the last two equations we obtain the matrix of expectations of ζ_{ij}

$$\begin{bmatrix} \mathbb{E}(\zeta_{11}) & \cdots & \mathbb{E}(\zeta_{1n}) \\ \vdots & \ddots & \vdots \\ \mathbb{E}(\zeta_{n1}) & \cdots & \mathbb{E}(\zeta_{nn}) \end{bmatrix} = \sum_{t=1}^{\infty} \mathbb{P}(T=t) \sum_{k=0}^{t-1} D^k = \mathbb{E}\left(\sum_{k=0}^{T-1} D^k \right). \tag{4.2}$$

Let $\lambda_1, \ldots, \lambda_n$ be the eigenvalues of the stochastic matrix $D = (\sigma_{ij})$. Since D is a Markov matrix, $\lambda_i = 1$ for some i and $|\lambda_i| \leqslant 1 \ \forall i$. If D is diagonalizable, then there exists a nonsingular matrix Λ such that $D^k = \Lambda \ \mathrm{diag}(1, \lambda_2^k, \ldots, \lambda_n^k) \ \Lambda^{-1}$, so that

$$\sum_{k=0}^{t-1} D^k = \Lambda \ \mathrm{diag}\left(t, \sum_{k=0}^{t-1} \lambda_2^k, \ldots, \sum_{k=0}^{t-1} \lambda_n^k \right) \ \Lambda^{-1}. \tag{4.3}$$

Substitution of (4.3) into (4.2) yields

$$\begin{aligned} \begin{bmatrix} \mathbb{E}(\zeta_{11}) & \cdots & \mathbb{E}(\zeta_{1n}) \\ \vdots & \ddots & \vdots \\ \mathbb{E}(\zeta_{n1}) & \cdots & \mathbb{E}(\zeta_{nn}) \end{bmatrix} &= \Lambda \left[\sum_{t=1}^{\infty} \mathbb{P}(T=t) \ \mathrm{diag}\left(t, \sum_{k=0}^{t-1} \lambda_2^k, \ldots, \sum_{k=0}^{t-1} \lambda_n^k \right) \right] \Lambda^{-1} \\ &= \Lambda \ \mathrm{diag}\big(\varphi(1), \varphi(\lambda_2), \ldots, \varphi(\lambda_n)\big) \ \Lambda^{-1}, \end{aligned} \tag{4.4}$$

where φ is the function defined by

$$\varphi(s) = \sum_{t=1}^{\infty} \mathbb{P}(T=t) \sum_{k=0}^{t-1} s^k = \begin{cases} \mathbb{E}(T) & \text{if} \quad s = 1, \\ \mathbb{E}\left(\frac{1-s^T}{1-s} \right) & \text{if} \quad s \neq 1. \end{cases} \tag{4.5}$$

The following theorem, a discrete equivalent of a result presented in [85], is obtained using equalities (4.1) and (4.4).

Theorem 4.2.1 *$\mathcal{R}_0$ is given by the spectral radius of M, $\varrho(M)$, where*

$$M = \mathbb{E}\left(1 + D + \cdots + D^{T-1}\right) \mathit{diag}(\beta_1, \ldots, \beta_n).$$

Moreover, if the Markov matrix D is diagonalizable then

$$M = \Lambda \ \mathit{diag}\big(\varphi(1), \varphi(\lambda_2), \ldots, \varphi(\lambda_n)\big) \ \Lambda^{-1} \ \mathit{diag}(\beta_1, \ldots, \beta_n).$$

Remark. Notice that the trivial case $T = 0$ yields $M = 0$ and $\mathcal{R}_0 = 0$. For this reason $T \neq 0$ is assumed from now on.

This result can also be expressed using the probability generating function (pgf) of T, which we denote by $\phi(s)$, i.e.,

$$\phi(s) = \mathbb{E}\left(s^T\right). \tag{4.6}$$

For $s \neq 1$ (see (4.5)),

$$\varphi(s) = \frac{1 - \phi(s)}{1 - s}. \tag{4.7}$$

The series $\phi(s) = \sum_{t=1}^{\infty} s^t \mathbb{P}(T = t)$ is absolutely convergent in $|s| \leqslant 1$, and so is $\varphi(s)$. An explicit formula for the pgf is usually available for most commonly used discrete distributions. In addition, it is easily verified that $0 \leqslant \varphi(s) \leqslant \mathbb{E}(T)\ \forall s \in [-1, 1]$.

Applications of Theorem 4.2.1 are illustrated later when specific distributions for T are considered in the model with $n = 2$ patches (see Section 4.3.1). This result also allows us to compare the reproduction numbers $\mathcal{R}_0$ corresponding to different distributions of T (see Section 4.3.2).

4.2.2 Probabilities of minor and major epidemics

When it comes to stochastic models, the probability of extinction of the branching process, also known as the probability of a minor epidemic,($\mathbb{P}_0$), provides insightful results about the model [50, 51, 65, 68]. In this section, a formula for $\mathbb{P}_0$ is derived using the probability generating function of the offspring distribution.

Obtaining an expression for the pgf of the offspring distribution, denoted by G, is important because the probability of extinction of a branching process can be determined using G [72]. Let η_{ij} be the number of offsprings (secondary infections) generated in population j by an individual from population i. Since the sum of inde-

pendent Poisson random variables is still Poisson we have that $\eta_{ij}|\zeta_{ij} = \text{Poisson}(\beta_j\zeta_{ij})$. Let $\vec{s} = (s_1, \ldots, s_n)$. Then the function $G : [0,1]^n \to [0,1]^n$ can be expressed as

$$\begin{aligned} G_i(\vec{s}) &= \mathbb{E}\left(\prod_{j=1}^n s_j^{\eta_{ij}}\right) = \mathbb{E}\left(\mathbb{E}\left(\prod_{j=1}^n s_j^{\eta_{ij}} \middle| \zeta_{i1}, \ldots, \zeta_{in}\right)\right) \\ &= \mathbb{E}\left(\prod_{j=1}^n \mathbb{E}\left(s_j^{\eta_{ij}} \middle| \zeta_{i1}, \ldots, \zeta_{in}\right)\right) = \mathbb{E}\left(e^{-\sum_{j=1}^n \beta_j\zeta_{ij}(1-s_j)}\right). \end{aligned} \tag{4.8}$$

Define $\zeta_{ij}(t)$ to be the time spent in group j by an individual from group i up to time t, and

$$X_i(t) = \sum_{j=1}^n \beta_j\zeta_{ij}(t)(1-s_j).$$

Using the conditional expectation formula, equation (4.8) becomes

$$\begin{aligned} G_i(\vec{s}) &= \mathbb{E}\left(e^{-\sum_{j=1}^n \beta_j\zeta_{ij}(1-s_j)}\right) = \sum_{t=1}^\infty \mathbb{E}\left(e^{-\sum_{j=1}^n \beta_j\zeta_{ij}(1-s_j)}\middle| T=t\right)\mathbb{P}(T=t) \\ &= \sum_{t=1}^\infty \mathbb{E}\left(e^{-X_i(t)}\right)\mathbb{P}(T=t) \end{aligned} \tag{4.9}$$

An explicit formula for G is provided in the following

Theorem 4.2.2 *Let $A(\vec{s})$ be the $n \times n$ matrix given by $A(\vec{s})_{ij} = e^{-\theta_i}\sigma_{ij}$. Let $E(\vec{s})$ be the $n\times 1$ matrix given by $E(\vec{s})_i = e^{-\theta_i}$, where $\theta_j = \beta_j(1-s_j)$. Then $G : [0,1]^n \to [0,1]^n$ is given by*

$$G(\vec{s})^{tr} = \left(G_1(\vec{s}), \ldots, G_n(\vec{s})\right)^{tr} = \sum_{t=1}^\infty A(\vec{s})^{t-1}E(\vec{s})\ \mathbb{P}(T=t)$$

Proof To simplify notation, let $\theta_j = \beta_j(1-s_j)$. Then

$$X_i(t) = \theta_1\zeta_{i1}(t) + \theta_2\zeta_{i2}(t) + \cdots + \theta_n\zeta_{in}(t).$$

Alternatively, $X_i(t) = \theta_i + \theta_{U_i(1)} + \cdots + \theta_{U_i(t-1)}$. Thus, by conditional expectation

$$\begin{aligned} \mathbb{E}(e^{-X_i(t+1)}) &= \mathbb{E}\left[\mathbb{E}\left(e^{-X_i(t+1)}|U_i(1)\right)\right] = \sum_{j=1}^n \mathbb{E}\left(e^{-X_i(t+1)}|U_i(1)=k\right)\mathbb{P}(U_i(1)=k) \\ &= \sum_{j=1}^n \mathbb{E}\left(e^{\theta_i+\theta_k+\cdots+\theta_{U_i(t)}}|U_i(1)=k\right)\sigma_{ik} = \sum_{j=1}^n e^{\theta_i}\mathbb{E}\left(e^{-X_k(t)}\right)\sigma_{ik} \end{aligned}$$

The last equality makes use of the stationary property of the Markov Chain U_i. For ease of notation, let A and E represent the matrices $A(\vec{s})$ and $E(\vec{s})$, this is

$$A = \begin{bmatrix} e^{-\theta_1}\sigma_{11} & e^{-\theta_1}\sigma_{12} & \cdots & e^{-\theta_1}\sigma_{1n} \\ e^{-\theta_2}\sigma_{21} & e^{-\theta_2}\sigma_{22} & \cdots & e^{-\theta_2}\sigma_{2n} \\ \vdots & \vdots & \ddots & \vdots \\ e^{-\theta_n}\sigma_{n1} & e^{-\theta_n}\sigma_{n2} & \cdots & e^{-\theta_n}\sigma_{nn} \end{bmatrix}, \qquad E = \begin{bmatrix} e^{-\theta_1} \\ e^{-\theta_2} \\ \vdots \\ e^{-\theta_n} \end{bmatrix}$$

It follows by induction that $\left(\mathbb{E}(e^{-X_1(t)}), \ldots, \mathbb{E}(e^{-X_n(t)})\right)^{tr} = A^{t-1}E$: clearly, for $t = 1$, $\mathbb{E}(e^{-X_i(1)}) = e^{-\theta_i}$ and $A^0E = E$. Now, assume the statement is true for t and prove for $t + 1$:

$$A^tE = A(A^{t-1}E) = A\begin{bmatrix} \mathbb{E}(e^{-X_1(t)}) \\ \mathbb{E}(e^{-X_2(t)}) \\ \vdots \\ \mathbb{E}(e^{-X_n(t)}) \end{bmatrix} = \begin{bmatrix} \sum_{k=1}^{n} e^{-\theta_1}\sigma_{1k}\mathbb{E}(e^{-X_k(t)}) \\ \sum_{k=1}^{n} e^{-\theta_2}\sigma_{2k}\mathbb{E}(e^{-X_k(t)}) \\ \vdots \\ \sum_{k=1}^{n} e^{-\theta_n}\sigma_{nk}\mathbb{E}(e^{-X_k(t)}) \end{bmatrix} = \begin{bmatrix} \mathbb{E}(e^{-X_1(t+1)}) \\ \mathbb{E}(e^{-X_2(t+1)}) \\ \vdots \\ \mathbb{E}(e^{-X_n(t+1)}) \end{bmatrix}$$

From equation (4.9), the i^{th} component of G is given by

$$G_i(\vec{s}) = \sum_{t=1}^{\infty} \mathbb{E}\left(e^{-X_i(t)}\right) \mathbb{P}(T = t),$$

therefore

$$G(\vec{s}) = \left(G_1(\vec{s}), \ldots, G_n(\vec{s})\right) = \sum_{t=1}^{\infty} A^{t-1}E \ \mathbb{P}(T = t)$$

■

The extinction probability (or probability of minor epidemic) is determined by the equation $G(\vec{s}) = \vec{s}$. This is a well known fact from the theory of branching process [72], see Section 1.3.2 for a discussion on this topic. If $\mathcal{R}_0 < 1$, the only fixed point of $G(\vec{s})$ is $(1, 1, \ldots, 1)$. If $\mathcal{R}_0 > 1$, the equation $G(\vec{s}) = \vec{s}$ has a nontrivial solution $\vec{z} = (z_1, \ldots, z_n) \in (0, 1)^n$. Each value z_i represents the extinction probability given the initial condition $I_i(0) = 1$ and $I_j(0) = 0 \ \forall j \neq i$. Thus, if there are m_i

initial infective individuals in population i at $t = 0$, then the extinction probability $\mathbb{P}_0$ (probability of minor epidemic) is

$$\mathbb{P}_0 = \prod_{i=1}^{n} z_i^{m_i}. \tag{4.10}$$

Naturally, the probability that a major epidemic occurs is $1 - \mathbb{P}_0$.

Theorem 2 is valid for any distribution of T and any number n of subpopulations. When a specific distribution of T is used, the formula may simplify and (4.10) can be determined numerically. Examples with $n = 2$ patches are presented in Section 4.3.3.

4.3 Additional insights from the two-patch model

When n is large, an explicit expression for the spectral radius of the matrix M can be difficult to obtain. However, for $n = 2$ patches, most formulas can be dramatically simplified, especially when specific distributions of T are used. In Section 4.3.1, explicit formulas for $\mathcal{R}_0$ and the pgf of offspring distribution $G(\vec{s})$ are derived. In Section 4.3.2, the effect of the distribution of T on $\mathcal{R}_0$ is analyzed.Finally, Section 4.3.3 includes some simulation results and Section 4.3.4 presents a more detailed formula for G, which is used to compute the probabilities of major and minor epidemics.

4.3.1 Properties of $\mathcal{R}_0$

Without loss of generality, assume that the transmission parameters β_i satisfy $\beta_1 \geqslant \beta_2$. To simplify the notation, let $a = \sigma_{11}$ and $b = \sigma_{22}$. Then, the transition matrix of the Markov chain becomes

$$D = \begin{bmatrix} a & 1-a \\ 1-b & b \end{bmatrix}. \tag{4.11}$$

To avoid extreme cases, let $a, b \in (0, 1)$. The eigenvalues of D are 1 and

$$\lambda = a + b - 1. \tag{4.12}$$

Let π denote the stationary probability distribution of the Markov chain described by D (i.e. $\pi D = \pi$). It is easy to verify that $\pi = [\pi_1, \pi_2]$ with

$$\pi_1 = \frac{1-b}{2-a-b} \in (0,1), \qquad \pi_2 = \frac{1-a}{2-a-b} \in (0,1).$$

The matrix D can be diagonalized and rewritten as

$$D = \Lambda \begin{bmatrix} 1 & 0 \\ 0 & \lambda \end{bmatrix} \Lambda^{-1}, \quad \text{where} \quad \Lambda = \begin{bmatrix} 1 & 1-a \\ 1 & -(1-b) \end{bmatrix}. \tag{4.13}$$

From Theorem 1, the mean offspring matrix is given by

$$M = \Lambda \begin{bmatrix} \mathbb{E}(T) & 0 \\ 0 & \varphi(\lambda) \end{bmatrix} \Lambda^{-1} \begin{bmatrix} \beta_1 & 0 \\ 0 & \beta_2 \end{bmatrix} = \begin{bmatrix} \beta_1[\pi_1\mathbb{E}(T) + \pi_2\varphi(\lambda)] & \beta_2\pi_2[\mathbb{E}(T) - \varphi(\lambda)] \\ \beta_1\pi_1[\mathbb{E}(T) - \varphi(\lambda)] & \beta_2[\pi_2\mathbb{E}(T) + \pi_1\varphi(\lambda)] \end{bmatrix}.$$

Recall from (4.5) that $\varphi(1) = \mathbb{E}(T)$ is the mean infectious period and $\varphi(\lambda) = \mathbb{E}\left(\frac{1-\lambda^T}{1-\lambda}\right)$. For ease of notation, let

$$\mathcal{R}_{0i} = \beta_i \mathbb{E}(T), \qquad \overline{\mathcal{R}}_0 = \pi_1\mathcal{R}_{01} + \pi_2\mathcal{R}_{02}. \tag{4.14}$$

$\overline{\mathcal{R}}_0$ can be interpreted as the weighted average of $\mathcal{R}_{01}$ and $\mathcal{R}_{02}$, the intuitive patch reproduction numbers. Finally, by analyzing M we can find not only the exact value of $\mathcal{R}_0$ but also other important properties that are listed in the next Theorem.

Theorem 4.3.1 *Let $z = \varphi(\lambda)$ and $\phi(\lambda)$, $\varphi(\lambda)$, λ, $\overline{\mathcal{R}}_0$, $\mathcal{R}_{01}$ be defined as in* (4.6), (4.7), (4.12), (4.14). *For $n = 2$ patches,*

(i) An explicit expression for $\mathcal{R}_0$ is

$$\mathcal{R}_0 = \frac{\overline{\mathcal{R}}_0 + z(\beta_1\pi_2 + \beta_2\pi_1) + \sqrt{\left[\overline{\mathcal{R}}_0 + z(\beta_1\pi_2 + \beta_2\pi_1)\right]^2 - 4\beta_1\beta_2\mathbb{E}(T)z}}{2}; \tag{4.15}$$

(ii) $\mathcal{R}_0$ has the following upper and lower bounds:

$$\overline{\mathcal{R}}_0 \leqslant \mathcal{R}_0 \leqslant \mathcal{R}_{01};$$

(iii) $\mathcal{R}_0$ is decreasing with respect to $\phi(\lambda)$ and increasing with respect to z.

Proof Following a similar approach that the one presented in [85], define $z = \varphi(\lambda)$. Denote by

$$f_z(x) = [\mathcal{R}_{01}\pi_1 + z\beta_1\pi_2 - x][\mathcal{R}_{02}\pi_2 + z\beta_2\pi_1 - x] - (\mathbb{E}(T) - z)^2\beta_1\beta_2\pi_1\pi_2$$

the characteristic polynomial of M. Straightforward calculations yield

$$f_z(0) > 0, \quad f_z(\mathcal{R}_{02}) \leqslant 0, \quad f_z(\overline{\mathcal{R}}_0) \leqslant 0, \quad \text{and} \quad f_z(\mathcal{R}_{01}) \geqslant 0.$$

Therefore, $f_z(x)$ has two real roots. $\mathcal{R}_0$, the dominant eigenvalue of M, is in the interval $[\overline{\mathcal{R}}_0, \mathcal{R}_{01}]$, as illustrated in Figure 4.2. To analyze the connection between the distribution of T and $\mathcal{R}_0$, consider two random variables with different distributions but the same mean, i.e., $\mathbb{E}(T_1) = \mathbb{E}(T_2)$ (so that the two distributions are "comparable"). Let $z_i = \varphi(\lambda, T_i) = \frac{1-\mathbb{E}(\lambda^{T_i})}{1-\lambda}$. Through z_i, the two distributions may yield different reproduction numbers, which we denote by $\mathcal{R}_0^{T_1}$ and $\mathcal{R}_0^{T_2}$. Notice that $\mathcal{R}_{01}, \mathcal{R}_{02}$ and $\overline{\mathcal{R}}_0$ do not depend on z_i (see (4.14)). Assume that $z_1 \leqslant z_2$, then it can be verified that

$$f_{z_1}(\mathcal{R}_0^{T_2}) = \frac{z_2 - z_1}{\mathbb{E}(T_1)}\left[(\mathcal{R}_{01} - \mathcal{R}_0^{T_2})(\mathcal{R}_0^{T_2} - \mathcal{R}_{02}) + \mathcal{R}_0^{T_2}(\mathcal{R}_0^{T_2} - \overline{\mathcal{R}}_0)\right] \geqslant 0.$$

Thus, $f_{z_1}(\mathcal{R}_0^{T_2}) \geqslant f_{z_1}(\mathcal{R}_0^{T_1}) = 0$. Since $\overline{\mathcal{R}}_0 \leqslant \mathcal{R}_0^{T_i} \leqslant \mathcal{R}_{01}$ $(i = 1, 2)$ and f is an increasing function on $(\overline{\mathcal{R}}_0, \mathcal{R}_{01})$, it follows that $\mathcal{R}_0^{T_1} \leqslant \mathcal{R}_0^{T_2}$. A graphical representation of this argument is provided in Figure 4.2. Finally, since $z_1 \leqslant z_2$ if and only if $\mathbb{E}(\lambda^{T_2}) \leqslant \mathbb{E}(\lambda^{T_1})$, we conclude that $\mathcal{R}_0$ is a decreasing (increasing) function of $\phi(\lambda)$ $(\varphi(\lambda))$. This completes the proof of Theorem 4.3.1.

■

Remark. If $\beta = \beta_1 = \beta_2$ (i.e., identical transmission in both sub-populations), formula (4.15) reduces to $\mathcal{R}_0 = \mathcal{R}_{0i} = \overline{\mathcal{R}}_0 = \beta\mathbb{E}(T)$, which is consistent with the standard simple SIR model with a single population. In the following sections we assume that $\beta_1 > \beta_2$, to avoid this trivial case.

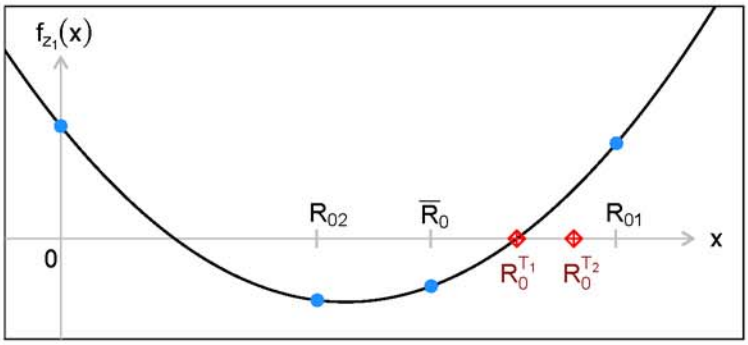

Figure 4.2. Plot of the characteristic polynomial $f_{z_1}(x)$.

4.3.2 Effect of the distribution of infectious period T on $\mathcal{R}_0$

To investigate how the choice of the IP distribution may affect $\mathcal{R}_0$, we examine our model under several distributions for T and compare the corresponding $\mathcal{R}_0$ values. We consider two models to be *comparable* if they have the same values for β_1, β_2, π, and mean infectious period $\mathbb{E}(T)$.

The following four distributions will be considered: **A.** shifted Geometric (sGeom); **B.** shifted Negative Binomial (sNegBinom); **C.** shifted Poisson (sPoisson); and **D.** discrete with finitely many points (for example the empirical distribution obtained from data). In all cases the support of T lies in $\mathbb{N}$. For convenience of, we list below the specifics of each distribution as well as relevant quantities involved in $\mathcal{R}_0$.

A. $T \sim \text{sGeom}(\gamma)$. The probability mass function (pmf) is $\mathbb{P}(T = t) = \gamma(1-\gamma)^{t-1}$ for $t \in \{1, 2, 3, \dots\}$ and $0 < \gamma < 1$. The mean and pgf are given by

$$\mathbb{E}(T) = \frac{1}{\gamma}, \quad \phi_g(\lambda) = \mathbb{E}\left(\lambda^T\right) = \frac{\gamma\lambda}{1-\lambda(1-\gamma)} = \frac{\lambda}{\mathbb{E}(T) - \lambda[\mathbb{E}(T)-1]}.$$

B. $T \sim \text{sNegBinom}(k, \eta)$. The pmf is given by

$$\mathbb{P}(T = t) = \binom{t-1+k-1}{t-1}\eta^k(1-\eta)^{t-1} \quad \text{for } t \in \{1, 2, 3, \dots\},$$

and $\eta = \frac{k}{\mathbb{E}(T)+k-1}$ for $k \in \mathbb{N}$. The mean is $\mathbb{E}(T) = \frac{(1-\eta)k}{\eta} + 1$ and pgf is given by

$$\phi_{nb_k}(\lambda) = \mathbb{E}\left(\lambda^T\right) = \lambda\left(\frac{\eta}{1-\lambda(1-\eta)}\right)^k = \lambda\left(\frac{k}{\mathbb{E}(T)-\lambda[\mathbb{E}(T)-1]-1+k}\right)^k.$$

If $k = 1$, this distribution is equivalent to a sGeom(γ).

C. T is sPoisson(κ) with parameter κ. The pmf is $\mathbb{P}(X = t) = e^{-\kappa}\frac{\kappa^{t-1}}{(t-1)!}$ for $t \in \{1, 2, 3, \dots\}$ and $\kappa > 0$. The mean and pgf are

$$\mathbb{E}(T) = \kappa + 1, \quad \phi_p(\lambda) = \mathbb{E}\left(\lambda^T\right) = \lambda e^{-\kappa(1-\lambda)} = \lambda e^{-[\mathbb{E}(T)-1](1-\lambda)}.$$

D. T is discrete with support on $\{1, 2, \dots, m\}$. The pmf is

$$\mathbb{P}(X = x) = \begin{cases} p_k & \text{if } x = k, \quad k = 1, \cdots, m \\ 0 & \text{otherwise.} \end{cases}$$

The mean and pgf are

$$\mathbb{E}(T) = \sum_{k=1}^{m} k p_k, \quad \phi_e(\lambda) = \mathbb{E}\left(\lambda^T\right) = \sum_{k=1}^{m} p_k \lambda^k.$$

Plots of the pgf $\phi(\lambda)$ for the distributions **A**–**C** are shown in Figure 4.3. We observed that the order of the pgfs can be very different depending on the sign of λ, the smallest eigenvalue of the transition matrix D (4.12). By Theorem 4.3.1, $\phi(\lambda)$ can be used to compare the $\mathcal{R}_0$ values associated with these specific distributions. Denote the reproduction numbers corresponding to distributions **A - C** by $\mathcal{R}_0^g$, $\mathcal{R}_0^{nb}$, and $\mathcal{R}_0^p$, respectively. Figure 4.3 suggests that these numbers follow a certain order based on the corresponding distributions. This finding is described in the following result.

Theorem 4.3.2 *Let $\lambda = a + b - 1$ be the smaller eigenvalue of the Markov matrix D. Let $T \neq 0$. The reproduction numbers corresponding to the distributions **A**–**C** can be ordered as follows:*

$$\begin{aligned} &\mathcal{R}_0^g \leqslant \mathcal{R}_0^{nb_k} \leqslant \mathcal{R}_0^{nb_{k+1}} \leqslant \mathcal{R}_0^p \quad \textit{if} \ \ \lambda \in [0, 1), \\ &\mathcal{R}_0^p \leqslant \mathcal{R}_0^{nb_{k+1}} \leqslant \mathcal{R}_0^{nb_k} \leqslant \mathcal{R}_0^g \quad \textit{if} \ \ \lambda \in (-1, 0]. \end{aligned} \tag{4.16}$$

Moreover,

$$\mathcal{R}_0^{nb_k} \to \mathcal{R}_0^p \ \textit{as} \ k \to \infty.$$

Equality is attained only if $\lambda = 0$ or $k = 1$.

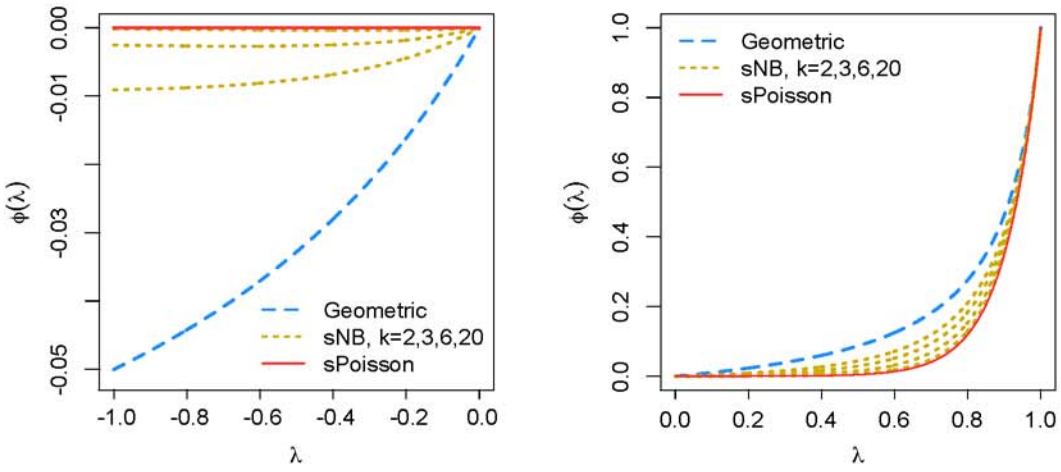

Figure 4.3. Plots of the pgf $\phi(\lambda) = \mathbb{E}(\lambda^T)$ for sGeom, sNegBinom and sPoisson distributions for $\lambda \in (-1, 0)$ (left) and $\lambda \in (0, 1)$ (right). In all cases, the mean infectious period is $\mathbb{E}(T) = 10.5$.

Proof Let $-1 < \lambda < 1$. From the Binomial Theorem

$$\left(1 + \frac{\mathbb{E}(T) - \lambda[\mathbb{E}(T) - 1] - 1}{k}\right)^k \geqslant \mathbb{E}(T) - \lambda[\mathbb{E}(T) - 1].$$

This, combined with the fact that $\mathbb{E}(T) - \lambda[\mathbb{E}(T) - 1] \geqslant 1$ yield

$$\frac{1}{\mathbb{E}(T) - \lambda[\mathbb{E}(T) - 1]} \geqslant \left(\frac{k}{k + \mathbb{E}(T) - \lambda[\mathbb{E}(T) - 1] - 1}\right)^k.$$

Since

$$\left(\frac{k}{k+\mathbb{E}(T)-\lambda[\mathbb{E}(T)-1]-1}\right)^k = \left(1 + \frac{(1-\lambda)[\mathbb{E}(T)-1]}{k}\right)^{-k} \searrow e^{-(1-\lambda)[\mathbb{E}(T)-1]}$$

as $k \to \infty$, we can conclude that $\phi_g(\lambda) \geqslant \phi_{nb_k}(\lambda) \geqslant \phi_{nb_{k+1}}(\lambda) \geqslant \phi_p(\lambda)$ if $\lambda \in [0, 1)$, and $\phi_g(\lambda) \leqslant \phi_{nb_k}(\lambda) \leqslant \phi_{nb_{k+1}}(\lambda) \leqslant \phi_p(\lambda)$ if $\lambda \in (-1, 0]$.

■

Remark: Theorem 4.3.2 clearly shows that the effect of the IP distribution on $\mathcal{R}_0$ depends on the sign of λ. This phenomenon is not observed in the continuous-time models, for which the value of $\mathcal{R}_0$ is (i) smaller for Exponential than for Gamma distribution (with shape parameter larger 1); and (ii) maximized with fixed duration

for the IP [85]. The similarity between continuous and discrete models exists for $\lambda > 0$ because the pgf can be expressed in terms of the mgf

$$\phi(\lambda) = \mathbb{E}(\lambda^T) = \mathbb{E}(e^{T \log \lambda}). \tag{4.17}$$

On the other hand, the above equality is no longer valid for $\lambda < 0$. A possible biological reason for this discrepancy between continuous and discrete models has not been identified. In practice, most models would assume that individuals are more likely to stay in their patch than to migrate to the other patch. This implies $a, b \geqslant 0.5$, and therefore $\lambda = a + b - 1 \geqslant 0$.

If $\lambda > 0$, sharper bounds than those given in Theorem 4.3.1 can be obtained for $\mathcal{R}_0$, regardless of the distribution of T.

Theorem 4.3.3 *Let $\lambda > 0$.*

(i) An upper bound for $\mathcal{R}_0$ is given by

$$\frac{1}{2}\Bigg\{ \overline{\mathcal{R}}_0 + \tfrac{1-\lambda^{\mathbb{E}(T)}}{1-\lambda}(\beta_1\pi_2 + \beta_2\pi_1) + \sqrt{\left[\overline{\mathcal{R}}_0 + \tfrac{1-\lambda^{\mathbb{E}(T)}}{1-\lambda}(\beta_1\pi_2 + \beta_2\pi_1)\right]^2 - 4\beta_1\beta_2\mathbb{E}(T)\tfrac{1-\lambda^{\mathbb{E}(T)}}{1-\lambda}} \Bigg\}$$

This value is attained when T has a constant distribution with fixed duration $\mathbb{E}(T)$.

(ii) If $Var(T) \leqslant \sigma^2$, a lower bound for $\mathcal{R}_0$ is given by

$$\frac{1}{2}\left[\overline{\mathcal{R}}_0 + \underline{z}(\beta_1\pi_2 + \beta_2\pi_1) + \sqrt{\left[\overline{\mathcal{R}}_0 + \underline{z}(\beta_1\pi_2 + \beta_2\pi_1)\right]^2 - 4\beta_1\beta_2\mathbb{E}(T)\underline{z}}\right],$$

where

$$\underline{z} = \frac{\mathbb{E}(T)^2\left(1 - \lambda^{\frac{\mathbb{E}(T)^2+\sigma^2}{\mathbb{E}(T)}}\right)}{\left[\mathbb{E}(T)^2 + \sigma^2\right](1-\lambda)}.$$

This value is attained if T is the two point distribution

$$\underline{T} = \begin{cases} 0 & \text{with probability } \frac{\sigma^2}{\mathbb{E}(T)^2+\sigma^2}, \\ \frac{\mathbb{E}(T)^2+\sigma^2}{\mathbb{E}(T)} & \text{with probability } \frac{\mathbb{E}(T)^2}{\mathbb{E}(T)^2+\sigma^2}. \end{cases}$$

Proof For the upper bound, by Jensen's inequality $\mathbb{E}(e^{T\log\lambda}) \geqslant e^{\mathbb{E}(T)\log\lambda}$. Therefore, for all comparable T, $\phi(\lambda) > \lambda^{\mathbb{E}(T)}$. Substitution of this value in (4.15) leads to the upper bound expression.

For the lower bound, let $\underline{\phi}(\lambda) = \mathbb{E}(\lambda^{\underline{T}})$ then it is easy to check that

$$\mathrm{Var}(\underline{T}) = \tfrac{\mathbb{E}(T)^2\sigma^2}{\mathbb{E}(T)^2+\sigma^2} + \left[\tfrac{\mathbb{E}(T)^2+\sigma^2}{\mathbb{E}(T)} - \mathbb{E}(T)\right]^2 \tfrac{\mathbb{E}(T)^2}{\mathbb{E}(T)^2+\sigma^2} = \sigma^2,$$

$$\underline{\phi}(\lambda) = \mathbb{E}\left(\lambda^{\underline{T}}\right) = \tfrac{\sigma^2}{\mathbb{E}(T)^2+\sigma^2} + \tfrac{\mathbb{E}(T)^2}{\mathbb{E}(T)^2+\sigma^2}\lambda^{\frac{\mathbb{E}(T)^2+\sigma^2}{\mathbb{E}(T)}}.$$

It is known that the mgf of a non-negative random variable with variance σ^2 is maximized by $\underline{T}$ (see Theorem 1 in [74]). From (4.17) $\underline{T}$ also maximizes the pgf of all comparable infectious periods T. Moreover,

$$g(\sigma) = \frac{\sigma^2}{\mathbb{E}(T)^2+\sigma^2} + \frac{\mathbb{E}(T)^2}{\mathbb{E}(T)^2+\sigma^2}\lambda^{\frac{\mathbb{E}(T)^2+\sigma^2}{\mathbb{E}(T)}}$$

is an increasing function of σ. Consider g as a function of $z = \sigma^2$. Then

$$g(z) = \frac{z + \mathbb{E}(T)^2\lambda^{\frac{\mathbb{E}(T)^2+z}{\mathbb{E}(T)}}}{\mathbb{E}(T)^2+z} \quad \text{and} \quad g'(z) = \frac{\mathbb{E}(T)g_1(t)}{(\mathbb{E}(T)^2+z)^2},$$

where $g_1(z) = \mathbb{E}(T) + \left[\log(\lambda)\mathbb{E}(T)^2 + \log(\lambda)z - \mathbb{E}(T)\right]\lambda^{\frac{\mathbb{E}(T)^2+z}{\mathbb{E}(T)}}$. Clearly, the sign of $g'(z)$ is determined by $g_1(z)$. Since $e^{-\mathbb{E}(T)\log(\lambda)} \geqslant -\mathbb{E}(T)\log(\lambda) + 1$, then

$$1 \geqslant \left[-\mathbb{E}(T)\log(\lambda) + 1\right]\lambda^{\mathbb{E}(T)} \quad \Rightarrow \quad 1 + \left[\mathbb{E}(T)\log(\lambda) - 1\right]\lambda^{\mathbb{E}(T)} \geqslant 0.$$

Therefore $g_1(0) = \mathbb{E}(T)\left[1 + \left[\log(\lambda)\mathbb{E}(T) - 1\right]\lambda^{\mathbb{E}(T)}\right] \geqslant 0$. Since

$$\begin{aligned} g_1'(z) &= \left[\log(\lambda)\mathbb{E}(T)^2 + \log(\lambda)z - \mathbb{E}(T)\right]\frac{\log(\lambda)}{\mathbb{E}(T)}\lambda^{\frac{\mathbb{E}(T)^2+z}{\mathbb{E}(T)}} + \log(\lambda)\lambda^{\frac{\mathbb{E}(T)^2+z}{\mathbb{E}(T)}} \\ &= \left[\log(\lambda)^2\mathbb{E}(T) + \frac{z\log(\lambda)^2}{\mathbb{E}(T)}\right]\lambda^{\frac{\mathbb{E}(T)^2+z}{\mathbb{E}(T)}} \;\geqslant\; 0, \end{aligned}$$

it follows that $g_1(z)$ is an increasing function of z. Thus, $g_1(z) \geqslant g_1(0) \geqslant 0\ \forall z \geqslant 0$; and, $g'(z) \geqslant 0\ \forall z \geqslant 0$. Therefore, conclude $g(\sigma_1) \leqslant g(\sigma_2)\ \forall \sigma_1 \leqslant \sigma_2$. This implies that, if T satisfies $\mathrm{Var}(T) \leqslant \sigma^2$, then its pgf is no greater than $\underline{\phi}$ for any $\lambda \in [0,1]$. Since $\mathcal{R}_0$ is a decreasing function with respect to the pgf ϕ, we conclude that $\mathcal{R}_0$ is minimized when $T = \underline{T}$. Finally, substituting the expression $\underline{z} = \underline{\varphi}(\lambda) = \frac{1-\underline{\phi}(\lambda)}{1-\lambda}$ for z in (4.15) we obtain the expression for the lower bound. ■

Remark Since our model is discrete, we consider random variables with support on the set $\{0, 1, \dots\}$, thus if $\mathbb{E}(T)$ or $\frac{\mathbb{E}(T)^2+\sigma^2}{\mathbb{E}(T)} \notin \mathbb{N}_0$ are not integers, then the upper and lower bound might not be attained.

4.3.3 Results of stochastic simulations

Numerical simulations of the model with $n = 2$ subpopulations have been conducted. Let $S_i(t), I_i(t), R_i(t)$ denote the numbers of susceptible, infective, and recovered individuals, respectively, of the population i at time t ($i = 1, 2,\ t \in \mathbb{N}$). Initial populations $N_1(0)$ and $N_2(0)$ are chosen near the Markov equilibrium, i.e., $N_1(0) \approx \pi_1 N,\ N_2(0) \approx \pi_2 N$. Recall that the total population size $N = N_1(t) + N_2(t)$ remains constant for all time. Assume $I_i(0) > 0$ for at least one sub-population i. To determine the number of individuals in each epidemiological classes at time t, we first run the epidemic process (updating the number of susceptible, infected, recovered), and then shuffle the population from one patch to the other according to the Markov matrix D (4.13). The epidemiological process is simulated using a similar approach as in [28]. Since the number of effective contacts per person in population i is Poisson(β_i), the number of secondary infections is determined by $x(t) \sim \text{Poiss}\left(\beta_i I_i(t-1)\frac{S_i(t-1)}{N_i(t-1)}\right)$.

If $T \sim \text{sGeom}(\gamma)$ (see distribution **A** in Section 4.3.2), then the probability that an infected individual recovers at time t is equal to γ. Let $x_i(t)$ and $y_i(t)$ denote the newly infected and newly recovered individuals at time t, respectively, in population i. Note that $y_i(t)$ is distributed as Binomial($I_i(t-1), \gamma$). Then

$$S_i(t_-) = S(t-1) - x(t), \qquad I_i(t_-) = I_i(t-1) + x(t) - y(t),$$

$$R_i(t_-) = R_i(t-1) + y(t)$$

The notation t_- is used because of the following consideration. To obtain $S_i(t)$, $I_i(t)$, and $R_i(t)$ we must simulate the movement from patch i to patch j. Let $s_{i\to i}$ denote the number of susceptible individuals staying in patch i ($i = 1, 2$). Then, the number of susceptible individuals staying in patch 1, $s_{1\to 1}$, is distributed as Binomial($S_1(t_-), a$).

Similarly $s_{2\to 2} \sim \text{Binomial}(S_2(t_-), b)$. Define $s_{1\to 2} = S_1(t_-) - s_{1\to 1}$ and $s_{2\to 1} = S_2(t_-) - s_{2\to 2}$. Note that

$$S_1(t) = s_{1\to 1} + s_{2\to 1} \qquad \text{and} \qquad S_2(t) = s_{2\to 2} + s_{1\to 2}.$$

In the same fashion $i_{i\to j}$ and $r_{i\to j}$ are defined. Then,

$$I_1(t) = i_{1\to 1} + i_{2\to 1}, \qquad I_2(t) = i_{2\to 2} + i_{1\to 2},$$

$$R_1(t) = r_{1\to 1} + r_{2\to 1}, \qquad R_2(t) = r_{2\to 2} + r_{1\to 2}.$$

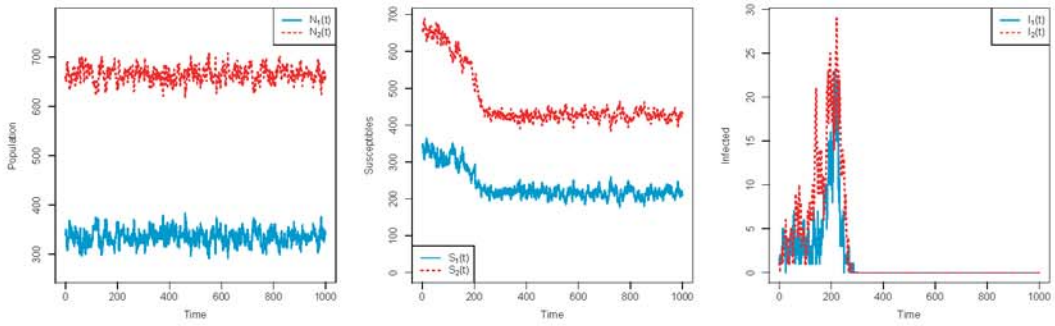

Figure 4.4. Sample path of an epidemic with $T \sim$ sGeom. Parameter values, $N_1(0) = 340$, $N_2(0) = 660$, $I_1(0) = I_2(0) = 1$, $a = .8$, $b = .9$ $\beta_1 = .27$, $\beta_2 = .15$ and $\mathbb{E}(T) = 10$, produce $\mathcal{R}_0^{geom} = 1.964408$.

Based on these rules, numerical simulations have been conducted. A sample path of the simulated epidemic with sGeometric distribution is illustrated in Figure 4.4. The set of parameter values used in this figure are $N_1(0) = 340$, $N_2(0) = 660$, $I_1(0) = I_2(0) = 1$, $a = .8$, $b = .9$ $\beta_1 = .27$, $\beta_2 = .15$ and $\mathbb{E}(T) = 10$, which produce $\mathcal{R}_0^{geom} \approx 1.96$. In this realization, the epidemic ended at around $t = 250$.

Taking advantage of the fact that a Negative Binomial r.v. with parameters (k, η) (see **B** in Section 4.3.2) can be written as the sum of k Geometric r.v. with parameter η, the infectious class I_i has been artificially subdivide into $k = 5$ subclasses. The above ideas were then used to generate an epidemic with this distribution for T.

To complement the numeric results, the case $T \sim \text{Unif}(\{5, 6, \ldots, 15\})$ was considered (i.e. $\mathbb{P}(T = i) = \frac{1}{11}$ for $i \in \{5, 6, \ldots, 15\}$). This distribution was chosen

to emphasize the fact that *any* distribution for T is allowed by our model. $T \sim$ Unif represents the absolutely lack of a priori information, other than recovery takes place 5 to 10 days after acquiring the disease. Figure 4.5 shows the three *comparable* distributions for which simulations were performed.

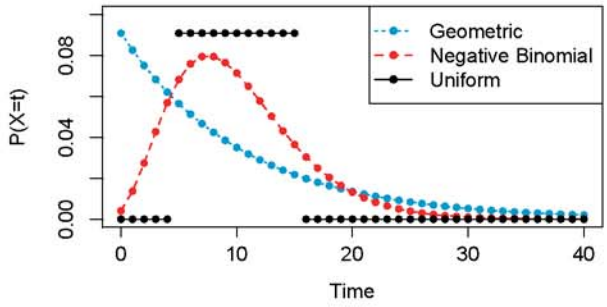

Figure 4.5. Probability mass function $\mathbb{P}(T = t)$ of three comparable distributions: sGeom$\left(\gamma = \frac{1}{10}\right)$; sNegBinom$(k = 5, \eta = \frac{5}{14})$ and Uniform in $\{5, \ldots, 15\}$. All three distributions have mean equal to 10.

The influence of the distribution of T on the final size $\mathcal{F}$, the duration $\mathcal{D}$ and peak $\mathcal{P}$ of an epidemic can also be examined by comparing results from multiple epidemic paths [49,87,88]. Figures 4.6, 4.7 and 4.7 collect the outcomes of 50,000 simulations of the models with $T \sim$ sGeom (i.e., the Geometric Distribution Model or GDM); $T \sim$ sNegBinom with shape parameter $k = 5$ (i.e., the Negative Binomial Distribution Model or NBDM); and $T \sim$Unif $\{5, \ldots, 15\}$ (i.e., the Uniform Distribution Model or UDM). Parameter values for these figures are the same as in Figure 4.4. The corresponding basic reproduction numbers can be computed using (4.15) and the pdf formulas provided in Section 4.3.2:

$$\mathcal{R}_0^{Geom} = 1.964408 \; < \; \mathcal{R}_0^{NegBin} = 1.977059 \; < \; \mathcal{R}_0^{Unif} = 1.98091. \tag{4.18}$$

In Figure 4.6, histograms show the overall distribution of $\mathcal{F}$. The large bin near zero (representing lower $\mathcal{F}$ values) collects observations that can be cataloged as minor epidemics, whereas all other bins collect major epidemics. The average of $\mathcal{F}$, from smaller to larger is given by Geometric, NegBinomial and Uniform distribution. This

confirms (4.18), which indicates that the Geom distribution is likely to predict a less severe epidemic than the predicted by NegBinom and Uniform. In particular, a much lower level of final epidemic size was predicted. Figure 4.7 captures the distribution of the duration of the epidemic $\mathcal{D}$. Our observations indicate that epidemics with $T \sim$ Geometric tend to be milder but longer than those with $T \sim$ NegBinomial and $T \sim$ Uniform. Figure 4.8 shows the distribution of the epidemic peak. One more time we observed that the Geometric model predicts a milder epidemic when measured by the average peak of the outbreak. The uniform model, on the other hand, predicts a more severe epidemic under the same criteria.

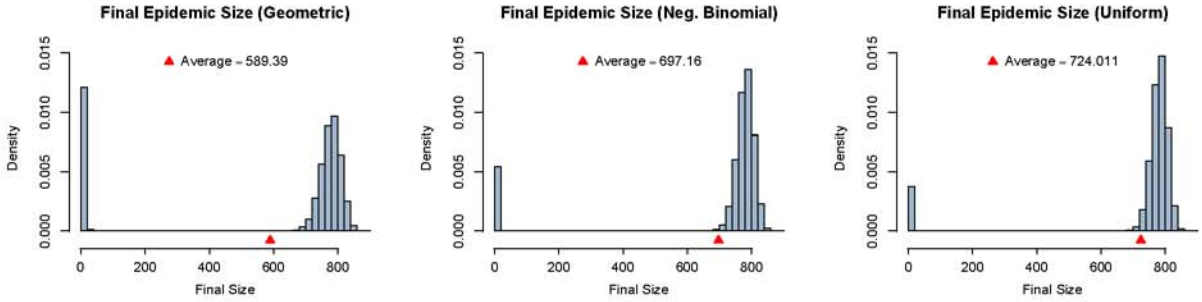

Figure 4.6. Distribution of the final size $\mathcal{F}$ obtained from 50,000 simulations from the GDM (left), the NBDM (middle) and UDM (right). $\mathcal{R}_0^{Geom} \approx 1.96$, $\mathcal{R}_0^{NegBin} \approx 1.97$ and $\mathcal{R}_0^{Unif} \approx 1.98$.

4.3.4 Probabilities of minor and major epidemics

Recall that the Markov matrix D for $n = 2$ patches is given in (4.11). From Theorem 4.2.2

$$A(s_1, s_2) = \begin{bmatrix} e^{-\theta_1}a & e^{-\theta_1}(1-a) \\ e^{-\theta_2}(1-b) & e^{-\theta_2}b \end{bmatrix}, \quad E(s_1, s_2) = \begin{bmatrix} e^{-\theta_1} \\ e^{-\theta_2} \end{bmatrix}, \quad \begin{matrix} \theta_1 = \beta_1(1-s_1) \\ \theta_2 = \beta_2(1-s_2) \end{matrix}$$

$$G(s_1, s_2)^{tr} = \begin{bmatrix} G_1(s_1, s_2) \\ G_1(s_1, s_2) \end{bmatrix} = \sum_{t=1}^{\infty} A(s_1, s_2)^{t-1} E(s_1, s_2)\ \mathbb{P}(T = t)$$

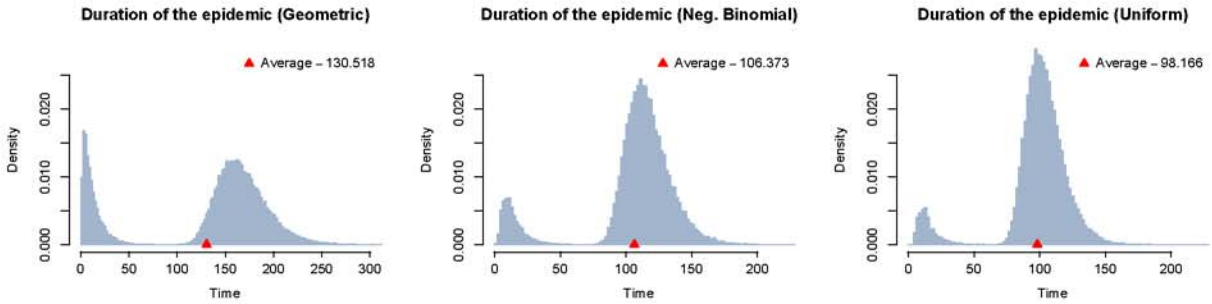

Figure 4.7. Distribution of the epidemic duration $\mathcal{D}$ obtained from 50,000 observations for the GDM (left), the NBDM (middle) and UDM (right).

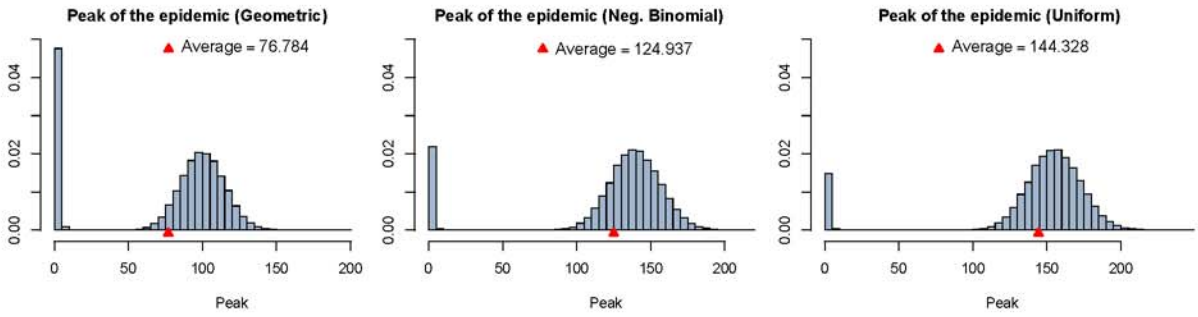

Figure 4.8. Distribution of the epidemic peak $\mathcal{P}$ obtained from 50,000 observations for the GDM (left), the NBDM (middle) and UDM (right).

Although it is difficult to find an analytic expression for the solution of $G(s_1, s_2) = (s_1, s_2)$, numerical solutions can be obtained for a given distribution of T by substituting appropriate expressions for $\mathbb{P}(T = t)$ in the above equations. For example, for the three models GDM, NBDM and UDM (see Figures 4.6, 4.7 and 4.8), the extinction probabilities $\mathbb{P}_0$ (or probability of a minor epidemic) are obtained numerically using the fixed point approach. Results are listed in Table 4.2. These probabilities are given by $\mathbb{P}_0 = z_1^{I_1(0)} z_2^{I_2(0)}$, as defined in equation (4.9) and (4.10). For each model, three pairs of initial conditions $(I_1(0), I_2(0))$ are considered.

To examine how good these approximations are, the second column in Table 4.2 contains the "empirical" probabilities of minor epidemic. These quantities have been determined by the proportion of observations that have total infections $\leqslant 10$ (see Figure 4.6). The last (Error) column shows the difference between the analytic value $\mathbb{P}_0$ and the value from model simulations. Our simulations suggest that $\mathbb{P}_0$ provides a very good approximation.

Table 4.2.
Comparison of the probabilities of minor epidemic (extinction probability $\mathbb{P}_0$) and simulation results for different initial values $I_1(0)$ and $I_2(0)$. A sample path for which the final size is less than 10 was considered to be a minor epidemic.

	Initial value $\big(I_1(0), I_2(0)\big)$	$\mathbb{P}_0$	Proportion from simulations	Error
Geometric	(1,0)	0.4426690	0.43962	0.003048985
	(0,1)	0.5324051	0.52236	0.010045121
	(1,1)	0.2356792	0.22546	0.010219235
NegBinom	(1,0)	0.2815446	0.28798	-0.006435354
	(0,1)	0.3728444	0.37072	0.002124375
	(1,1)	0.1049723	0.10308	0.001892338
Uniform	(1,0)	0.18068085	0.2353	-0.05461915
	(0,1)	0.25198173	0.31478	-0.06279827
	(1,1)	0.04552827	0.07218	-0.02665173

4.4 Discussion

In this chapter, discrete-time stochastic epidemic models in a metapopulation setting were studied. Although some of the ideas and methods are adopted from [85], which deals with an analogous continuous-time model, new findings and results were obtained. A particular new behavior that is absent in continuous models is that, in the two patch model, the effect of distributions of T on $\mathcal{R}_0$ depends critically on the sign of λ (the smaller eigenvalue of the Markov matrix D). The consideration of a (random) arbitrarily distributed infectious period T in the discrete model is also a new feature that has not been studied previously. The results obtained for the general distribution allow us to compare model outcomes under different assumptions on the distribution of infectious period.

For the model with n populations and an arbitrary infectious period T, we derived the expression for $\mathcal{R}_0$ (Theorem 1) and the equation for the probability of disease extinction $\mathbb{P}_0$ (see (4.9) and (4.10)). These general results are applied to the case of $n = 2$ populations, from which an explicit formula for $\mathcal{R}_0$ was derived in terms of the pgf ϕ of T. More importantly, it was proved that $\mathcal{R}_0$ is a decreasing function of ϕ, which allows us to obtain an order relation among the $\mathcal{R}_0$ that is dependent on the distributions of T (including sGeometric; sNegative Binomial; sPoisson; and a discrete distribution with finite support, representing the case of empirical data). It was shown that, when $\lambda > 0$ the Geometric distribution gives the smallest reproduction number ($\mathcal{R}_0^g$) while the Poisson distribution gives the largest ($\mathcal{R}_0^p$). However, when $\lambda < 0$, the order is reversed (see Theorem 3). In addition, an upper and lower bounds for $\mathcal{R}_0$ were provided for the case $\lambda > 0$. Notice that, if individuals in population i are more likely to stay than to move to the other population, i.e., $a, b > 0.5$, then $\lambda > 0$ will be a more likely scenario.

Because our model includes several random factors, e.g., the infectious period T and the number of effective contacts β_i, some of the results are obtained by carrying out a large number of numerical simulations for the model with $n = 2$ populations.

From these simulation results we can obtain insights into the effect of distributions of T on the final epidemic size $\mathcal{F}$, duration of an epidemic $\mathcal{D}$, peak of an epidemic $\mathcal{P}$ and probability of minor epidemic $\mathbb{P}_0$ (e.g., see Figures 4.6 - 4.8). Traditionally, models with Geometric infectious period are preferred due to its tractability. However, our findings suggest that when the model with $T \sim$ Geom is compared with the model with $T \sim$NegBinom and $T \sim$Uniform, the GDM predicts a **milder** epidemic (when $\lambda > 0$). This is supported by our analytical (see (4.16), (4.18)) and numerical results (see Figures 4.6-4.8). From the numerical simulations we also observe that the GDM is likely to generate a **longer** duration when compared to the NBDM and UDM.

A formula for the probability of disease extinction $\mathbb{P}_0$ has also been derived based on the approximations by a branching process. Comparisons of the $\mathbb{P}_0$ value with the proportion of minor epidemics from simulations of the three models (GDM, NBDM and UDM) suggest that the formula for $\mathbb{P}_0$ provides very good approximations (see Table 4.2). From the results shown in Table 4.2 we also observe that the Geometric model predicts a higher (smaller) probability of minor (major) epidemic.

5. SUMMARY AND DISCUSSION

In this thesis several discrete-time epidemic models, both deterministic and stochastic, are developed and studied. The driving questions that motivated most of these models are the following:

(i) What are the drawbacks of Geometric distribution assumption on disease stages when the model is used to evaluate control measures?

(ii) How will the model predictions alter when the Geometric distribution is replaced by more realistic distributions?

(iii) Can we derive a formula for the reproduction numbers $\mathcal{R}_0$ ($\mathcal{R}_C$) and a final epidemic size relation when an arbitrarily distributed disease duration is used in a discrete SEIR type of model?

These questions are addressed in this thesis, and the results obtained can be very useful for providing important insights into disease transmission dynamics and evaluations of disease control strategies such as quarantine and isolation.

In Chapter 2, a systematic derivations for the reproduction numbers of various discrete-time epidemic models are presented. Models without disease control (Sections 2.2 and 2.3) and with isolation (Section 2.4) are considered, most of which allow for an arbitrarily distributed (bounded) infectious period. The inclusion of the general distribution makes the model analysis challenging, particularly the computation of $\mathcal{R}_0$ and $\mathcal{R}_C$ due to the fact that the commonly employed method, the next generation matrix approach, cannot be applied. The technique developed in this thesis is one of the main novelties, which provides a useful method for analyzing discrete-time epidemic models.

Because $\mathcal{R}_C$ depends on the mean infectious period and the isolation-adjusted mean sojourn time (see formula (2.23)), among other factors, we demonstrated that

models assuming Geometric distributions can lead to biased or misleading evaluations on disease control strategies. For example, Figure 2.13 in Section 2.4 illustrates that the choice of distributions may have significant influence on the applications of the model in evaluating control strategies. This is in agreement with previous findings, suggesting the importance of using more realistic assumptions on disease stage distributions in some cases.

Chapter 3 presents more examples of using discrete-time epidemic models to evaluate control strategies and the effect of stage-duration distributions on the quantitative dynamics. To the best of our knowledge, no discrete-time epidemic models have been previously developed and analyzed that include quarantine and isolation while allowing the disease stages to have arbitrary distributions. The analyses presented in this chapter provide useful tools for evaluating the final epidemic size. The results are discussed in particular within the context of three classical discrete parametric distributions: Geometric, Poisson and Binomial. The results suggest that the use of distinct parametric distributions can lead to contradictory model predictions (see Figure 3.8).

The framework introduced in Chapter 3 also allows for the incorporation of empirical stage-duration distributions. This can provide a particular advantage of using data directly in the application of the model due to the flexibility in the distribution assumption. Another major contribution of this study is the derivation of the analytic formulas for $\mathcal{R}_C$ and final epidemic sizes. The general formula for $\mathcal{R}_C$ makes it possible to further examine the role of its additive components ($\mathcal{R}_I$, $\mathcal{R}_{IH}$ and $\mathcal{R}_{QH}$), which can help identify critical factors for the most effectively control of the disease.

Finally, in Chapter 4 a discrete-time stochastic epidemic model in a metapopulation setting was studied. The (random) infectious period T is assumed to be arbitrarily distributed, which represents a new feature that has not been studied previously in the stochastic/discrete setting. For the model with n sub-populations, an expression for $\mathcal{R}_0$ (Theorem 4.2.1) and the probability of disease extinction $\mathbb{P}_0$ (Theorem 4.2.2 and equation (4.10)) are obtained. These general results are then

applied to the case of $n = 2$ sub-populations, from which an explicit formula for $\mathcal{R}_0$ can be derived in terms of the pgf ϕ of T. More importantly, we proved that $\mathcal{R}_0$ is a decreasing function of ϕ, which allows us to obtain an order relationship among the $\mathcal{R}_0$ values corresponding to the distributions of T. We compared these reproduction numbers under specific distributions (e.g., Geometric, Poisson and Negative Binomial) and established a hierarchical relationship. More generally, upper and lower bounds for $\mathcal{R}_0$ are provided for the case $\lambda > 0$.

Because our model includes several random factors, some of the results are obtained by carrying out a large number of numerical simulations for the model with $n = 2$ sub-populations. From these simulation results we can obtain insights into the effect of distributions of T on the final epidemic size $\mathcal{F}$, duration of an epidemic $\mathcal{D}$, and probability of minor epidemic $\mathbb{P}_0$ (e.g., see Figs. 4.6 and 4.7). Traditionally, models with Geometric infectious period are preferred due to the tractability of the model. However, our findings suggest that when the model with $T \sim$ Geom is compared with the model with $T \sim$NegBinom or $T \sim$Uniform, the geometric distribution model (GDM) predicts a **milder** epidemic (when $\lambda > 0$). This is supported by our analytical (see (4.16), (4.18)) and numerical results (see Fig. 4.6, 4.7). From the numerical simulations we also observe that the GDM is likely to generate a **longer** duration when compared to the negative binomial distribution model (NBDM) and the uniform distribution model (UDM).

We have also derived a formula for the probability of disease extinction $\mathbb{P}_0$ based on the approximations by a branching process. Comparisons of the $\mathbb{P}_0$ value with the proportion of minor epidemics from simulations of the three models (GDM, NBDM and UDM) suggest that the formula for $\mathbb{P}_0$ provides very good approximations (see Table 4.2). From the results shown in Table 4.2 we also observe that the Geometric model predicts a higher (smaller) probability of minor (major) epidemic.

In summary, the studies included in this thesis provide new methods and frameworks for formulating and analyzing discrete-time epidemic models, particularly when more realistic distributions for disease stages need to be considered. The use of ar-

bitrarily distributed stage durations in the general model provide formulas for several quantities including $\mathcal{R}_0$ ($\mathcal{R}_C$), final epidemic size relation, and probability of minor/major epidemic that can be easily applied when specific distributions are considered. Model results provide useful tools for evaluating disease control strategies.

REFERENCES

REFERENCES

[1] Klaus Dietz and J.A.P. Heesterbeek. Daniel Bernoulli's epidemiological model revisited. *Mathematical Biosciences*, 180:1–21, 2002.

[2] Ronald Ross. *The Prevention of Malaria*. Dutton, New York, 2nd edition, 1911.

[3] William O. Kermack and Anderson G. McKendrick. Contributions to the mathematical theory of epidemics. I. *Proceedings of the Royal society of London. Series A*, 115:700–721, 1927. Reprinted in Bull. Math. Biol. 53 (1991) 33-55.

[4] William O. Kermack and Anderson G. McKendrick. Contributions to the mathematical theory of epidemics. II. The problem of endemicity. *Proceedings of the Royal society of London*, 138(834):55–83, 1932.

[5] William O. Kermack and Anderson G. McKendrick. Contributions to the mathematical theory of epidemics. III. Further studies of the problem of endemicity. *Proceedings of the Royal Society of London*, 141(843):94–122, 1933. Reprinted in Bull. Math. Biol. 53 (1991) 89-118.

[6] C. Castillo Chavez, Z. Feng, and W. Huang. On the computation of ∇_0 and its role on global stability. *Mathematical approaches for emerging and reemerging infectious diseases: an introduction*, 1:229–250, 2002.

[7] T. de Camino-Beck, M.A. Lewis, and P. van den Driessche. A graph-theoretic method for the basic reproduction number in continuous time epidemiological models. *Journal of Mathematical Biology*, 59(4):503–516, 2009.

[8] O. Diekmann and J.A.P. Heesterbeek. *Mathematical Epidemiology of Infectious Diseases: Model Building, Analysis and Interpretation*, volume 5. Wiley, 2000.

[9] O. Diekmann, J.A.P. Heesterbeek, and MG Roberts. The construction of next-generation matrices for compartmental epidemic models. *Journal of the Royal Society Interface*, 7(47):873–885, 2010.

[10] J.A. Jacquez, C.P. Simon, and J.S. Koopman. Core groups and the $\nabla_0' s$ for subgroups in heterogeneous sis and si models. *Epidemic Models: Their Structure and Relation to Data (D. Mollison, ed.)*, pages 279–301, 1995.

[11] H.R. Thieme. Spectral bound and reproduction number for infinite-dimensional population structure and time heterogeneity. *SIAM Journal on Applied Mathematics*, 70(1):188–211, 2009.

[12] P. van den Driessche and J. Watmough. Reproduction numbers and subthreshold endemic equilibria for compartmental models of disease transmission. *Mathematical Biosciences*, 180(1):29–48, 2002.

[13] Gerardo Chowell, Carlos Castillo-Chavez, Paul W. Fenimore, Christopher M. Kribs-Zaleta, Leon Arriola, and James M. Hyman. Model parameters and outbreak control for SARS. *Emerging Infectious Diseases*, 10(7):1258–1263, 2004.

[14] Gerardo Chowell, Paul W. Fenimore, Melissa A. Castillo-Garsow, and Carlos Castillo-Chavez. SARS outbreaks in Ontario, Hong Kong and Singapore: the role of diagnosis and isolation as a control mechanism. *Journal of Theoretical Biology*, 224(1):1–8, 2003.

[15] A. Gumel, S. Ruan, T Day, J. Watmough, P. van den Driessche, F. Brauer, D. Gabrielson, C. Bowman, M.E. Alexander, S. Ardal, J. Wu, and B.M Sahai. Modeling strategies for controlling SARS outbreaks based on Toronto, Hong Kong, Singapore and Beijing experience. *Proc. Roy. Soc. London*, 271:2223–2232, 2004.

[16] L.J.S. Allen, A.M. Burgin, et al. Comparison of deterministic and stochastic SIS and SIR models in discrete time. *Mathematical biosciences*, 163(1):1–34, 2000.

[17] L.J.S. Allen and P. van den Driessche. The basic reproduction number in some discrete-time epidemic models. *Journal of Difference Equations and Applications*, 14(10-11):1127–1147, 2008.

[18] J.M. Cushing and A.S. Ackleh. A net reproductive number for periodic matrix models. *Journal of Biological Dynamics*, 6(2):166–188, 2012.

[19] T. de Camino-Beck and M.A. Lewis. A new method for calculating net reproductive rate from graph reduction with applications to the control of invasive species. *Bulletin of Mathematical Biology*, 69(4):1341–1354, 2007.

[20] M.C.M. De Jong, O. Diekmann, and J.A.P. Heesterbeek. The computation of ∇_0 for discrete-time epidemic models with dynamic heterogeneity. *Mathematical biosciences*, 119(1):97–114, 1994.

[21] Nancy Hernandez-Ceron, Zhilan Feng, and Carlos Castillo-Chavez. Discrete epidemic models with arbitrary stage distributions and applications to disease control. *Bulletin of Mathematical Biology*, 75(10):1716–1746, 2013.

[22] M.A. Lewis, J. Renclawowicz, P. van den Driessche, and M. Wonham. A comparison of continuous and discrete-time West Nile virus models. *Bulletin of Mathematical Biology*, 68(3):491–509, 2006.

[23] C.L. Wesley, L.J.S. Allen, C.B. Jonsson, Y.K. Chu, and R.D. Owen. A discrete-time rodent-hantavirus model structured by infection and developmental stages. *Advanced Studies in Pure Mathematics*, 53:1–12, 2009.

[24] Yicang Zhou, Zhien Ma, and F. Brauer. A discrete epidemic model for SARS transmission and control in China. *Mathematical and Computer Modelling*, 40(13):1491 – 1506, 2004.

[25] L.J.S. Allen, M.A. Jones, and C.F. Martin. A discrete-time model with vaccination for a measles epidemic. *Mathematical Biosciences*, 105(1):111 – 131, 1991.

[26] Hui Cao and Yicang Zhou. The discrete age-structured SEIT model with application to tuberculosis transmission in China. *Mathematical and Computer Modelling*, 55(3–4):385–395, 2012.

[27] Yueli Luo, Shujing Gao, Dehui Xie, and Yanfei Dai. A discrete plant disease model with roguing and replanting. *Advances in Difference Equations*, 2015(1), 2015.

[28] Linda J.S. Allen and P. van den Driessche. Relations between deterministic and stochastic thresholds for disease extinction in continuous- and discrete-time infectious disease models. *Mathematical Biosciences*, 2013.

[29] Juping Zhang and Zhen Jin. Discrete time SI and SIS epidemic models with vertical transmission. *Journal of Biological Systems*, 17(2):201 – 212, 2009.

[30] Masaki Sekiguchi. Permanence of some discrete epidemic models. *International Journal of Biomathematics*, 02(04):443–461, 2009.

[31] Masaki Sekiguchi. Permanence of a discrete SIRS epidemic model with time delays. *Applied Mathematics Letters*, 23(10):1280 – 1285, 2010.

[32] Zengyun Hu, Zhidong Teng, and Haijun Jiang. Stability analysis in a class of discrete SIRS epidemic models. *Nonlinear Analysis: Real World Applications*, 13(5):2017 – 2033, 2012.

[33] Yoichi Enatsu, Yukihiko Nakata, and Yoshiaki Muroya. Global stability for a class of discrete SIR epidemic models. *Mathematical Biosciences and Engineering*, 7(2):347, 2010.

[34] Carlos Castillo-Chavez and Abdul-Aziz Yakubu. Discrete-time S-I-S models with complex dynamics. *Nonlinear Analysis: Theory, Methods & Applications*, 47(7):4753 – 4762, 2001.

[35] Junhong Li and Ning Cui. Bifurcation and chaotic behavior of a discrete-time SIS model. *Discrete Dynamics in Nature and Society*, 2013, 2013.

[36] Lorenzo Pellis, Neil M. Ferguson, and Christophe Fraser Fraser. The relationship between real-time and discrete-generation models of epidemic spread. *Mathematical Biosciences*, 216(1):63–70, 2008.

[37] Donald Ludwig. Final size distribution for epidemics. *Mathematical Biosciences*, 23(1):33 – 46, 1975.

[38] Linda J.S. Allen. Some discrete-time SI, SIR, and SIS epidemic models. *Mathematical Biosciences*, 124(1):83 – 105, 1994.

[39] F. Brauer, Z. Feng, and C. Castillo-Chavez. Discrete epidemic models. *Mathematical Biosciences*, 7:1–15, 2010.

[40] Xiuying Li and Wendi Wang. A discrete epidemic model with stage structure. *Chaos, Solitons & Fractals*, 26(3):947 – 958, 2005.

[41] F. Brauer and C. Castillo-Chavez. *Mathematical Models in Population Biology and Epidemiology*. Springer, 2nd edition, 2012.

[42] Hal Smith. *An Introduction to Delay Differential Equations with Applications to the Life Sciences*, volume 57 of *Texts in Applied Mathematics*. Springer-Verlag New York, 1 edition, 2011.

[43] Zhilan Feng, Dashun Xu, and Haiyun Zhao. Epidemiological models with non-exponentially distributed disease stages and applications to disease control. *Bulletin of Mathematical Biology*, 69:1511–1536, 2007.

[44] Herbert W Hethcote and David W Tudor. Integral equation models for endemic infectious diseases. *Journal of Mathematical Biology*, 9(1):37–47, 1980.

[45] Alun L. Lloyd. Realistic distributions of infectious periods in epidemic models: Changing patterns of persistence and dynamics. *Theoretical Population Biology*, 60(1):59–71, 2001.

[46] Norman MacDonald. *Time lags in biological models*, volume 27. Springer-Verlag Heidelberg, 1978.

[47] Norman T. J. Bailey. Some stochastic models for small epidemics in large populations. *Journal of the Royal Statistical Society. Series C (Applied Statistics)*, 13(1):pp. 9–19, 1964.

[48] Dorothy Anderson and Ray Watson. On the spread of a disease with gamma distributed latent and infectious periods. *Biometrika*, 67(1):191–198, 1980.

[49] Cheryl L. Addy, Jr. Longini, Ira M., and Michael Haber. A generalized stochastic model for the analysis of infectious disease final size data. *Biometrics*, 47(3):961–974, 1991.

[50] Linda J.S. Allen and Glenn E. Lahodny, Jr. Extinction thresholds in deterministic and stochastic epidemic models. *Journal of Biological Dynamics*, 6(2):590–611, 2012.

[51] Glenn E. Lahodny, Jr. and Linda J.S. Allen. Probability of a disease outbreak in stochastic multipatch epidemic models. *Bulletin of Mathematical Biology*, 75(7):1157–1180, 2013.

[52] Ira M. Longini Jr. The generalized discrete-time epidemic model with immunity: a synthesis. *Mathematical Biosciences*, 82(1):19 – 41, 1986.

[53] Carlos Castillo-Chávez. *Mathematical and statistical approaches to AIDS epidemiology.* Number 83 in Lecture Notes in Biomathematics. Springer-Verlag, 1989.

[54] H.J. Wearing, P. Rohani, and M.J. Keeling. Appropriate models for the management of infectious diseases. *PLoS Medicine*, 2(7):e174, 2005.

[55] A. L. Lloyd. The dependence of viral parameter estimates on the assumed viral life cycle: limitations of studies of viral load data. *Proceedings of the Royal Society of London B: Biological Sciences*, 268(1469):847–854, 2001.

[56] A. L. Lloyd. Destabilization of epidemic models with the inclusion of realistic distributions of infectious periods. *Proceedings of the Royal Society of London. Series B: Biological Sciences*, 268(1470):985–993, 2001.

[57] Nancy Hernandez-Ceron, Zhilan Feng, and P. van den Driessche. Reproduction numbers for discrete-time epidemic models with arbitrary stage distributions. *Journal of Difference Equations and Applications*, 19(10):1671–1693, 2013.

[58] Elisabeta Vergu, Henri Busson, and Pauline Ezanno. Impact of the infection period distribution on the epidemic spread in a metapopulation model. *PloS one*, 5(2):e9371, 2010.

[59] J. Lessler, N. G. Reich, R. Brookmeyer, T. M. Perl, K. E. Nelson, and D. A. Cummings. Incubation periods of acute respiratory viral infections: a systematic review. *The Lancet Infectious Diseases*, 9(5):291 – 300, 2009.

[60] Gianpaolo Scalia-Tomba. Asymptotic final-size distribution for some chain-binomial processes. *Advances in Applied Probability*, 17(3):477–495, 1985.

[61] Joel C. Miller, Anja C. Slim, and Erik M Volz. Edge-based compartmental modelling for infectious disease spread. *Journal of the Royal Society Interface*, 9(70):890–906, 2012.

[62] Norman T. J. Bailey. A simple stochastic epidemic. *Biometrika*, pages 193–202, 1950.

[63] P. Whittle. The Outcome of a Stochastic Epidemic–A Note on Bailey's Paper. *Biometrika*, 42(1/2):116–122, 1955.

[64] J.A.J. Metz. The epidemic in a closed population with all susceptibles equally vulnerable; some results for large susceptible populations and small initial infections. *Acta Biotheoretica*, 27:75–123, 1978.

[65] Frank Ball. A unified approach to the distribution of total size and total area under the trajectory of infectives in epidemic models. *Advances in Applied Probability*, 18:289–310, 1986.

[66] Frank Ball. Coupling methods in epidemic theory. In Denis Mollison, editor, *Epidemic Models: Their Structure and Relation to Data*, chapter 1, pages 34–52. Cambridge University Press, 1995.

[67] Thomas Sellke. On the Asymptotic Distribution of the Size of a Stochastic Epidemic. *Journal of Applied Probability*, 20(2):390–394, 1983.

[68] Frank Ball. The threshold behavior of epidemic models. *Journal of Applied Probability*, 20(2):227–241, 1983.

[69] Frank Ball and Peter Donnelly. Strong approximations for epidemic models. *Stochastic Processes and their Applications*, 55(1):1–21, 1995.

[70] Damian Clancy. Strong approximations for mobile population epidemic models. *The Annals of Applied Probability*, 6(3):883–895, 08 1996.

[71] L.J.S. Allen. *An Introduction to Stochastic Processes with Applications to Biology*. Pearson Education Upper Saddle River, New Jersey, 2nd edition, 2010.

[72] P. Jagers. *Branching Processes with Biological Applications*. John Wiley & Sons London, 1975.

[73] Robert B. Ash. *Real Analysis and Probability*. Academic Press, New York, 1972.

[74] E. Seneta and N. C. Weber. Attainable bounds for expectations. *Journal of the Australian Mathematical Society (Series A)*, 33(03):411 – 420, 11 1982.

[75] George Casella and Roger L Berger. *Statistical Inference*, volume 70. Duxbury Advance Series, 2nd edition, 2001.

[76] Willliam Feller. *An Introduction to Probability Theory and its Applications*, volume 1. John Wiley & Sons, New York, 1971.

[77] Ronald E Walpole, Raymond H Myers, Sharon L Myers, and Keying Ye. *Probability and statistics for engineers and scientists*, volume 5. Macmillan New York, 1993.

[78] Junling Ma and David J.D. Earn. Generality of the final size formula for an epidemic of a newly invading infectious disease. *Bulletin of Mathematical Biology*, 68(3):679–702, 2006.

[79] Michael J. Tildesley and Matt J. Keeling. Is a good predictor of final epidemic size: Foot-and-mouth disease in the UK. *Journal of Theoretical Biology*, 258(4):623 – 629, 2009.

[80] Viggo Andreasen. The final size of an epidemic and its relation to the basic reproduction number. *Bulletin of Mathematical Biology*, 73(10):2305–2321, 2011.

[81] F. Brauer. Age-of-infection and the final size relation. *Mathematical Biosciences and Engineering*, 5(4):681–690, 2008.

[82] Nancy Hernandez-Ceron, Jonathan A. Chavez-Casillas, and Zhilan Feng. Discrete stochastic metapopulation model with arbitrarily distributed infectious period. *Mathematical Biosciences*, 261(0):74 – 82, 2015.

[83] Niels G. Becker. On a general stochastic epidemic model. *Theoretical Population Biology*, 11(1):23 – 36, 1977.

[84] Frank Ball. Dynamic population epidemic models. *Mathematical Biosciences*, 107(2):299 – 324, 1991.

[85] Peter Neal. The basic reproduction number and the probability of extinction for a dynamic epidemic model. *Mathematical Biosciences*, 236(1):31 – 35, 2012.

[86] John A. Jacquez and Philip O'Neil. Reproduction numbers and thresholds in stochastic epidemic models I. homogeneous populations. *Mathematical Biosciences*, 107(2):161–186, 1991.

[87] Frank Ball and Ingemar Nåsell. The shape of the size distribution of an epidemic in a finite population. *Mathematical Biosciences*, 123(2):167–181, 1994.

[88] Andrew D. Barbour. The duration of the closed stochastic epidemic. *Biometrika*, 62(2):477–482, 1975.